A functional study of blood-pressure-associated SNPs at natriuretic peptide receptor C gene locus

by

Meixia Ren MB.BS

December 2015

This thesis is submitted for the degree of Doctor of Philosophy of the University of London

Clinical Pharmacology

William Harvey Research Institute,

Barts and the London School of Medicine and Dentistry,

London

I dedicate this thesis to my parents.

Their altruism, love and encouragement has steered me where I am today

ABSTRACT

Background: Essential hypertension is regarded as a complex disease, the phenotype of which results from interactions between numerous genes and environmental factors. Genome-wide association studies of blood pressure (BP) and hypertension have been developed to explore the potential genes involved in blood pressure and identified a number of trait-associated variants. Among those variants, single nucleotide polymorphisms (SNPs) rs1173771 (G/A) and rs1421811 (G/C) are located at the natriuretic peptide receptor C (*NPR3*) gene locus. Their major alleles are related with blood pressure elevation. Studies have implicated NPR-C in mediating some of the cardio-protective actions of natriuretic peptides and its direct involvement in the pathogenesis of hypertension. However, the precise role of these association between genetic variants at *NPR3* and blood pressure control has not been elucidated.

Objective: To functionally characterise the effect of BP-associated SNPs at the *NPR3* gene locus in the context of BP regulatory pathways.

Methods: Primary human umbilical artery smooth muscle (HUASMCs) and vein endothelial (HUVECs) cells were genotyped for BP-associated *NPR3* variants. Endogenous mRNA and protein expression levels were assessed by qRT-PCR, allelic expression imbalance assay and western blotting. Open chromatin regions were assayed using formaldehyde-assisted isolation of regulatory elements (FAIRE). Interaction between variants flanking region with nuclear protein was detected by electrophoretic mobility shift assay (EMSA). Cell proliferation and migration were

determined by cell counting and scratch assays. Angiotensin II (Ang II)-induced calcium flux was evaluated using the intracellular fluorescent probe.

Results: The BP-elevating allele of the *NPR3* variants in rs1173771 linkage disequilibrium (LD) block was associated with lower endogenous mRNA and protein levels in HUASMCs. This is consistent with the finding that BP-elevating allele is less located within open chromatin. The decreased *NPR3* expression in HUASMCs carrying the BP-elevating allele is associated with increased cell proliferation and intracellular calcium flux in response to Ang II stimulation. No differences in migration rates were detected. No genotype-dependent characteristics were observed in HUVECs *NPR3* expression and cell proliferation.

Moreover, RT-PCR showed a linkage between of the BP-elevating allele of the *NPR3* variants in rs1421811 LD block and lower endogenous mRNA in HUASMCs. Intracellular calcium flux detection also revealed a trend of higher response to Ang II stimulation in BP-elevating allele homozygous HUASMCs. However, No genetic differences were detected in proliferation and migration rates of HUASMCs, and HUVECs *NPR3* expression and cell proliferation studies did not present any significant genotype-dependent association.

Conclusions: This study has identified a potential mechanism for BP-associated SNPs at *NPR3* locus to influence BP predominantly *via* an effect on vascular smooth muscle cell behaviours.

TABLE OF CONTENTS

ABSTRACT ---------- 3

TABLE OF CONTENTS ---------- 5

ACKNOWLEDGEMENT ---------- 11

INDEX OF FIGURES ---------- 13

INDEX OF TABLES ---------- 19

LIST OF ABBREVIATIONS ---------- 21

1. INTRODUCTION ---------- 25

1.1. Blood pressure control ---------- 26

1.1.1 Cardiac output ---------- 26

1.1.2 Kidney sodium excretion ---------- 26

1.1.3 Vascular tone /peripheral vascular resistance ---------- 27

1.1.4 Autonomic nervous system ---------- 27

1.2 Hypertension ---------- 28

1.3 Essential hypertension and genes ---------- 29

1.3.1 Genetic variants/biomarkers ---------- 31

1.3.2 SNPs to gene expression/function and phenotype ---------- 32

1.3.3 Strategies for identifying blood pressure genes/biomarkers ---------- 33

1.3.4 Mendelian forms of hypertension /monogenic hypertension ---------- 37

1.4 Essential hypertension and GWAS ---------- 40

1.4.1 Advances in blood-pressure GWAS ---- 42

1.5 Blood-pressure associated SNPs at *NPR3* gene locus ---- 49

1.5.1 rs1173771 linkage disequilibrium block ---- 49

1.5.2 rs1421811 linkage disequilibrium block ---- 53

1.6 NPR-C signalling system and regulation ---- 55

1.6.1 NPR-C ---- 55

1.6.2 NPR-C associated signalling pathways ---- 56

1.6.3 Regulation of NPR-C expression ---- 58

1.6.4 NPR-C and diseases ---- 60

1.7 CNP/NPR-C signalling transduction system and hypertension ---- 64

1.8 Original hypothesis ---- 66

1.9 Aims and objectives ---- 66

2. MATERIALS & METHODS ---- 68

2.1 Human cell samples ---- 69

2.1.1 Isolation of human umbilical cords arterial smooth muscle cells (HUASMCs) 69

2.1.2 Isolation of human umbilical cords endothelial cells (HUVECs) ---- 69

2.1.3 Cell culturing ---- 70

2.1.4 Cell counting using a haemocytometer ---- 71

2.1.5 Preservation and recovery of cells ---- 72

2.2 Bioinformatics analysis ---- 73

2.3 Genotyping (KASPar SNP Genotyping system) ---- 74

2.3.1 DNA extraction ---- 76

2.3.2 KASPar genotyping ---- 76

2.4 Quantitative Real-Time Reverse Transcription PCR (q RT-PCR) ---- 79

2.4.1 RNA extraction ---- 81

2.4.2 Conversion of RNA to complementary DNA ---------- 81
2.4.3 SYBR-Green quantitative PCR---------- 82

2.5. Allelic expression imbalance (AEI)---------- 85
2.5.1 Preparation of DNA samples---------- 86
2.5.2 Polymerase chain reaction (PCR) ---------- 86
2.5.4 DNA purification from gel and quantification---------- 89
2.5.5 Sanger sequencing---------- 89

2.6 Western Blot Analysis ---------- 90
2.6.1 Preparation of lysate from cell culture---------- 90
2.6.2 Quantification of protein using bicinchoninic acid assay (BCA) kit ---------- 91
2.6.4 Electro transfer ---------- 93
2.6.5 Antibody staining and detection---------- 94
2.6.6 Blocking peptide competition ---------- 95

2.7 Electrophoretic mobility shift assay (EMSA) ---------- 96
2.7.1 Preparation of probes ---------- 97
2.7.2 Cytosolic and nuclear protein extraction ---------- 98
2.7.3 Pre-running ---------- 99
2.7.4 Electrophoretic binding reaction ---------- 100
2.7.5 Electrophoretic transferring and crosslinking. ---------- 101
2.7.6 Detection with Pierce kit---------- 101
2.7.7 Efficiency test of biotin-labelled probes by dot blot assay ---------- 101
2.7.8 Annealing efficiency test ---------- 102

2.8 Cross-linked chromatin immune-precipitation (X-ChIP)---------- 103
2.8.1 Cross-linking and sonication. ---------- 103
2.8.2 Immunoselection with specific antibody---------- 103
2.8.3 Reversing of the cross-linking ---------- 104
2.8.4 Purification of DNA and detection of DNA sequence ---------- 104
2.8.5 Optimization of sonication time---------- 104

2.9 Formaldehyde-assisted isolation of regulatory elements (FAIRE) ---------- 105

2.9.1 Cross-linking and sonication ---------- 106

2.9.2 Preparation of DNA ---------- 107

2.9.3 Purification of DNA ---------- 108

2.9.4 Detection of FAIRE enrichment by sequencing ---------- 108

2.10 Cell proliferation assay ---------- 108

2.10.1 Optimization of CNP concentration in HUASMCs ----------110

2.11 *In vitro* scratch assay ----------111

2.12 Fluorescent imaging plate reader (FLIPR) calcium flux assay ----------112

2.12.1 Optimization of loading dyes and Ang II concentrations in HUASMCs -------115

2.12.2 Optimization of CNP/C-ANF$_{4-23}$ concentrations in calcium flux in HUASMCs ----------116

2.12.3 Preliminary test for agonists of calcium flux in HUVECs ----------119

2.13 Data and statistical analysis. ---------- 120

3. RESULT OF FUNCTIONAL STUDY OF BP-ASSOCIATED VARIANTS AT THE *NPR3* GENE LOCUS IN HUASMCS ----------121

3.1 Genotyping results of BP- associated SNPs at the *NPR3* locus in HUASMCs. --- 122

3.2 Functional study of variants in the rs1173771 linkage disequilibrium block in HUASMCs ---------- 124

3.2.1 Effect of BP-associated SNPs on *NPR3* mRNA level in HUASMCs ---------- 124

3.2.2 Effects of variants in the rs1173771 LD block on NPR-C protein level --------- 127

3.2.3 Interaction of BP-associated SNPs in rs1173771 LD block with nuclear proteins ---------- 129

3.2.4 BP-associated variants reside in open chromatins in HUASMCs ---------- 131

3.2.5 BP-elevating allele of variants in the rs1173771 LD block increases HUASMC proliferation ---------- 134

3.2.6 BP-associated variants at the *NPR3* locus have no effect on HUASMC migration ---------- 137

3.2.7 BP-elevating allele of variants in the rs1173771 LD block increases intracellular calcium flux in response to Ang II in HUASMCs. ---------- 139

3.3 Functional study of variants in the rs1421811 LD block in HUASMCs ---------- 144

3.3.1 Effect of BP-associated SNPs on *NPR3* mRNA level in HUASMCs ---------- 144

3.3.2 No significant effect of variants in the rs1421811 LD block on NPR-C expression level ---------- 145

3.3.3 No significant association between variants in the rs1421811 LD block at NPR3 gene locus and HUASMC proliferation ---------- 146

3.3.4 No significant association between variants in the rs1421811 LD block at the *NPR3* gene locus and HUASMC migration ---------- 148

3.3.5 Impact of variants in the rs1421811 LD block in HUASMC calcium flux. ------ 150

4. RESULT OF FUNCTIONAL STUDY OF BP-ASSOCIATED VARIANTS AT THE *NPR3* GENE LOCUS IN HUVECS ----------153

4.1 Genotyping result of BP-associated SNPs at the *NPR3* locus in HUVECs --------- 154

4.2 Functional study of variants in the rs1173771 LD block in HUVECs ---------- 155

4.2.1 Effect of BP-associated SNPs in the rs173771 LD block on *NPR3* mRNA level in HUVECs ---------- 155

4.2.2 No effect of BP-associated SNPs on the NPR-C protein level in HUVECs ---- 157

4.2.3 Interaction of BP-associated SNP rs1173756 with nuclear proteins from HUVECs ---------- 159

4.2.4 Effect of BP-associated SNPs in HUVECs cell proliferation ---------- 160

4.3 Functional study of variants in the rs1421811 LD block in HUVECs ---------- 163

4.3.1 No effect of BP-associated SNPs on the *NPR3* mRNA level in HUVECs------- 163

4.3.2 Effect of BP-associated SNPs on HUVEC proliferation ---------- 164

5. DISCUSSION AND FUTURE WORK---------- 166

5.1 BP-associated SNPs in rs1173771 LD block influence *NPR3* gene expression in HUASMCs. ---------- 169

5.2 BP-associated SNPs in rs1173771 LD block influence HUASMC proliferation *via* NPR-C signalling pathway. ---------- 172

5.3 BP-associated SNPs in rs1173771 LD block affect HUASMC calcium flux in response to Ang II ---------- 175

5.4 No significant correlation of genetic impact on cell proliferation and calcium flux in response to Ang II ---------- 177

5.5 Effect of BP-associated variants in rs173771 LD block on HUVECs---------- 179

5.6 Effect of other LD block at *NPR3* gene locus in HUASMCs and HUVECs---------- 181

5.7 Conclusion ---------- 182

5.8 Future work ---------- 184

5.8.1 Original hypothesis ---------- 184

5.8.2 Future work ---------- 185

6. REFERENCES ---------- 187

7. APPENDIX ---------- 212

Reagents, buffers and solution ---------- 212

ACKNOWLEDGEMENT

Many people have provided me with help and support through my time as a PhD student, and I am extremely grateful for that.

I would like to thank my parents, my younger sister and my finance for their endless love and encouragement to help me to stay strong during four years of my PhD study in UK. They are always my solid backup no matter where I am.

I would like to express my thanks to Professor Mark Caulfield for his guidance and very kind support during my PhD study. I am very grateful that he has provided me a lot of opportunities to expand my horizon in the science filed. I believe I would benefit a lot in the future from the critical thinking I have been trained during the PhD. I would like to express my thanks to Professor Shu Ye for his supervision and very kind help in my PhD subject. He was very nice to share me with his experiences in research and gave me a lot of suggestion not only for academic life.

I would like to thank Dr. Fu Liang Ng, Dr. Kate Witkowska and clinical pharmacology team for their company and support during these years. They has done a good job in organizing the lab and provided me a lot of fantastic advices in the design and daily work of this project.

I would like to thank my advisors Professor Adrian Hobbs and Dr. Qingzhong Xiao. They are very nice to help me to design the experiments and have provided me a lot of good suggestion in CNP and cloning work in my subject.

I would like to express thanks to my collaborators in UCL, Professor Andrea Townsend and Dr. Michael Barren. Thanks to their kindness, I could finish my calcium work with their generous help and had a very nice time in UCL.

I would like to thank Helen Warren, Zhilong Jia and Bori Mifsud for their very kind support for the bioinformatics work involved in subject.

This work was supported by National Institute for Health Research, and I would like to acknowledge the financial support from Chinese Scholarship Council.

INDEX OF FIGURES

Figure 1.1 Pathophysiological mechanisms involved in hypertension. 28

Figure 1.2 Hierarchy in genetics of cardiovascular disease. 30

Figure 1.3 Relation of risk allele frequencies, penetrance / effect sizes (odds ratios) and feasibility of identifying risk variants by common genetic tests. [37] 32

Figure 1.4 Genome-wide –log$_{10}$ *P*-value plots and effects for significant loci. 50

Figure 1.5 Regional plots of SNP rs1173771 in CEU (A) and CHB+JPT (B) at the *NPR3* locus. 52

Figure 1.6 Regional plots of SNP rs1421811 in CEU (A) and CHB+JPT (B) at the *NPR3* locus. 54

Figure 1.7 Structure of *NPR3* gene and its protein NPR-C. 56

Figure 1.8 Summary of NPR-C-coupled signalling systems. 58

Figure 1.9 Schematic description of the intracellular mechanisms activated by NPR-C stimulation. 63

Figure 1.10 Activation of natriuretic peptide receptor (NPR)-C by endothelial CNP underlies a key mechanism regulating vascular tone and local blood flow. 65

Figure 2.1 Human umbilical cords arteries and vein. 70

Figure 2.2 Haemocytometer gridlines. 72

Figure 2.3 Systemic principles of KASPar genotyping system. 75

Figure 2.4 KASPar genotyping data plotted showing the four separate clusters. 78

Figure 2.5 Representative amplification curve of RT-PCR. 80

Figure 2.9 The DNA fragments under a UV transilluminator. 88

Figure 2.10 A representative sequencing result. 89

Figure 2.11 Standard curve for protein concentration quantification in bicinchoninic acid assay (BCA) assay. 92

Figure 2.12 Assembly of a transfer 'sandwich' in western Blot 94

Figure 2.13 Blocking competition with NPR-C blocking peptide in HUASMCs. 96

Figure 2.14 The diagram of biotin-labelled probes after dot blot assay. 102

Figure 2.15 The annealed oligos under a UV transilluminator. 102

Figure 2.16 The DNA fragments range under different sonication times. 105

Figure 2.17 Principles of formaldehyde-assisted isolation of regulatory elements (FAIRE). 106

Figure 2.18 Principle of the cell viability detection with Cell Counting Kit-8. 109

Figure 2.19 Optimization of CNP concentration in HUASMC proliferation. 111

Figure 2.20 Calcium flux assay principle 113

Figure 2.21 Representative trace of intracellular calcium changes in response to Ang II in HUASMCs. 115

Figure 2.22 Optimization of three different loading dyes (A) and Ang II concentration with calcium 6 (B) in HUASMCs. 116

Figure 2.23 Optimization of concentrations of CNP (1pM to 1μM) (A) and C-ANF$_{4-23}$ (1pM to 1μM) (B) with Losartan (1μM) as antagonist control in Ang II (10nM) - induced intracellular calcium changes in HUASMCs. .. 118

Figure 2.24 Optimization for agonist of calcium flux in HUVECs. 120

Figure 3.1 An allelic discrimination plot for SNP rs1173771 in HUASMCs analysed by SDS 2.3. 122

Figure 3.2 Quantitative analysis of mRNA levels of *NPR3* among BP-associated SNPs in linkage disequilibrium block of rs1173771 in HUASMCs. 126

Figure 3.3 Allelic expression imbalance of 3-UTR SNP rs1173756 in the *NPR3* gene in HUASMCs. 127

Figure 3.4 Blood pressure-associated variant in rs1173771 LD block significantly affect natriuretic peptide receptor C (NPR3) protein level in human umbilical arterial smooth muscle cells (HUASMCs). 128

Figure 3.5 Interaction of *NPR3*-intronic SNPs rs1173743 and rs1173747with HUASMC nuclear proteins *in vitro*. 130

Figure 3.6 Interaction of *NPR3* SNPs rs1173771 (intergenic) and rs1173756 (located in 3'-UTR) with HUASMC nuclear proteins *in vitro*. 131

Figure 3.7 Allele-specific difference of rs1173747 in open chromatin in HUASMCs. 132

Figure 3.8 Allele-specific difference of rs1173756 in open chromatin in HUASMCs. 133

Figure 3.9 Effect of BP-associated variants in the rs1173771 LD block in *NPR3* on HUASMCs proliferation. 135

Figure 3.10 Inhibitory effect of CNP/ C-ANF$_{4-23}$ on HUASMC proliferation. 136

Figure 3.11 No significant effect of blood pressure (BP)-associated variants in rs1173771 LD block at the *NPR3* locus on cell migration in HUASMCs. 138

Figure 3.12 Representative figures to show cell density of human umbilical arterial smooth muscle cells in each genotype after incubated with fluorescent loading dye calcium 6. 140

Figure 3.13 Effect of *NPR3* BP-associated variants in the rs1173771 LD block on the intracellular calcium changes induced by angiotensin II (Ang II) in HUASMCs. 141

Figure 3.14 Effect of C-type natriuretic peptide and natriuretic peptide receptor C-specific agonist CANF4-23 on angiotensin II induced intracellular calcium changes in HUASMCs. 142

Figure 3.15 Effect of C-type natriuretic peptide and natriuretic peptide receptor C-specific agonist C-ANF$_{4-23}$ on angiotensin II induced intracellular calcium changes in HUASMCs. 143

Figure 3.16 Quantitative analysis of mRNA levels of *NPR3* among BP-associated SNPs in rs1421811 LD block in HUASMCs. 145

Figure 3.17 Effect of Blood pressure-associated variant in rs1421811 LD block on natriuretic peptide receptor C (NPR-C) protein level in human umbilical arterial smooth muscle cells (HUASMCs). 146

Figure 3.18 No significant effect of BP-associated variant in rs1421811 LD block in *NPR3* on HUASMC proliferation. 147

Figure 3.19 No effect of blood pressure (BP)-associated variants in the rs1421811 LD block at the *NPR3* locus on HUASMC migration. 149

Figure 3.20 Effect of variants in the rs142181 LD block on angiotensin II induced intracellular calcium changes in human umbilical arterial smooth muscle cells. 151

Figure 3.21 No effect of C-type natriuretic peptide and natriuretic peptide receptor C-specific agonist $CANF_{4-23}$ on angiotensin II induced intracellular calcium changes in human umbilical arterial smooth muscle cells. 152

Figure 4.1 Quantitative analysis of mRNA levels of NPR3 among BP-associated SNPs in the rs1173771 LD block in HUVECs. 156

Figure 4.2 Allelic expression imbalance of 3-UTR SNP- rs1173756 in *NPR3* gene in HUVECs. 157

Figure 4.3 No effect of BP-associated variant on NPR3 protein level in HUVECs. 158

Figure 4.4 Detection of relative binding affinities of DNA sequences flanking BP-associated SNPs to HUVEC nuclear extract *in vitro*. 160

Figure 4.5 No effect of BP-associated variants in the rs1173771 LD block at *NPR3* locus on human umbilical vein endothelial cells proliferation. 161

Figure 4.6 No effect of CNP/ $CANF_{4-23}$ on human umbilical vein endothelial cells proliferation. 162

Figure 4.7 Quantitative analysis of mRNA levels of *NPR3* among BP-associated SNPs in the rs1421811 LD block in HUVECs. 164

Figure 4.8 No effect of BP-associated variants in the rs1421811 LD block in *NPR3* on human umbilical vein endothelial cells proliferation. 165

Figure 5.1 No correlation between cell viability in 24 hours and calcium flux in response to Ang II. 178

Figure 5.2 A much higher relative expression level of *NPR3* mRNA was detected in HUASMCs compared with HUVECs. 180

Figure 5.3 A proposed model to show the systemic mechanism between risk variants in natriuretic peptide receptor C (*NPR3*) gene and hypertension risk. 183

INDEX OF TABLES

Table 1.1 Characteristics of Mendelian Disorders of Hypertension and Hypotension. 37

Table 1.2 Summary of genetic variants robustly associated with blood pressure traits. 43

Table 2.1 Bioinformatics update about BP-associated SNPs in rs1173771 LD block. 74

Table 2.2 Primers sequence information for KASPar genotyping for variants in rs1173771 LD block. 78

Table 2.3 Primers sequence information for KASPar genotyping for variants in rs1421811 LD block. 79

Table 2.4 Information of primers for rs1173756 DNA fragments. 86

Table 2.5 Constitute reagents volume in PCR system. 87

Table 2.6 Components in protease inhibitor cocktail. 91

Table 2.7 Constitute reagents volume in separating gel and stacking gel. 93

Table 2.8 Information on the antibodies used in Western Blot analysis. 95

Table 2.9 Components in ECL solutions. 95

Table 2.10 Information of oligos in EMSA. 98

Table 2.11 Constitute in buffer A and buffer B. 99

Table 2.12 Components in 6% non-denaturing polyacrylamide gel. 99

Table 2.13 Preparation of reaction mix. 100

Table 2.14 Working media for *in vitro* scratch assay. 112

Table 2.15 The working concentrations of compounds used in FLIPR assay. 114

Table 2.16 Agonists used in HUVECs calcium flux. 119

Table 3.1 BP-associated SNPs genotyping result in HUASMCs. 123

Table 3.2 Linkage disequilibrium (LD) values between *NPR3* SNPs..... 124

Table 4.1 BP-associated SNPs genotyping results in HUVECs and HWE calculation..... 154

LIST OF ABBREVIATIONS

Abbreviation	Full name
ANP	Atrial natriuretic peptide
AEI	Allelic Expression Imbalance
Ang II	Angiotensin II
AVP	Arginine–vasopressin
bp	Base pair
BP	Blood pressure
BMI	Body mass index
BSA	Bovine serum albumin
cAMP	Cyclic adenosine monophosphate
cGMP	Cyclic guanosine monophosphate
CANF $_{4\text{-}23}$	(Cys18)-atrial natriuretic factor (4-23) amide
CARe	Candidate Gene Association Resource
CVD	Cardiovascular disease
CO	Cardiac output
CNP	C type of Natriuretic peptide
CPT	Cold presser test
Ct	Threshold cycle
DBP	Diastolic blood pressure

dNTP	deoxynucleoside triphosphates
DMEM	Dulbecco's Modified Eagle Medium
EC	Endothelial cell
ECL	Enhanced chemiluminescence
ED	Endothelium dysfunction
EDHF	Endothelium-derived hyperpolarizing factor
EDTA	Ethylene diamine tetra-acetic acid
EMSA	Electrophoretic Mobility Shift Assay
ERK	Extracellular-signal-regulated kinases
ET-1	Endothelin-1
eNOS	Endothelial nitric oxide synthase
g	Gravitational-force
G_i	Inhibitory guannine nucleotide regulatory protein
G_q	Guanine nucleotide regulatory protein, q polypeptide
GWLAs	Genome-wide linkage studies
GWASs	Genome-wide association studies
H_2O	Water
HR	Heart rate
HUASMCs	Human Umbilical Vein Smooth Muscle Cells
HUVECs	Human Umbilical Vein Endothelial Cells
LD	Linkage disequilibrium
KASPar	

ICBP-GWAS	The Kbiosciences Competitive Allelic-specific PCR SNP genotyping system International Consortium for Blood Pressure Genome-Wide Association Studies
MAF	Minor allele frequencies
MAPK	Mitogen-activated protein kinase
MAP	Mean arterial pressure
$MgCl_2$	Magnesium chloride
MI	Myocardial infarction
$NaNO_3$	Sodium nitrate
NaOH	Sodium hydroxide
NADPH	nicotinamide adenine dinucleotide phosphate
NO	Nitric oxide
NOS	Nitric oxide synthase
NP-40	Nonidet P-40
NPR3	Natriuretic peptide receptor C
NPR-A	Natriuretic peptide receptor A
NPR-B	Natriuretic peptide receptor B
PBS	Phosphate buffered saline
PCI	Percutaneous trans-luminal revascularisation
PCR	Polymerase chain reaction
PI	Protease Inhibitor

PNS	Parasympathetic nervous system
PP	Pulse pressure
PSS	physiological saline solution
QTLs	Quantitative trait locus
RSA system	Renin–angiotensin–aldosterone system
R37A	37 amino acid peptide
SBP	Systolic blood pressure
SNP	single nucleotide polymorphism
SNS	Sympathetic nervous system
SHR	Spontaneously hypertensive rat
SMC	Smooth muscle cell
SsDNA	Single-stranded DNA
SV	Stroke volume
TFBS	Transcriptional factor binding sites
3’ UTR	3 primer untranslated region
UV	Ultraviolet
vol	Volume

1. Introduction

1.1. Blood pressure control

At the basic level, blood pressure can be approximated by Ohm's Law modified for fluid dynamics, pressure = flow X resistance. Blood flow depends on the cardiac output (CO) and blood volume, whereas resistance is primarily determined by the contractile state of small arteries and arterioles throughout the body, also called total peripheral vascular resistance. These components of blood pressure are subject to a range of regulatory influences.

1.1.1 Cardiac output

Cardiac output is the volume of blood pumped per minute by left ventricle of the heart, and it is equal to the stroke volume (SV) times the heart rate (HR). SV is defined as the volume of blood ejected per contraction and is controlled by the energy with which the myocytes contract and the pressure required to force out the blood.[1] Both HR and SV are important in adapting the cardiac output to its metabolic demands. Heart rate itself is highly variable and therefore acts as a driving force for cardiovascular regulation.[2]

1.1.2 Kidney sodium excretion

As sodium is the major cation in the extracellular fluid (e.g. increased dietary salt intake could increase the extracellular fluid volume), renal sodium excretion provides a crucial pathway for reducing body fluid volumes and returning systemic pressures to normal. Due to the capacity of the kidney to rapidly increase urinary sodium excretion in response to elevations in blood pressure, also called 'pressure natriuresis', the kidney has been regarded as one of central organs in circulatory homeostasis and blood pressure control.[3] The peptide hormone angiotensin II, which

increases thirst, promotes salt retention by the kidney, causes vasoconstriction, and enhances the release of catecholamine from neurones and the adrenal gland.[4]

1.1.3 Vascular tone /peripheral vascular resistance

Along with changes in circulating volumes, peripheral vascular resistance is also an important determinant of blood pressure. Vascular resistance is the force that opposes the flow of blood through a vascular bed. It is equal to the difference in blood pressure across the vascular bed divided by the cardiac output.[5–7] Most phenotypes of hypertension result from an increased vascular tone that leads to an elevated total peripheral resistance.[8,9] Vascular resistance under both normotensive and hypertensive conditions is under control of multiple hormonal mediators. For instance, G protein–coupled receptors on vascular smooth muscle cells and their associated signalling pathways are required for maintenance and control of blood pressure.[10,11] Peripheral vascular resistance could also be modified, e.g. by arterial wall modifications due to ageing, medial hypertrophy due to obesity.[12]

1.1.4 Autonomic nervous system

Vascular resistance and cardiac output are both controlled by the autonomic nervous system. This in turn is divided into two subsystems: the parasympathetic nervous system (PNS) and the sympathetic nervous system (SNS).[13] A major role of the SNS is the maintenance of BP (short-term) and the regulation of blood flow via the arterial baroreflex. The arterial baroreflex works by sensing changes in BP via baroreceptors which respond to vessel wall stretch. Longer term control of arterial pressure however has traditionally been attributed to the kidney.[14,15]

In summary, normal control of blood pressure requires complex integration of regulatory mechanisms across multiple physiological systems, including the kidney, skin, the vasculature, the central and sympathetic nervous systems, and various hormonal regulators (Figure 1.1).[16]

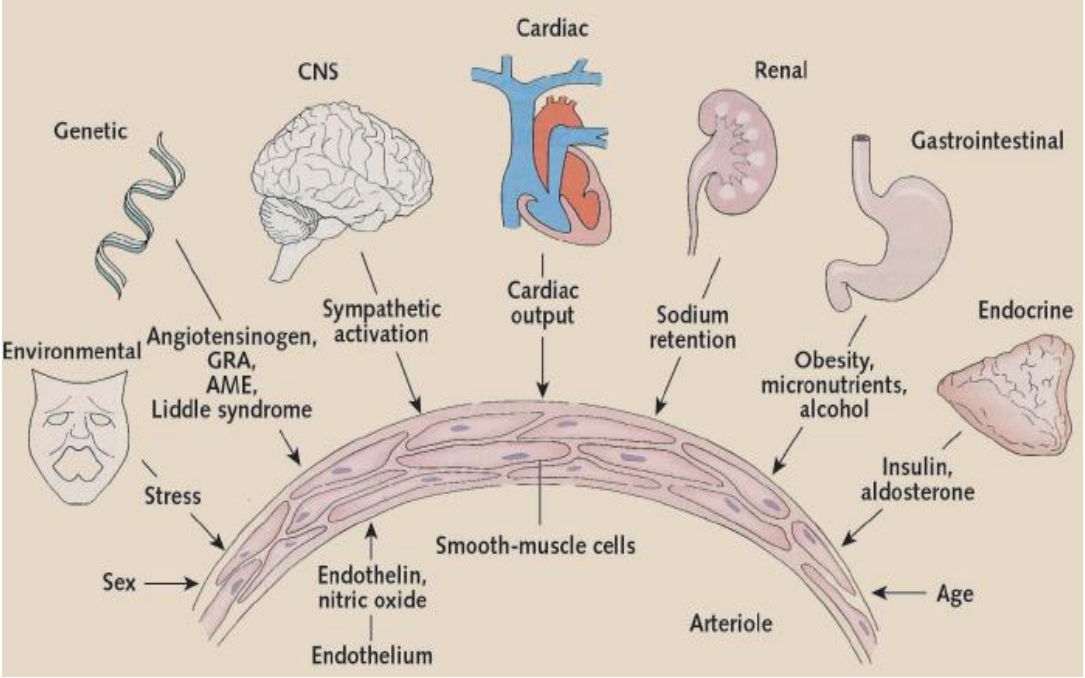

Figure 1.1 Pathophysiological mechanisms involved in hypertension.
AME = apparent mineralocorticoid excess; CNS = central nervous system; GRA = glucocorticoid-remediable aldosteronism.[16]

1.2 Hypertension

Hypertension is defined as a systolic blood pressure (SBP) of 140 mm Hg or more, or a diastolic blood pressure (DBP) of 90 mm Hg or more, or taking antihypertensive medication.[17] It is one of the most common chronic diseases in the human population. It is predicted to be prevalent in 30% of the worldwide population by 2025, with approximately 1.56 billion suffering from hypertension.[18] Cardiovascular diseases

including stroke, myocardial infarction (MI), congestive heart failure, arterial aneurysm and chronic renal failure are complications of hypertension and are major sources of morbidity and mortality [19]. The relationship between blood pressure and risk of cerebrovascular disease events is continuous, consistent and independent of other risk factors. [20]

Advances in the diagnosis of hypertension and multiple different therapeutic strategies targeting the disease have played a major role in recent dramatic declines in coronary heart diseases and stroke mortality all over the world and the public has been more aware of this disorder and its risks. However, control rates remain unsatisfactory, and a substantial proportion of people with hypertension under treatment do not achieve the target levels of blood pressure control recommended by current guidelines. Public health data have confirmed inadequate control of BP under various anti-hypertensive medications among treated hypertension patients. Indeed, only 20% to 30% of treated individuals achieve current targets.[21,22] Similar numbers were observed in a ten-year study (1998-2008) in hypertensive patients in America.[23] These findings highlight the need for a more effective way of hypertension prevention.

1.3 Essential hypertension and genes

In approximately 5% of all hypertension cases, the cause is secondary to conditions such as primary hyperaldosteronism (Conn's syndrome), Cushing's syndrome (excessive glucocorticoids), phaeochromocytoma or renal diseases; it may also be drug-induced. The majority of hypertension cases are labelled as essential hypertension, defined as high blood pressure without any known secondary cause, constituting the remainder 95% of cases.[24,25] Essential hypertension is regarded as a complex disease, the phenotype of which results from interactions between numerous genes and environmental factors including high salt intake, smoking, alcohol

consumption, BMI (body mass index), age and stress. The genetic contribution to essential hypertension comes in the form of multiple alleles in polygenes that can alter the function and/or the expression level of the encoded protein, creating endo-phenotypes that complicate into hypertension with other risk factors [26] (Figure 1.2).

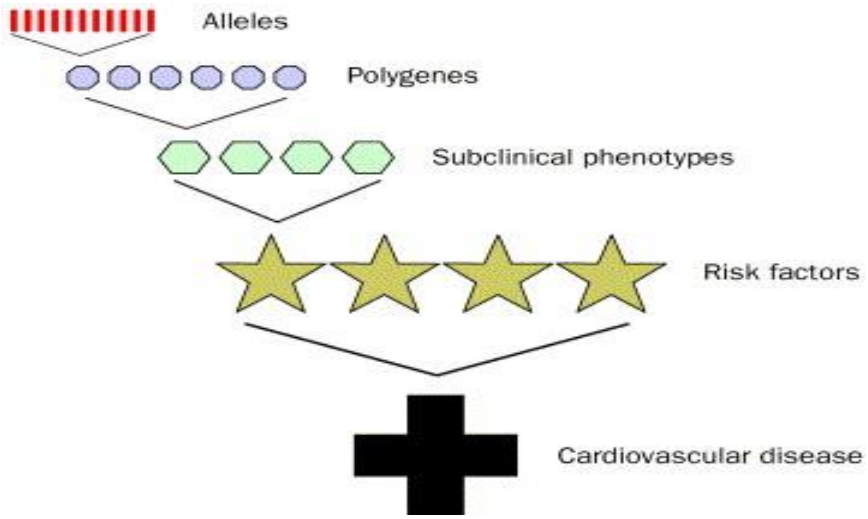

Figure 1.2 Hierarchy in genetics of cardiovascular disease.
Several subclinical physiological phenotypes contribute to each cardiovascular risk factor. Phenotypes depend on unknown number of polygenes; polygenic effects depend on an unknown number of alleles. [26]

Epidemiological and familial aggregation studies have established that there is a significant heritability component (30%-50%) for both blood pressure and hypertension.[27] The importance of genetic influence is perhaps best illustrated by the observation that the risk of developing hypertension for people with a family history of hypertension is increased by approximately four times compared with the general population[28]. The role attributable to genetic factors amounts to some 25% among hypertensive families and can reach 65% when monozygotic twins are compared. Unravelling the genetics of hypertension holds promise for providing an unbiased

approach for understanding its pathogenesis, risk profiling and identifying therapeutic targets.[29]

1.3.1 Genetic variants/biomarkers

Substantial genetic variations exist in human genome, such as insertions and deletions (indels), structural variation, and epigenetic modification.[30,31] The majority (90%) of human genetic variants are single nucleotide polymorphism (SNP) that is a single-nucleotide substitutions of one base for another occurring every 100–300 genome bases in a DNA sequence, and has a population frequency of at least 1%.[32,33]. However, not all single-nucleotide changes are SNPs. Some specific disease-causing point mutations are also caused by single allelic variants which often occur within a gene's coding or regulatory regions and affect the function of the protein encoded by the gene.[34] With advances in high-throughput genome-wide chip-based strategies, their interrogation at large scale is now feasible, and tens of thousands of SNPs in their first versions can interrogate more than 5 million variants across the human genome.[35]

Each SNP is usually constituted by two, rarely more, different possible nucleotide bases (alleles) at the same genetic position. The allele with a higher frequency (>50%) in a population is regarded as the major allele, otherwise, the other is the minor allele (<50%). It is widely accepted that gene variants with minor allele frequencies (MAF) from 5% to 50% are considered common, those with MAF between 1% and 5% are considered less common, and those with MAF less than 1% are considered rare. Different MAF classes of variant determine its optimal research strategies.[36]

To date, two principal heritable types of BP-associated variants are recognised (Figure 1.3). The first type is monogenic hypertension involved with variants occurring near exclusively in rare familial syndromes. These are usually exonic mutations with

large effect sizes usually causing catastrophically high BP levels with severe and early onset cardiovascular morbidity and mortality in many cases. The other type is common essential hypertension which to date is mostly caused by a mixture of common variants with modest effect sizes.[37]

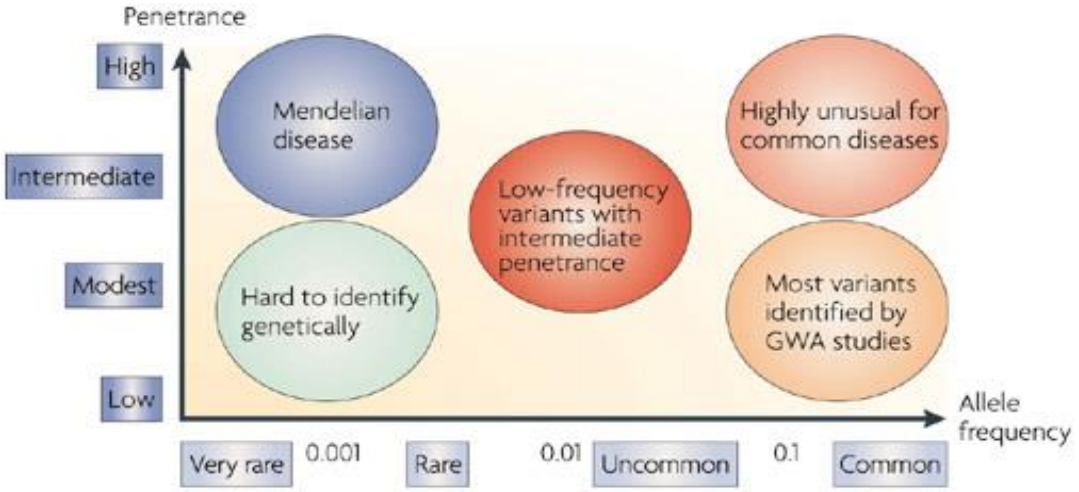

Figure 1.3 Relation of risk allele frequencies, penetrance / effect sizes (odds ratios) and feasibility of identifying risk variants by common genetic tests. [37]

1.3.2 SNPs to gene expression/function and phenotype

Based on the genetic position of variants, SNPs are mainly classified into five groups:

1) exonic SNPs: Nonsynonymous SNPs, SNPs may change the encoded amino acids (nonsynonymous); and synonymous SNPs: those nucleotide substitutions that do not change the amino acid.

2) Intronic SNPs: SNPs within introns;

3) 5' UTR SNPs: SNPs at the 5' end of the gene;

4) 3' UTR SNPs: SNPs at the 3' end of the gene including the region of the mRNA between the stop codon and the poly-A tail;

5) intergenic SNPs: those nucleotides located in the intergenic regions between genes.[38]

It is intuitive that nonsynonymous SNPs (amino acid substitutions) can change the gene expression or subsequently alter function of a protein. Intronic, 3-UTR, 5'-UTR and synonymous SNPs which can be catalogued as non-coding SNPs could also influence gene expression.[39] Cis-regulatory sequences have been regarded as critical regions to regulate the transcription of nearby genes. They are typically composed of non-coding DNA containing binding sites for transcription factors (TFs) and/or other regulatory molecules. Tighter or looser binding of regulatory proteins will lead to up- or down-regulated transcription, change gene expression and hence may produce phenotype difference.[40]

In addition, SNPs located in intron or exon can function as part of cis-acting RNA sequence elements presenting in pre-mRNAs. They can impact alternative splicing, subsequently resulting in a single gene coding for multiple proteins.[41]

1.3.3 Strategies for identifying blood pressure genes/biomarkers

1.3.3.1 Candidate-gene studies

The candidate gene approach is a common strategy in the hunt for genes that are involved in essential hypertension with the use of classic epidemiological techniques. The aim of this approach is to determine whether hypertension is associated with 'candidate gene' markers, most frequently consisting of single nucleotide polymorphisms (SNPs).[42] The selection of candidate genes for such studies has generally been based on a mechanistic understanding of the roles of the encoded

proteins in blood pressure regulation. These candidates are mainly involved in the renin–angiotensin–aldosterone system (RSA system) or other determinants of sodium and blood-volume regulation, adrenergic pathways, vascular-associated genes; metabolism-associated genes, other miscellaneous' roles. [43]

Human candidate gene studies have examined more than 60 genes likely to be implicated in essential hypertension,[42] but most of the studies were often dependent on prior knowledge of the gene product in question, and genes whose products are unknown or believed to be "unimportant" in the pathogenesis of hypertension were likely to be ignored. It is common phenomenon that candidate genes did not provide accurate and consistent evidence in hypertension associated analysis.[44]

1.3.2.2 Genome-wide linkage studies

Genome-wide linkage studies (GWLS) utilize genetic markers - notably microsatellite (also called simple sequence repeats) polymorphisms and SNPs that are linked with a disease phenotype and located anywhere within the genome. This approach is carried out without any prior knowledge of a likely contribution to the phenotype of interest.

Since the mid-1990s, with the availability of increased numbers of markers, genome-wide linkage studies have now identified well more than 60 hypertension-associated quantitative trait locus (QTLs) across the genome [45] QTL refers to a position in the chromosome that may influence the trait of interest.[46]

These results indicate that no single genomic region has a uniformly large effect on predisposition to hypertension. [47] At present, all human autosomal chromosomes have been reported to contain regions linked to BP and hypertension.[43]

1.3.3.3 Genome-wide association studies

Genome-wide association studies (GWAS) is an approach that involves scanning markers across the genomes of many people to find genetic variations associated with a particular disease. It is based on the concept that common complex diseases are governed by several SNPs having subtle effects and are context-dependent.

Association studies are carried out with a categorical (often binary case/control) or quantitative design. From the statistical perspective, quantitative traits are preferred because they improve power to detect a genetic effect, and often have a more interpretable outcome. Other disease traits do not have well-established quantitative measures. In these circumstances, individuals are usually classified as either affected or unaffected – a binary categorical variable. [48] The basic paradigm used in GWAS recently is to catalogue very common variants and genotype them based on arrays directly or indirectly through linkage disequilibrium (LD) in individuals. [36]

There has been a recent increase in the number of publications of GWAS data for complex diseases in different populations and ethnic groups. The first large GWAS experiment for hypertension was carried out by The Wellcome Trust Case Control Consortium (WTCCC) in 2007 which studied 7 complex diseases including: bipolar disorder (BD), coronary artery disease (CAD), Crohn's disease (CD), hypertension (HTN), rheumatoid arthritis (RA), type I diabetes (T1D), and type II diabetes (T2D) (WTCCC 2007).

In contrast to linkage studies, association studies have good sensitivity and successfully represent variants with a MAF frequency of ~5% or higher in the general population, but they are prone to false positive results. Even an association between a particular allele and high blood pressure is found but it does not imply ‘cause’, and determination of the causative variant among possibly hundreds of variants in LD with association is also challenging. It has been showed that interactions between the various alleles of different genes may be more important than allelic variation at a single locus in the determination of blood pressure,[49] until now, GWAS study have reported more than 60 loci associated with blood pressure.[45]

Association studies to date have largely focused on studying individual common variants, because they could be more readily assayed with initial genomic technologies. Nonetheless, the genetic variants identified thus far appear to explain less than half of the estimated heritability in most diseases and traits. The 'missing heritability' of complex diseases highlights the importance of exploring the potential rare variants. Association studies are now increasingly being applied to sets of rare variants as well.[50]

1.3.3.4 Next generation sequencing

Nucleic acid sequencing is a method for determining the exact order of nucleotides present in a given DNA or RNA molecule. The Human Genome Project was accomplished in 2003 with first-generation sequencing, known as Sanger sequencing. With the growing demand for a cheap and rapid approach for sequencing, next generation sequencing (NGS) has been developed. Its platforms perform massively

parallel high-throughput sequencing, allowing millions of fragments of DNA from a single sample are sequenced in unison.[51] The base methodology includes template preparation, sequencing and imaging, and data analysis.[52] In many cases, targeted sequencing for specific genes or genomic regions, e.g. whole exome, RNA messenger, is preferred to detect a suspected disease. For instance, exome sequencing could identify the causative mutations in pathogenic presentations where the exact genetic cause is not known.[53]

1.3.4 Mendelian forms of hypertension /monogenic hypertension

There are several rare Mendelian forms of hypertension with distinctive co-phenotypes, such as the hypertension and hypokalemia seen in Liddle's syndrome with causal proteins SCNN1B, SCNN1G encoded by 16p13-p21.[54] Lifton et al have found mutations of more than 20 genes are responsible for those rare disorders.[9] To date, dozens of genes have been identified, leading to a number of distinguishable Mendelian syndromes causing hypertension (Table 1.1). They mainly influence two main pathways: renal salt excretion/sodium homeostasis and steroid hormone metabolism.[9,55]

Table 1.1 Characteristics of Mendelian Disorders of Hypertension and Hypotension.

Locus	Gene(s)	Mode of inheritance	Genomic and biological mechanism	Phenotypic annotation	OMIM	Therapeutic notes/clinical management
1p32.3	*BSND*	Autosomal recessive	Mutations in a beta-subunit for CLCNKA and CLCNKB chloride channels	**Bartter syndrome, type 4**	#602522	Aldosterone inhibitors and angiotensin-converting enzyme (ACE) inhibitors

1p36.13	*CLCNKB*	Autosomal recessive	Loss of function mutations in chloride channels, impaired chloride reaborsportion in the thick ascending loop of Henle	**Bartter syndrome, type 3** Low blood pressure hypokalaemic metabolic alkalosis elevated plasma renin and aldosterone	#607364	Aldosterone inhibitors and angiotensin-converting enzyme (ACE) inhibitors
1p36.13	*SDHB*	Autosomal dominant	Tumors or extra-adrenal paraganglia associated pheochromocytoma	**Paragangliomas 4**	#115310	Alpha adrenergic blockers for pheochromocytoma
1q23.3	*SDHC*	Autosomal dominant	Tumors or extra-adrenal paraganglia associated pheochromocytoma.	**Paragangliomas 3**	#605373	Alpha adrenergic blockers for pheochromocytoma
2q36.2	*CUL3*	Autosomal dominant	Deficiency in cullin–ring E3 ligase complexes increase activity of cotransporter of NCCT and ROMK	**Pseudohypoaldosteronism, type IIE**	#614496	Thiazide diuretics, low-sodium diet
3q25.3	*VHL*	Autosomal dominant	Mutations in the VHL tumour suppressor gene	**Von Hippel-Lindau syndrome** Associated with retinal, cerebellar, and spinal hemangioblastoma, renal cell carcinoma (RCC), pheochromocytoma, and pancreatic tumors.	#193300	Alpha adrenergic blockers, surgical resection
4q31.23	*NR3C2*	Autosomal dominant	Gain of function in mineralocorticoid receptor; salt wasting with hyperkalemic acidosis resulting from renal unresponsiveness to mineralocorticoids	**Hypertension exacerbation in pregnancy Pseudohypoaldosteronism type I**	#605115 #177735	Spironolactone contraindicated and delivery of fetus
5q31.2	*KLHL3*	Autosomal dominant	Loss of function mutations lead to inhibition of KLHL3 and increase activity of cotransporter of NCCT and ROMK	**Pseudohypoaldosteronism, type IID** Hyperkalaemia. Hyperchloremic metabolic acidosis	#614495	Thiazide diuretics, low-sodium diet
6p21.33	*CYP21A2*	Autosomal recessive	Loss of function, impaired synthesis of aldosterone and following excessive salt loss	**Congenital adrenal hyperplasia**	#613815	Mineralocorticoid , sodium chloride
7p22.3-7p22.1				**Familial Hyperaldosteronism type 2**	#605635	Spironolactone, eplerenone
8p11.23	*STAR*	Autosomal recessive	Loss of steroidogenesis	**Lipoid congenital adrenal hyperplasia**	#201710	Glucocorticoid and mineralocorticoid replacement
8q24.3	*CYP11B1*	Autosomal dominant	Impaired reductions in cortisol and corticosterone synthesis	**Adrenal hyperplasia, congenital, due to 11-beta-hydroxylase deficiency;**	#610613	Glucocorticoids

8q24.3	*CYP11B2*	Autosomal recessive	Defect in the penultimate biochemical step of aldosterone biosynthesis	**Hypoaldosteronism, congenital, due to CMO I deficiency;** decreased aldosterone and salt-wasting, increased plasma corticosterone and 11-deoxycorticosterone	#610600	Glucocorticoids
10q11.2	*RET*	Autosomal dominant	Mutations in the *RET* oncogene	**Multiple Endocrine Neoplasia, Type IIA** Associated with multiple endocrine neoplasms, including medullary thyroid carcinoma, pheochromocytoma, and parathyroid adenomas.	#171400	Alpha adrenergic blockers, surgical resection
10q24.3	*CYP17A1*	Autosomal recessive	*CYP17A1* deficiency result in low levels of glucocorticoids with a consequent loss of the feedback inhibition of the hypothalamic-pituitary axis and elevated ACTH secretion	**Adrenal hyperplasia, congenital, due to 17-beta-hydroxylase deficiency**	#202110	Glucocorticoids
11q12.2	*SDHAF2*	Autosomal dominant	Tumors or extra-adrenal paraganglia associated pheochromocytoma.	**Paragangliomas 2**	#601650	Alpha adrenergic blockers, surgical resection
11q23.1	*SDHD*	Autosomal dominant	Tumors or extra-adrenal paraganglia associated pheochromocytoma.	**Paragangliomas 1**	#16800	Alpha adrenergic blockers, surgical resection
11q24.3	*KCNJ5*	Autosomal dominant	Mutations in potassium inwardly-rectifying channel	**Familial Hyperaldosteronism type 3;** elevated aldosteronism levels, and high levels of the hybrid steroids 18-oxocortisol and 18-hydroxycortisol	#613677	Adrenalectomy
11q24.3	*KCNJ1*	Autosomal recessive	Mutation in the potassium channel ROMK	**Bartter syndrome, antenatal, type 2**	#241200	Sodium and potassium supplement; cyclooxygenase (COX) inhibitor : indomethacin; some specific inhibitor of COX2
12p12.3	*WNK1*	Autosomal dominant	Gain of function mutation in *WNK1* results in salt retention via sodium and potassium transporters	**Pseudohypoaldosteronism type IIC Gordon's syndrome;** hypertension, hyperkalaemia	#614492	Thiazide diuretics, low-sodium diet
15q21.1	*SLC12A1*	Autosomal recessive	Loss of function in sodium-potassium-chloride cotransporter-2 in the thick ascending loop of Henle	**Bartter syndrome, antenatal, type 1** hyposthenuria, moderate hypokalaemic metabolic alkalosis	#601678	Sodium and potassium supplements; Aldosterone inhibitors and angiotensin-converting enzyme (ACE) inhibitors

12p13.31	*SCNN1A*	Autosomal recessive	Mutation in subunits of the renal epithelial sodium channel of the distal nephron leads to renal salt wasting	**Pseudohypoaldosteronism, type I;** hyponatremia, hyperkalaemia, and increased plasma renin activity	#264350	Aggressive salt replacement and control of hyperkalemia
16p12.2	*SCNN1B, SCNN1G*	Autosomal dominant	Mutation in subunits of the renal epithelial sodium channel (ENaC)of the distal nephron cause hyperactivity of ENaC	**Liddle's Syndrome;** frequently severe hypertension associated with hypokalaemic metabolic alkalosis	#177200	Low salt diet , amiloride and triamterene
16q13	*SLC12A3*	Autosomal recessive	Loss of function mutation in thiazide-sensitive Na-Cl cotransporter result in lower sodium reabsorption	**Gitelman syndrome ;** low blood pressure with elevated plasma renin	#263800	Potassium and magnesium supplement, NaCl intake
16q22.1	*HSD11B2*	Autosomal recessive	Loss of function mutations in HSD11B2 leads to inefficient conversion of cortisol to cortisone	**Apparent Mineralocorticoid Excess** low-renin hypertension associated with low aldosterone, metabolic alkalosis, hypernatremia, and hypokalaemia	#218030	Spironolactone, dexamethasone
17q21.2	*WNK4*	Autosomal dominant	Loss of function mutations in *WNK4* results in salt retention via sodium and potassium transporters	**Pseudohypoaldosteronism type IIB Gordon's syndrome;** hypertension with low plasma renin, normal or elevated potassium	#614491	Thiazide diuretics, low-sodium diet
tRNA	tRNA(Ile)	Mitochondrial	Loss of mitochondrial function	hypertension, hypercholesterolemia and hypermagnesemia	#500005	-

Notice: OMIM: Online Mendelian Inheritance in Man (http://www.omim.org/).

These discoveries in monogenic hypertension and resulted in new understanding of blood pressure regulation. However, these rare Mendelian blood pressure phenotypes account for less than 1% of human hypertension and in the main these genes have not been found to be associated with common forms.[56]

1.4 Essential hypertension and GWAS

Linkage analyses are very effective in identifying Mendelian forms of hypertension that are determined by rare alleles with large effect size. [57] However, the vast majority of the genetic contribution to blood pressure remains unexplained. This is probably

because of the complexity of the trait and the likelihood that blood pressure variation in the general population is determined by many genes that each have a modest effect and low penetrance.[43] Thus, very large sample sizes are needed to identify the possible variants using some approaches. Over the past few years, genome-wide association studies (GWAS) have begun to identify the primary genetic loci of hypertension. As compared to linkage analysis, GWAS provides a more powerful method of identifying the associated variants that underlie susceptibility to common disease, including hypertension,[58] and the science community has more interest in the complex haplotype-based association studies.[24]

This approach has the advantage of being an unbiased and comprehensive search across the genome for susceptibility of alleles. For instance, by allowing the recruitment of unrelated individuals and increasing the mapping resolution, GWAS provides a potential to discover novel candidate genes not identified through other methodological approaches.[36] From 2007, there have been several large-scale GWAS of blood pressure. The major genetic analysis in these studies focused on SBP and DBP as quantitative traits and there are tight correlation of two variables based on significant overlap between the genetic regions associated with SBP and DBP.[59,60]

In principle, GWAS tests for differences in allele frequency between cases and controls in unassociated individuals.[61] If a particular allele occurs more frequently in individuals with the disease (cases) than in those without the disease (controls), then the region or gene loci that the marker (typically single nucleotide polymorphism, SNP) lies within is said to be associated with the disease. The tested polymorphism might not the causative one but it will show an association if it is in linkage disequilibrium (LD) with an unknown causative, risk or protective variant. Thus these SNPs show unequivocal association with BP, the functional dissection of these signals is not

straightforward. For each SNP, an association test is performed yielding a p-value and a regression analysis which estimates its effect size (beta). Most current reports accept an association having a p-value smaller than 5×10^{-8} as genome-wide significant, which is reached by dividing the usual alpha of 0.05 by 1 million (the effective number of tests performed) using "Bonferroni Correction".[62]

1.4.1 Advances in blood-pressure GWAS

Since 2009, a sequential series of large-scale meta-analyses of genome-wide scans for blood pressure in individuals have identified a number of loci for SBP, DBP, pulse pressure (PP) and mean arterial pressure (MAP). A GWAS published in May 2009 reported that 4 loci for SBP and 6 for DBP and rs2681472 located in the plasma membrane calcium-transporting ATPase 1 gene (ATP2B1) is associated with elevation of hypertension.[59] Another study from Global BPgen consortium identified association between systolic or diastolic blood pressure and common variants in 8 regions near the CYP17A1, CYP1A2, FGF5, SH2B3, MTHFR, c10orf107, ZNF652 and PLCD3 genes.[63] Otherwise, the SNP rs13333226 in the promoter of the uromodulin (UMOD) gene was found associated with a reduction of hypertension and it is an expression SNP (eSNP) possibly decreasing urinary uromodulin excretion.[64]

To date, large GWAS in Europeans have totally reported more than 60 new loci for SBP, DBP, in which alleles have effect size of up to 0.5-1.0mmHg, [60,65–67][68] the summary of genetic variants robustly associated with blood pressure traits see the Table 1.2.

Table 1.2 Summary of genetic variants robustly associated with blood pressure traits.

Chr	SNP ID and dbSNP annotation		Gene locus name	Genes mapped to the locus	Biological function of gene candidate	Study type
1	*rs5068	UTR	*MTHFR-NPPA/NPPB*	*CLCN6, KIAA2013, MTHFR, NPPA*	N/a	GlobalBP GWAS
1	rs880315	INT	*CASZ1*	*CASZ1*	Zinc finger transcription factor necessary for cardiac and vascular morphogenesis.	meta
1	*rs17030613	INT	*ST7L-CAPZA1*	*CAPZA1, MOV10, RHOC, ST7L, WNT2B, PPM1J, LRRN2*	N/a	ICBP GWAS
1	rs2169137	INT	*MDM4*	*MDM4, PIK3C2B, RP11-430C7.4*	N/a	gene-centric
1	rs2004776	INT	*AGT*	*AGT*	Angiotensinogen is a liver-synthesised pro-peptide for angiotensin and angiotensin II, and a substrate for renin.	gene-centric
2	*rs16849225	INR	*FIGN-GRB14*	-	Region contains putative lincRNA of unknown function.	meta
2	rs16823124	INT	*PDE1A*	*PDE1A*	Ca^{2+}/calmodulin-dependent cyclic nucleotide phosphodiesterase	gene-centric
3	*rs1717027	INT	*ULK4*	*ULK4, TRAK1*	N/a	CHARGE GWAS
3	rs13082711	INR	*SLC4A7*	*SLC4A7, NEK10*	N/a	CHARGE GWAS
3	rs419076	INT	*MECOM*	*MECOM*	A transcriptional regulator and oncoprotein involved in hematopoiesis, apoptosis, development, and cell differentiation/proliferation.	ICBP GWAS
3	rs319690	INT	*MAP4*	*CSPG5, DHX30, MAP4, SMARCC1*	N/a	meta
3	rs347591	INT	*HRH1*	*HRH1, ATG7*	N/a	gene-centric

4	*rs16998073	INR	*FGF5*	-	Locus associated with intergenic region. Closest gene encodes an oncogene and key regulator of human hair growth.	GlobalBP GWAS
4	rs13107325	NS	*SLC39A8*	*SLC39A8*	Member of solute carrier family demonstrating divalent cation transport properties.	ICBP GWAS
4	rs13139571	INT	*GUCY1A3-GUCY1B3*	*GUCY1A3*	Subunit of guanylaye cyclase which catalyzes conversion of GTP to cGMP.	ICBP GWAS
4	rs6825911	INR	*ENPEP*	-	Locus associated with intergenic region. Closest gene encodes an ectopeptidase, expressed in nephrons with catabolic role in RAS.	meta
4	rs871606	INR	*CHIC2*	*FIP1L1*	A subunit of the cleavage and polyadenylation specificity factor complex that polyadenylates 3' end of mRNA precursors.	meta
5	*rs1173771	INR	*NPR3*	-	Locus associated with intergenic region. Closest gene encodes natriuretic peptide receptor 3.	ICBP GWAS
5	*rs11953630	INR	*EBF1*	-	Locus associated with intergenic region. Closest gene encodes a transcriptional activator COE1.	ICBP GWAS
6	rs805303	INT	*PRRC2A*	*PRRC2A, BAG6, GPANK1, CSNK2B, LY6G5B, ABHD16A, LY6G6F, C6orf25, DDAH2, MSH5, SAPCD1, VWA7, HSPA1A*	N/a	ICBP GWAS
6	rs1799945	NS	*HFE*	*HFE, HIST1H2AC, HISTH1T,*	N/a	ICBP GWAS

				HIST1H2BC, HISTH4C		
6	rs6924906	INR	-	*FAM46A*	Locus associated with intergenic region. Closest gene encodes a retina-expressed gene product of unknown function.	meta
6	rs13209747	INR	*RSPO3*	*RSPO3*	A soluble protein implicated in Wnt/ beta-catenin signalling.	meta
6	rs17080102	INT	*PLEKHG1*	*PLEKHG1*	Promotes protein-bound GDP to GTP exchange and activation of Rho, modulating cytoskeleton remodelling	meta
6	rs2854275	INT	*HLA-DQB1*	*HLA-DQB1, HLA-DRB1, HLA-DRB3, HLA-DOB*	N/a	gene-centric
7	rs3918226	INT	*NOS3*	*NOS3*	Enzyme catalysing L-arginine conversion to NO, a vasomotor tone and blood flow regulator.	gene-centric
7	*rs17477177	INT	*PIK3CG*	-	Locus associated with intergenic region. Closest gene encodes kinase protein mediating signalling regulating cell survival, proliferation, and motility.	meta
7	rs17428471	INR	*EVX1-HOXA*	-	Locus associated with intergenic region. Closest gene encodes a transcriptional repressor functioning during embryogenesis	meta
7	rs2949837	INR	*IGFBP3*	-	Locus associated with intergenic region. Closest gene encodes an insulin-like growth factor binding protein found in human endothelia.	meta
7	rs2282978	INT	*CDK6*	*CDK6, ERVWE1, GATAD1, PREX1*	N/a	gene-centric
7	rs10224002	INT	*PRKAG2*	*PRKAG2, NUB1,WDR86*	N/a	gene-centric

8	*rs2898290		*BLK-GATA4*	*C8orf14, BLK, C8orf8, C8orf12, C8orf13, C8orf16, C8orf49, CTSB, FDF1, GATA4, MTMR9, NEIL2, TDH, XKR6*	N/a	meta
8	rs2071518	UTR	*NOV*	*NOV*	A small secreted cysteine-rich regulatory protein which associates with ECM and plays a role in CV, skeletal, fibrosis and cancer development.	meta
8	rs12541063	INT	*MIR30D*	*MIR30D*	Small, non-coding RNA derived from miR30 precursor. miR30 members are highly expressed in the heart.	meta
8	rs2446849	INR	*CDH17*	-	Locus associated with intergenic region. Closest gene encodes a protein which is a cadherin-like, calcium-dependent, membrane-associated glycoprotein.	meta
10	*rs4373814	INR	*CACNB2*	*CACNB2*	Encodes the obligatory subunit for function of voltage-gated Ca^{+2} channel also associated with Bruguda syndrome.	CHARGE GWAS
10	*rs1530440	INT	*C10orf107*	*C10orf107*	Unknown	GlobalBP GWAS
10	rs932764	INT	*PLCE1*	*PLCE1*	Catalyses hydrolysis of polyphosphoinositides to initiate second messenger signalling cascades influencing cell differentiation.	ICBP GWAS
10	*rs1801253	INR	*ADRB1*	*ADRB1*	Encodes adrenergic receptor subtype beta 1 that mediates the physiological effects of neurohormone epinephrine	meta

10	rs7088591	INR	*IPMK*	-	Locus associated with intergenic region. Closest gene encodes inositol phosphate multikinase involved in intracellular secondary messenger pathways.	meta
10	*rs3824755	INT	*CYP17A1-NT5C2*	*AS3MT, C10orf32, CNNM2, NT5C2, CYP17A, C10orf26, INA*	N/a	CHARGE GWAS
10	rs4746172	INT	*VCL*	*ADK, AP3M1, VCL*	N/a	gene-centric
11	rs381815	INT	*PLEKHA7*	*PLEKHA7*	This protein is part of the adherents' junction complex regulating cell-cell interactions.	CHARGE GWAS
11	rs7129220	INT	*ADM*	*SBF2, ADM, AMPD3, SWAP70*	N/a	ICBP GWAS
11	rs633185	INT	*FLJ32810-TMEM133*	*ARHGAP42*	Encodes smooth-muscle specific RhoGAP regulating RHOA and tissue's contractility.	ICBP GWAS
11	rs661348	INT	*LSP1*	*LSP1, TNNT3*	N/a	gene-centric
11	rs11222084	INR	*ADAMTS8*	*ADAMTS8*	The enzyme metalloproteinase encoded by this gene contains two C-terminal TS motifs, and disrupts angiogenesis in vivo.	meta
11	*rs1401454	INT	*SOX6*	*SOX6*	Transcription factor binding to a specific DNA sequence. Involved in cardiac and skeletal muscle development.	meta
11	rs11041530	INR	*PPFIBP2*	*PPFIBP2, CYB5R2*	N/a	meta
11	rs217727	INR	*H19*	*H19, LSP1, MRPL23, TNNT3*	N/a	gene-centric
11	rs757081	NS	*NUCB2*	*NUCB2, ABCC8, KCNJ11, PIK3C2A, PLEKHA7, RPS13*	N/a	gene-centric

11	rs3741378	NS	*RELA*	*RELA, SIPA1, KAT5,*	N/a	gene centric
12	*rs17249754	INT	*ATP2B1*	*ATP2B1, POC1B*	N/a	CHARGE GWAS
12	*rs3184504	NS	*SH2B3-ATXN2*	*ATXN2, C12orf47, SH2B3, TRAFD1, PTPN1, C12orf51, ACAD10, NAA25, BRAP,ERP29,ALDH2*	N/a	CHARGE GWAS
12	*rs2384550	INR	*TBX3-TBX5*	-	Transcriptional repressor implicated in blood vessel development and cardiomyocyte cell fate determination.	CHARGE GWAS
12	rs11066289		*RPL6-ADLH1*	*HECTD4*	Encodes E3 ubiquitin-protein ligase which transfers conjugated ubiquitin from enzyme to substrate.	meta
12	rs7297416	INT	*HOXC4*	*HOXC4, HOXC5, HOXC6, HOXC8, HOXC9*	N/a	gene-centric
13	rs2315885	INR	*MIR5007*	*miR1297*	Locus associated with intergenic region encoding small non-coding RNAs that regulate post-transcriptional gene expression. This miR has been associated with oncogenesis.	meta
15	rs1378942	INT	*CYP1A1-CSK-ULK3*	*CPLX3, CSK, CYP1A2, LMAN1L, COX5A, ULK3, C15orf17, MPI, SCAMP5, RPP25, PPCDC*	N/a	GlobalBP GWAS
15	rs2521501	INT	*FES-FURIN*	*FES, FURIN*	N/a	ICBP GWAS
15	rs1036477	INT	*FBN1*	*FBN1, CEP152, DUT, SLC12A1*	N/a	gene-centric

16	rs13333226	-	*UMOD*	*UMOD*	Most abundant glycoprotein in normal urine. It localises to nephrons' distal tubules. Known to influence kidney stone formation.	extreme case control study
16	rs33063	INT	*NFAT5*	*NFAT5, WWP2*	N/a	gene-centric
17	rs12946454	INT	*PLCD3*	*HEXIM1, HEXIM2, PLCD3, ACBD4, DCAKD, NMT1*	N/a	GlobalBP GWAS
17	*rs16948048	INT	*ZNF652*	*LOC102724596, ABI3, B4GALNT2, PHOSPHO1, ZNF652*	N/a	GlobalBP GWAS
17	rs17608766	INT	*GOSR2*	*GOSR2, RPRML, CDC27*	N/a	ICBP GWAS
20	rs1327235	INR	*JAG1*	-	This locus is associated with intergenic region. The nearest gene encodes ligand for receptor notch 1.	ICBP GWAS
20	*rs6015450	INT	*GNAS-EDN3*	*ZNF831, C20orf174*	N/a	ICBP GWAS

Note: INT – intronic, INR – intergenic, NS – non synonymous, UTR – untranslated region. (*) denotes the first published SNP in instances where more than one rs number has been reported to be associated with a given gene locus.

1.5 Blood-pressure associated SNPs at *NPR3* gene locus

1.5.1 rs1173771 linkage disequilibrium block

Recently, the International Consortium for Blood Pressure Genome-Wide Association Studies (ICBP-GWAS) identified 29 variants associated with SBP, DBP or both from more than 200,000 individuals of European descent. Among those variants, is the index SNP rs1173771 (G/A) located at the natriuretic peptide receptor C (*NPR3)* locus. The major allele, G allele, is found to be associated with elevation of blood pressure. Its per-allele effect size is 0.504 mmHg for SBP and 0.261 mmHg for DBP (Figure 1.4).[65]

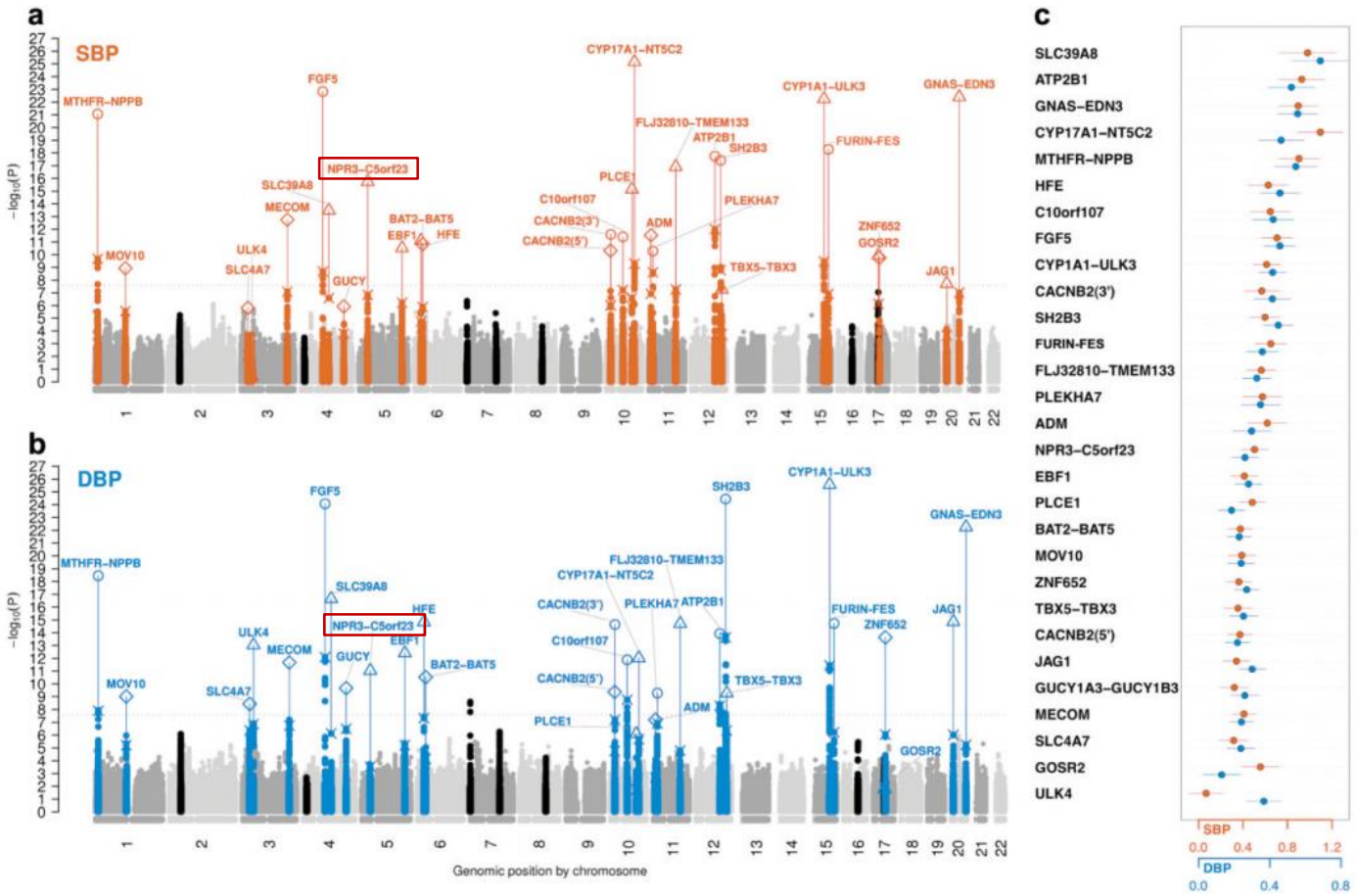

Figure 1.4 Genome-wide –log$_{10}$ *P*-value plots and effects for significant loci.

NPR3-C5orf23 locus is marked with red rectangle.[65]

SNP rs1173771 is an intergenic variant, 20 kb downstream flanking the gene coding for *NPR3*. It is in high linkage disequilibrium (LD) (r^2>0.75) with 14 SNPs in CEU population and 25 SNPs in CHB and JPT population in a 100kb sequence encompassing the *NPR3* gene according to the 1000 Genomes Project. In those SNPs, three are located at *NPR3* gene involving a 3 untranslated region (3' UTR) SNP and two intronic SNPs. The remaining are intergenic SNPs located downstream of *NPR3*.

Kato et al also identified a SNP rs1173766 (C/T) in 3' flanking region of *NPR3* ($P=1.9\times10^{-8}$ for SBP; $P=1.2\times10^{-7}$ for DBP) in a blood pressure GWAS in 19 414 subjects of East Asians,[69] a finding replicated by de novo genotyping in 10 461 Japanese subjects. This SNP is highly associated with rs1173771 (r^2=1.0 in CHB+JPT), and this supports the finding that SNP rs1173771 is a blood-pressure-associated SNP.

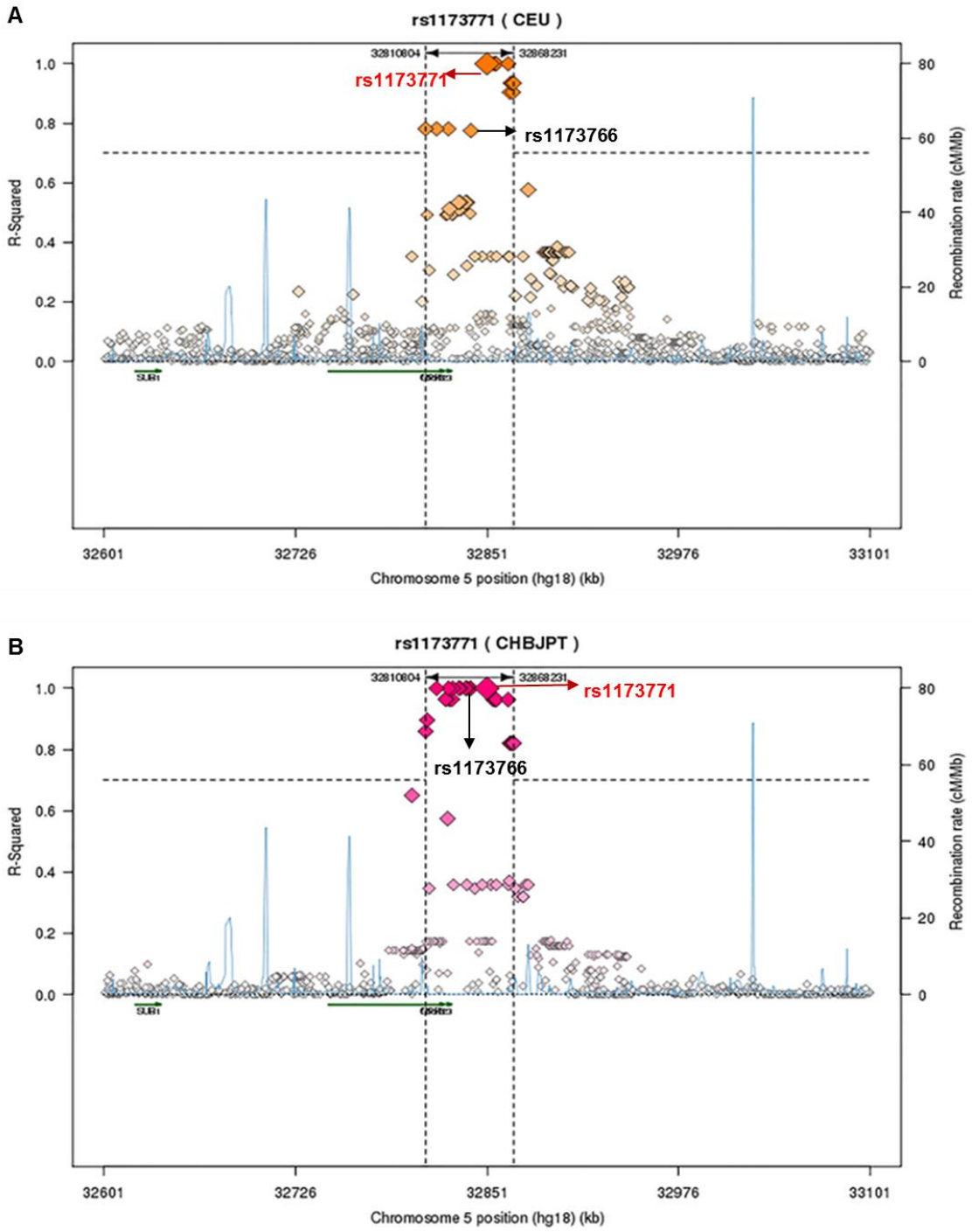

Figure 1.5 Regional plots of SNP rs1173771 in CEU (A) and CHB+JPT (B) at the *NPR3* locus.

SNPs (including rs173766) between the horizontal dashed lines are in high linkage disequilibrium (LD) (R-squared is 0.7) with SNP rs1173771 from the 1000 Genomes Project.

1.5.2 rs1421811 linkage disequilibrium block

In addition, an association of the intronic SNP rs1421811 with hypertension susceptibility was observed using a bespoke gene-centric array at the study-specific significance threshold of $p < 8.56 \times 10^{-7}$, and effect size for its minor allele (G) is −0.67mmHg in SBP.[70] SNP rs1421811 is an intronic variant located at *NPR3* intron 1. It is in high LD (r^2>0.7) with 20 SNPs in CEU population and 25 SNPs in CHB and JPT population in a 100kb sequence encompassing the NPR3 gene according to the 1000 Genomes Project (Figure 1.6). SNP rs1421811 is in low LD with rs1173771 (r^2=0.13 in CEU; r^2=0.05 in CHB+JPT).

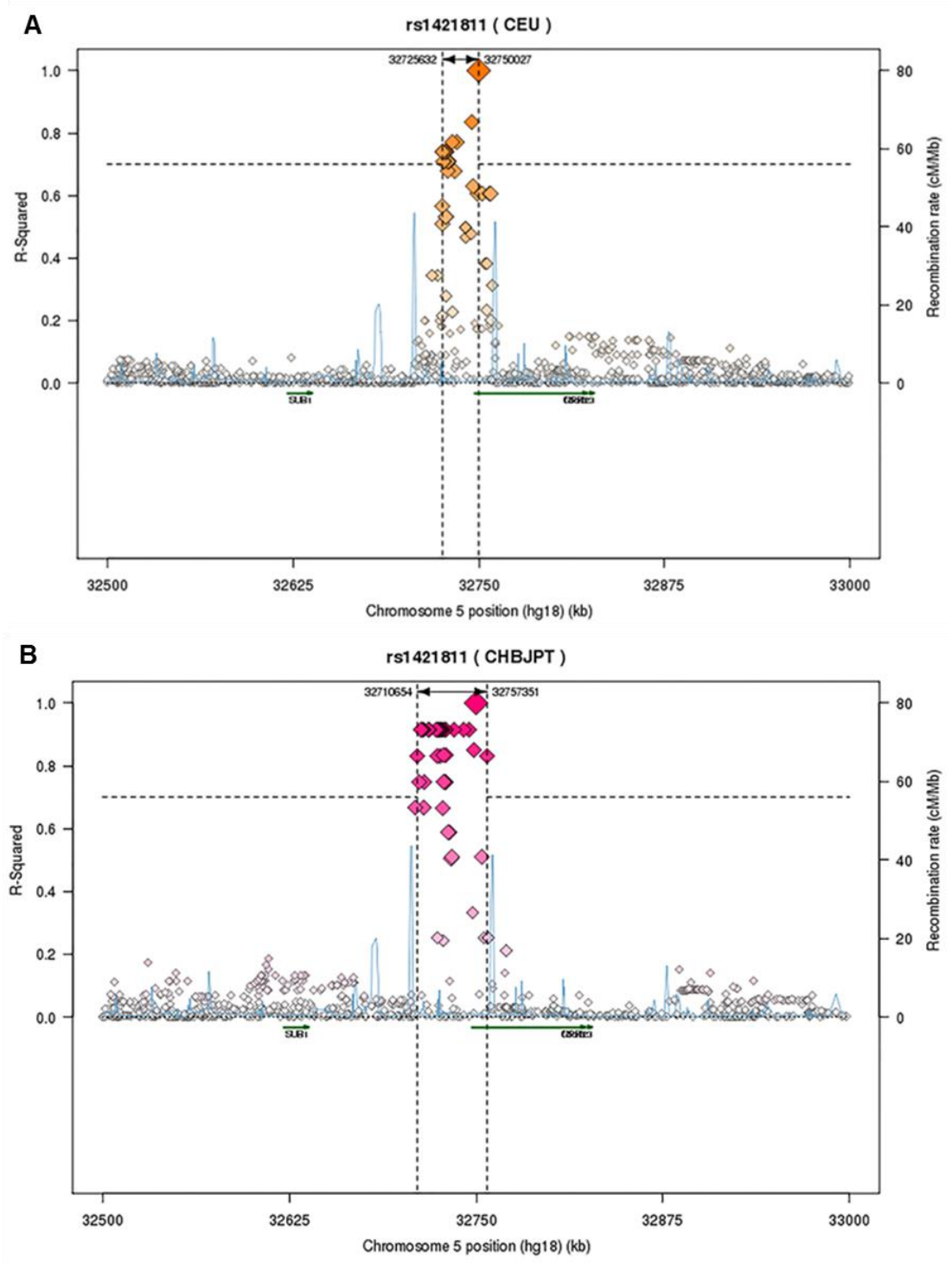

Figure 1.6 Regional plots of SNP rs1421811 in CEU (A) and CHB+JPT (B) at the *NPR3* locus.

SNPs between the horizontal dashed lines are in high linkage disequilibrium (R-squared is 0.7) with SNP rs1421811 from the 1000 Genomes Project.

In total, SNPs in these two LD blocks are mainly non-coding variants including the intronic and intergenic SNPs. As indicated in section 1.3.2, there is one possibility that these SNPs might be located in the regulatory elements interacting with transcriptional factors, or impacting alternative splicing, then influence gene expression, subsequent protein function and BP-related phenotypes.

1.6 NPR-C signalling system and regulation

1.6.1 NPR-C

The *NPR3* gene is located on human chromosome 5p14-p13. It has 8 exons, 7 transcripts, and finally translated 3 subtypes of natriuretic peptide receptor C (NPR-C). Subtype 1 (541aa) and 2 (540aa) are found to be functionally present in a variability of tissue and cells including vasculature.[71] NPR-C is composed of disulfide-linked homodimers of a single transmembrane 64–66 KDa protein. It contains a large extracellular domain of about 440 amino acids which is homologous to NPR-A and NPR-B, a single membrane-spanning domain and of a short cytoplasmic tail of 37 amino acids.[72] Its cytoplasmic domain contains a G_a inhibitory protein-activating sequence.[73] NPR-A and NPR-B can activate guanylyl cyclase, but NPR-C does not demonstrate guanylyl cyclase activity.[74] NPR-C is the most abundantly expressed NPR, comprising up to 95% of the total amount of NPR, and has similar affinity for all natriuretic peptides (NPs).[75] NPR-C is distributed widely in several cells and issues including vascular smooth muscle cells and mesangial cells,[76,77] the major endocrine glands, lungs, kidneys and the vascular wall including endothelium.[78]

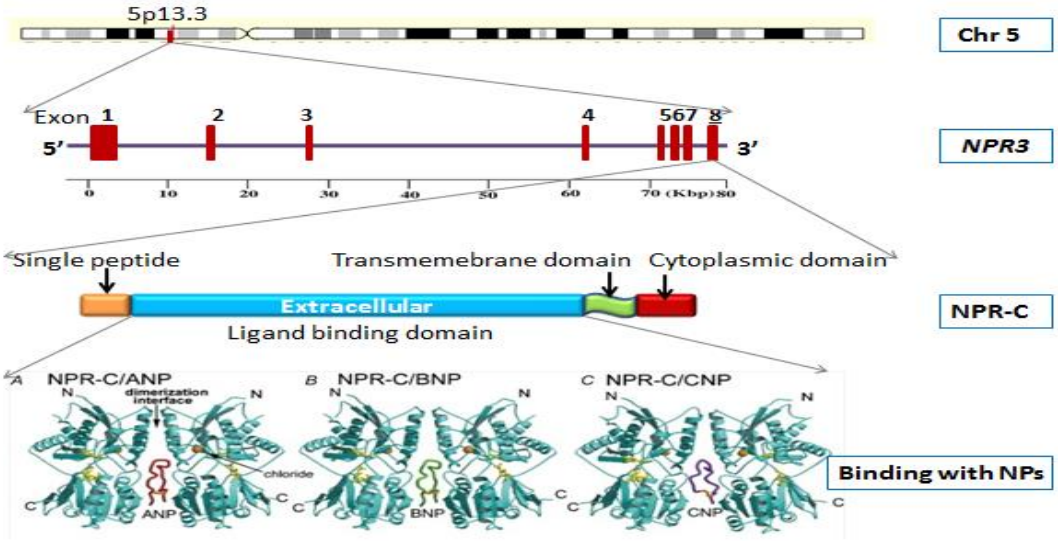

Figure 1.7 Structure of *NPR3* gene and its protein NPR-C.
NPR-C was coded by *NPR3* gene and its extracellular domain / ligand binding domain could bind with all natriuretic peptides (NPs) [75].

1.6.2 NPR-C associated signalling pathways

At the time of its discovery, NPR-C was primarily considered to be a systemic clearance receptor, removing natriuretic peptides (NP) from the circulation.[75,79] Binding of NP to NPR-C leads to internalization and removal of the peptides from blood.[73] However, accumulating evidence has modified the initial view and suggested a separate/different physiological role of NPR-C. It has since been demonstrated to be coupled to the adenylyl cyclase/cAMP signal transduction system through inhibitory guannine nucleotide regulatory protein (G_i) and elicits physiological function.[80–82] The cytoplasmic domain of NPR-C contains several G_i activator sequences which could bind and activate G_i regulatory protein.[83] The α subunit of this Gi protein inhibits adenylyl cyclase, resulting in lower intracellular formation of cAMP. [84] This inhibitory effect is supported by the application of C-ANF_{4-23}, a synthetic agonist of NPR-C, which inhibits adenylate cyclase activity in anterior pituitary, aorta, brain striatum and adrenal cortex in a concentration-dependent manner without

affecting cGMP levels.[81] In other words, NPR-C is a negative regulator of adenylate cyclase/cAMP system, whereas both NPR-A and NPR-B are coupled to guanylate cyclase/cGMP system.[72]

Moreover, when the Gi protein is activated, its β/γ subunit activates phospholipase C (PLC) and stimulates phosphatidyl inositol (PI) turnover in bovine and A10 vascular smooth muscle cells.[85] Stimulation of NPR-C has been found to inhibit vascular smooth muscle cell proliferation through mitogen-activated protein kinase (MAPK) and PI3-kinase pathways.[86] NPR-C has also been implicated in the modulation of other signalling pathways. Murthy *et al.* has shown NPR-C activation by C-ANF$_{4-23}$ can result in the activation of constitutive nitric oxide synthase (NOS) via $G_{i\alpha1}$ and $G_{i\alpha2}$ in gastrointestinal smooth muscle.[87] Furthermore, NPR-C binding to CNP or C-ANF$_{4-23}$ has been shown to inhibit L-type Ca^{2+} current (ICa,L) without modulating other voltage-gated Ca^{2+} currents in mouse atrial, ventricular, and sinoatrial node myocytes.[88]

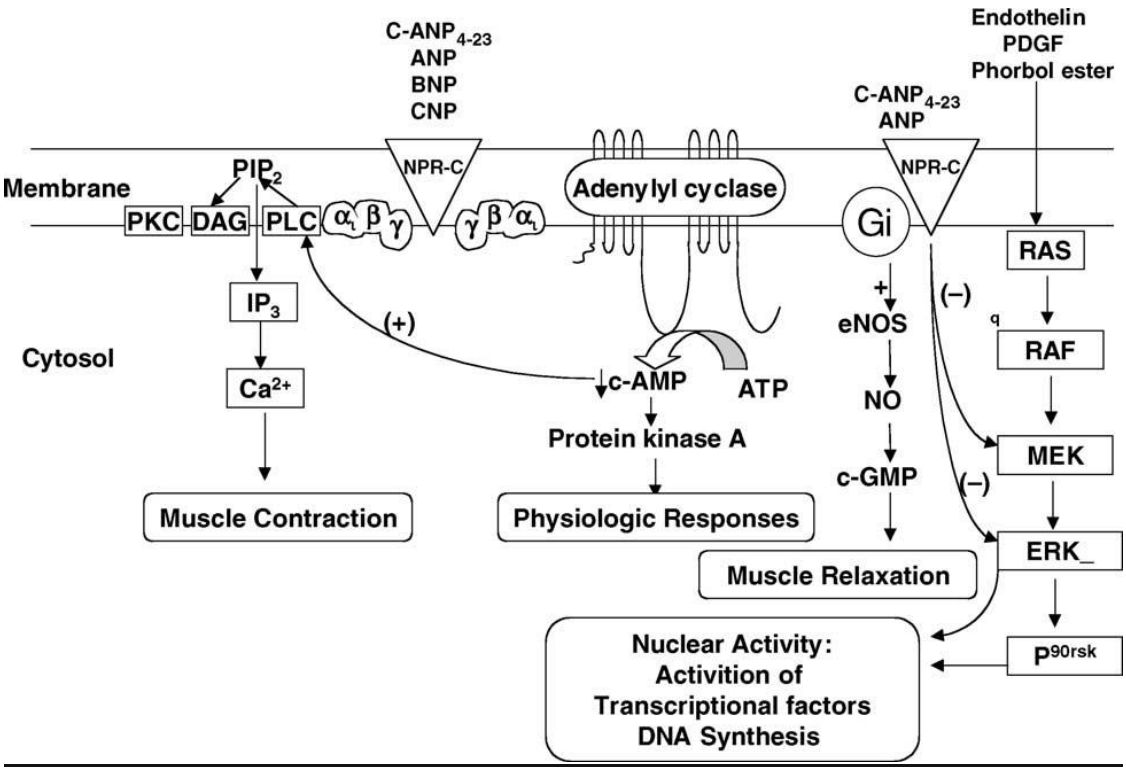

Figure 1.8 Summary of NPR-C-coupled signalling systems.

Natriuretic peptide (NP) receptors and associated signal transduction mechanisms activated by different natriuretic peptides. NPR-C, which is coupled to adenylyl cyclase through Gi protein. C-ANF$_{4–23}$, ANP, BNP, and CNP interact with this receptor and inhibit adenylyl cyclase activity and suppress cAMP concentrations.[72]

1.6.3 Regulation of NPR-C expression

NPR-C expression has been showed to be influenced under various conditions and by a variety of hormonal factors. Chabrier *et al.* found a down-regulation of NPR-C by the treatment of angiotensin II (Ang II) in rat vascular smooth muscle cells (VSMCs).[89] Similarly, Yasimoto *et al.* showed Ang II treatment induced a decrease of NPRC mRNA levels in cultured rat aortic smooth muscle cells, whereas NPRA and NPRB were not alternated by this treatment.[90] Other pro-hypertensive peptides, such as endothelin (ET-1) and arginine–vasopressin (AVP) have also been demonstrated to modulate NPR-C receptor expression. It is showed pre-treatment of endothelin (ET-1) attenuated NPR-C protein expression by about 60% in A-10 SMCs,[91] and was also

decreased by about 50% by AVP treatment in A-10 SMCs.[72] Moreover, norepinephrine or isoproterenol could also down-regulate NPR-C density mediated by the activation of the beta 2-adrenergic receptor, as the effect was blocked only by a antagonized by a beta 2-selective adrenergic antagonist, but not by an alpha 1-, alpha 2-, or beta 1-adrenergic antagonists in rat VSMCs.[92] Treatment of vascular endothelial cells with NaCl resulted in a marked reduction in the number of NPR-C, which may be related to the clearance function of NPR-C.[93] It is also revealed that fibroblast growth factors (FGF-1 and FGF-2) and platelet-derived growth factor-BB (PDGF-BB) that activate tyrosine kinase receptors can reduce expression of NPR-C in PASMCs.[94] In addition, nitric oxide (NO) was demonstrated to decrease the expression of natriuretic peptide receptor C (NPR-C) and adenylyl cyclase signalling in A10 SMC through cGMP-independent but MAPK-dependent pathway.[95] However, transforming growth factor-1 (TGF-1) has been reported to augment the expression of NPR-C at the transcriptional level in a murine thymic stromal cell line (MRL 104.8a) [96] and glucocorticoids could also increase NPR-C density on human cultured mesangial cells.[97]

Table1.2 Hormonal factors for regulating NPR-C.

Down-regulate	Up-regulate
Ang II, ET-1,AVP, NO, NaCl, isoproterenol FGF-1,FGF-2,DDGF-BB	TGF-1 Glucocorticoids

NPR-C is also regulated by various pathophysiological states. It is demonstrated fasting inhibits NPR-C expression in rat adipose tissue.[98] Several groups have shown that acute and chronic hypoxia cause the down-regulation of *NPR3* gene expression and binding in rat lung without affecting other NPRs.[99–101] Nagase *et al.* demonstrated that *NPR3* gene expression was selectively attenuated in the kidney

by chronic salt loading in Dahl salt-sensitive and salt-resistant rats.[102] More recently, it is indicated that the gene expression of NPR-C in aortic tissue of spontaneously hypertensive rats (SHR) was higher than that in normal rats(WKY).[103]

1.6.4 NPR-C and diseases

1.6.4.1 Hypertension

When physiologically activated (as described in Figure 1.8), NPR-C seems to exert protective vascular effects, suggesting a direct anti-hypertensive role. Indeed, a great deal of evidence has supported this. A lower NPR-A / NPR-C ratio is observed in obese hypertensive patients. This might result in a down-regulation of biological activity and/or an up-regulation of clearance of natriuretic peptide in adipose tissue, and plays an important role in obesity-associated hypertension.[104] An increased ANP receptor density has also been reported in cultured VSMC from spontaneously hypertensive rats (SHR) and other models of experimental hypertension suggesting that increased plasma levels of ANP in hypertension, may result in the down-regulation of NP receptors.[105] Nagase, Ando et al revealed that there is an exaggerated reduction of NPR-C number in the kidney in response to salt loading in Dahl salt-sensitive rats, suggesting a role of NPR-C in pathogenesis associated to renal sodium excretion in salt hypertension in this animal model.[102]

Moreover, it is demonstrated C-ANF_{4-23} (a specific synthetic NPR-C receptor agonist) increased nitric oxide synthase (NOS) activity in cardiac ventricle and atria, renal medulla and cortex and aorta artery, and ANP would interact with NPR-C coupled via Gi to activation Ca^{2+} -dependent NOS.[106] CNP/NPR-C signalling has also been revealed as an important pathway which underlies endothelium-derived hyperpolarizing factor (EDHF)-dependent regulation of vascular tone in the rat

mesenteric resistance arteries and in the coronary vasculature.[107] Li, et al. reported that the gene expression of NPR-C in aortic tissue of spontaneously hypertensive rats (SHR) was higher than that in normal rats(WKY).[103] In general, human hypertension is recognised as a state of NPR-C deficiency.

Recently, a downstream SNP located at the natriuretic peptide receptor C (*NPR3)* locus has been identified as associated with hypertension by International Consortium for Blood Pressure Genome-Wide Association Studies (ICBP-GWAS).[108] A separate combined study of admixture mapping and association analysis found an upstream SNP near *NPR3* being associated with SBP and DBP.[109] Furthermore, an intronic SNP in *NPR3* gene is reported with a gene-centric array.[110] This additional evidence also implies a potential role of *NPR3*/NPR-C in regulation of hypertension.

1.6.4.2 Cardiovascular atherosclerosis and myocardial infarction

NPR-C has also been implicated in the regulation of proliferative processes through various experimental *in vitro* studies. In particular, an anti-proliferative action has been described in smooth muscle, endothelial and astroglial cells.[111,112] NPR-C was strongly expressed in the neointimal SMCs, and seems to be important in controlling neointimal growth after percutaneous trans-luminal revascularization (PCI).[113] This is further supported by immunohistochemistry and immunofluorescence staining showed NPR-C near the luminal surface of the atherosclerotic plaque and in VSMCs.[114]

Hobbs et al. have showed binding of CNP to NPR-C could contribute to maintain coronary perfusion of myocardium and that activation of this molecular mechanism could protect against the ischemia/reperfusion (I/R) injury by reducing the infarct size in the rat model.[115] Thus, CNP/NPR-C signalling pathway may be viewed as important

in cardiovascular homeostasis. In addition, the mRNA levels of NPR-C were augmented in both the infarcted and non-infarcted regions of the left ventricular wall (LV), while it was decreased in the kidneys and lungs 28 days after MI.[116] It has also been demonstrated that low levels of the natriuretic peptides preferentially activate NPR-C and increase cardiomyocyte proliferation through inhibition of adenylate cyclase.[117]

1.6.4.3 Obesity

NPR-C has been identified to be highly expressed in adipocytes and adipose tissue, and is stimulated by a high fat diet, and conversely suppressed by fasting.[98,118,119] In addition, NPR-C gene expression in adipose tissue is higher in obese hypertensive than in obese normotensive subjects.[104] It has been reported that insulin, an antilipolytic hormone, significantly increased *NPR3* mRNA levels through the phosphatidylinositol 3-kinase (PI3-kinase) pathway.[118] NP receptors in adipose tissue are also under estrogenic control. Higher NPR-C gene expression is found in mesenteric adipose tissue and in the kidneys in the overweight estrogen-deficient follitropin receptor knockout mice, which could be associated with obesity and hypertension.[120]

1.6.4.4 Growth abnormality

Matsukawa, Grzesik et al found mice with *NPR3* gene disrupted (*Npr3* -/-) had a high rate of mortality(more than 50%) compared with other genotypes during growth before reproducing, and exhibited striking skeletal deformities with abnormal long bone growth and chondrocytes.[121] mRNA for *NPR3* is readily detected in osteoblasts and 1,25 dihydroxyvitamin D3, a key regulator of mineral metabolism, significantly increased *NPR3* mRNA in osteoblastic cells,[122] indicating a role for NPR-C in regulation of growth. Another study confirmed that mice that carry a mutation in *NPR3*

gene exhibited a skeletal overgrowth phenotype, resulting in an elongated body and kyphosis.[123]

A recent GWAS study indicated a SNP located on 5p14, 100 kb upstream of *NPR3* gene is associated with body height. Apart from *NPR3* locus, another SNP only away 6kb of natriuretic peptide precursor type C (*NPPC*) gene, which encodes CNP, is also found to be associated with overgrowth and skeletal abnormalities.[124] CNP is also revealed as a molecule that regulates endochondral ossification of the cartilaginous growth plate, resulting in longitudinal bone growth.[125] Thus, it might suggest CNP/ NPR-C signalling system represents an important pathway involved in determining of bone growth and height variation in humans.

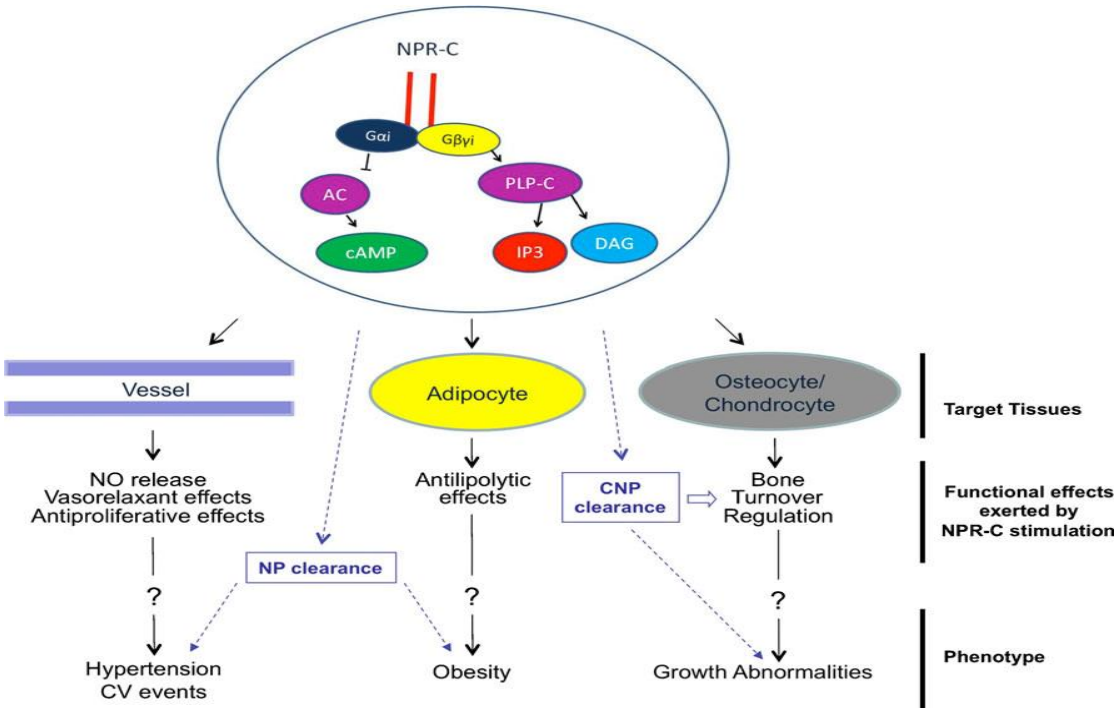

Figure 1.9 Schematic description of the intracellular mechanisms activated by NPR-C stimulation.

the direct effects (continuous lines) possibly exerted on main target tissues and the consequent potential contribution to pathological phenotypes.[126]

1.7 CNP/NPR-C signalling transduction system and hypertension

C-type natriuretic peptide (CNP) belongs to a family of natriuretic peptides and plays an important role in the cardiovascular homeostasis.[127,128] CNP is present in a high concentration in peripheral tissues, particularly vascular endothelial cells.[128–131] The relatively high expression of CNP in the vascular endothelial cells and the presence of its receptors NPR-C on the underlying smooth muscle cells, suggests that this peptide has the capacity to affect vascular tone. Indeed, local infusion of CNP increases the forearm blood flow, an effect that is independent from nitric oxide (NO).[131] Recent studies have revealed that the CNP/NPR-C signal transduction system is an important pathway in the regulation of peripheral blood flow and CNP acts as an endothelium-derived hyperpolarizing factor (EDHF) inducing relaxation mediated by the NPR-C pathway.[115,132]

Moreover, a facet of the vasoprotective profile of CNP is mediated via NPR-C-dependent ERK 1/2 phosphorylation, resulting in augmented endothelial cell proliferation and inhibition of vascular smooth muscle growth. This pathway may offer an innovative approach to reversing endothelial damage and vascular smooth muscle hyperplasia.[133] NPR-C binding to CNP or C-ANF$_{4\text{-}23}$ has been shown to inhibit L-type Ca^{2+} current (ICa,L) without modulating other voltage-gated Ca^{2+} currents in mouse atrial, ventricular,[88] which subsequently affect vascular contraction and blood pressure control. Indeed, the NPR-C agonist, C-ANF compound 118, caused relaxation of isolated mesenteric resistance arteries, which is inhabitable by NPR-C antagonism. It also promoted a reduction of blood pressure in wild-type mice (ED_{50}<1mg/kg), which could be blunted in NPR-C KO mice.[134]

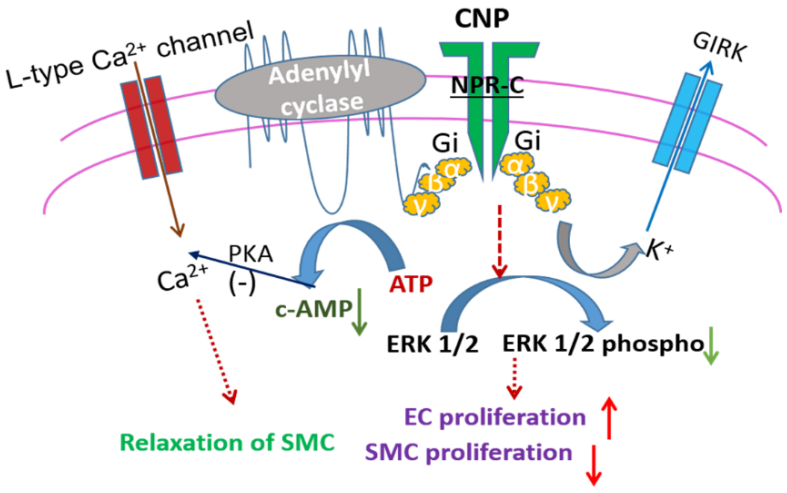

Figure 1.10 Activation of natriuretic peptide receptor (NPR)-C by endothelial CNP underlies a key mechanism regulating vascular tone and local blood flow. NPR-C binding with CNP/c-ANF lead to augmented endothelial cell proliferation and inhibition of vascular smooth muscle growth via ERK 1/2 phosphorylation, and decreased calcium influx. [88 ,133]

To the basic level, hypertension implies an increase in either blood volume or total peripheral resistance (TPR) regulatory influence, thus, any impact or pathway influencing both or either determinant could be associated with pathophysiology of hypertension.

As a candidate for endothelial derived hyperpolarising factor (EDHF), CNP potentially influences the peripheral blood flow and resistance of arteries and arterioles via NPR-C. It is reported CNP infusion reduced MAP in spontaneously hypertensive rats.[135] Skau, Goetze et al found a decrease of plasma pro-CNP concentration in idiopathic intracranial hypertension (IIH), reflecting a role of endothelial deregulation of vascular tone in this disease.[136] In addition, CNP also significantly attenuated the increases in right ventricular (RV) systolic pressure and the ratio of RV weight to body weight in monocrotaline-induced pulmonary hypertension.[137] In a study of age-related

myocardial fibrosis in Fisher rats, there was an inverse relationship between decreasing circulating CNP and increasing LV fibrosis that precedes subsequent reductions in diastolic and systolic function. It was found there was a significant and progressive decrease in plasma CNP from 2 to 11 to 20 months of rats, a modest but significant increase in MAP at 20 months with increasing LV fibrosis, and they also demonstrated that involved anti-proliferative action of CNP/NPR-C on cardiac fibroblasts (CFs).[138]

In summary, as indicated by studies described above, NPR-C/CNP signalling pathway plays an important role in the development of hypertension.

1.8 Original hypothesis

Given the central role of the natriuretic peptide system in cardiovascular homeostasis and association of genetic variants at *NPR3* with blood pressure level, we hypothesised that functional effects of these or nearby variants affect BP via regulating *NPR3* gene expression and its related pathways on cell phenotypes.

1.9 Aims and objectives

The overall aim of this thesis is to investigate the potential functional role of blood-pressure associated variants in *NPR3* gene in the development of hypertension.

Objectives:

1. To investigate effects of BP-associated variations in the *NPR3* gene on *NPR3* RNA and NPR-C protein expression in HUASMCs and HUVECs by quantitative RT-PCR, allelic expression imbalance assay and western blot analysis.

2. To study possible interaction of transcription factors with BP-associated variants at the *NPR3* locus in vitro and in vivo by electrophoretic mobility shift assay, chromatin immunoprecipitation, and formaldehyde-assisted isolation of regulatory elements analysis,

3. To investigate effects of BP-associated variants at the *NPR3* locus in CNP/NPR-C signalling pathway and on calcium flux, migration and proliferation of HUASMCs and HUVECs.

2. Materials & Methods

2.1 Human cell samples

2.1.1 Isolation of human umbilical cords arterial smooth muscle cells (HUASMCs)

VSMC cultures were isolated from human umbilical arteries (Figure 2.1) according to the previous technique[139] and approved by the appropriate ethics committee (08/H0704/140, AM05 Minor Amendment). Briefly, the umbilical cords were collected from The Royal London hospital and preserved in physiological saline solution (PSS) (0.85% w/v NaCl) before isolation. The arteries were isolated surgically from the cords and the tissue minced into small segments. The pieces were plated onto a 0.2 % w/v gelatin- (Sigma, G1890)-coated T25 flasks and incubated in a humidified incubator of 5 % CO_2 at 37^0C for 2 hours standing by, allowing arterial segments attach to the flasks. Then they were cultured in Dulbecco's Modified Eagle Medium (DMEM) (Sigma) supplemented with 20% fetal bovine serum (FBS) (Gibco), 2 mM L-glutamine (Sigma), 100 U/mL penicillin (Sigma) and 100 mg/mL streptomycin (Sigma). The flasks were allowed to stay in the incubator for 7 days until replacement of DMEM medium. After that, cells were detached with 0.25% trypsin-EDTA (Sigma) and sub-cultured to a fresh 0.04% gelatine-coated T25 flask when there was adequate proliferation of cells (70%-80% confluence).

2.1.2 Isolation of human umbilical cords endothelial cells (HUVECs)

Endothelial cells cultures were prepared from human umbilical veins (Figure 2.1) and generously donated by Biochemical Pharmacology at the William Harvey Research Institute. The cells were harvested by methods as previously described.[139] In brief, the umbilical vein was washed with cold phosphate buffered saline (PBS) (137mM NaCl, 2.7mM KCl, 10mM Na_2HPO4, and 2mM KH_2PO4), then injected with 0.1% collagenase (Gibco) and incubated for 30 min. The vessels was purged with PBS

and this PBS containing HUVECs was collected and centrifuged. Cell pellet was suspended in Medium 199 (Sigma) supplemented with 15% fetal bovine serum (Gibco), penicillin-streptomycin (Sigma) and endothelial cell growth factors (2.5μg/ml thymidine, 10 U/ml heparin, 4.5μg/ml endothelial cell growth supplement, 2.5μg/ml human β-endothelial cell growth factor)(Sigma) and cultured in gelatin-coated flasks until growing up to confluence. The cells were then detached by 0.25% trypsin-EDTA, resuspended into new flasks by certain dilution with fresh medium.

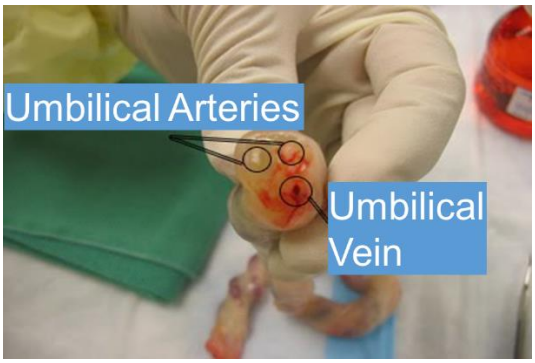

Figure 2.1 Human umbilical cords arteries and vein.

2.1.3 Cell culturing

Once HUASMCs and HUVECs were isolated and harvested, they were both maintained in specific media (see below). For HUASMCs, the culture medium used was DMEM that was supplemented with 15% FBS, 2mM L-glutamine, 100 U/mL penicillin, 100 mg/mL streptomycin and SMCs growth factors (0.5ng/ml recombinant human epidermal growth factor, 2ng/ml recombinant human basic fibroblast growth factor, 5μg/ml recombinant human insulin) (ProSpec). Otherwise, Medium 199 supplemented with 15% FBS, penicillin-streptomycin and endothelial cell growth factors (see section 2.1.2) were used for HUVECs. When the cells were grown up to about 80% confluence, they were detached by 0.25% trypsin-EDTA (Sigma) and sub-cultured into new 0.04% gelatine-coated flasks with fresh medium. Passages 2-

6 of HUASMCs and passages 2-5 of HUVECs were utilised for subsequent functional experiments.

In total, an amount of 282 umbilical cords were collected by the team during three years from 2012-2014. 247 cell samples were successfully obtained with 35 samples failed due to no cells growing or contaminations.

2.1.4 Cell counting using a haemocytometer

Cell counting was performed in several subsequent experiments including cell proliferation, migration and calcium flux assays by utilising haemocytometer. In brief, HUASMCs and HUVECs cell suspension were gently pipetted up and down to ensure the cells are evenly distributed. 10ul of cell suspension was then mixed with equal volume of 0.4% Trypan Blue (Sigma), and subjected at the edge of the coverslip on a pre-cleaned glass haemocytometer.

The live, unstained cells (live cells do not take up Trypan Blue) were counted in one set of 16 squares under a microscope (as shown in Figure 2.2).The cell concentration per ml was calculation by following equation:

Cell concentration = average number of cells in one large square × dilution factor $\times 10^4$

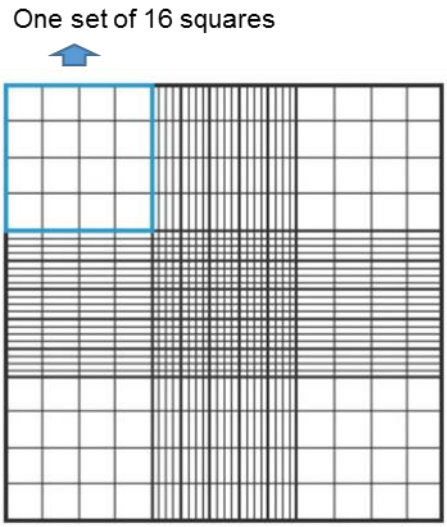

Figure 2.2 Haemocytometer gridlines.
Haemocytometer diagram indicating one of the sets of 16 squares that should be used for counting.

2.1.5 Preservation and recovery of cells

Both HUASMCs and HUVECs were preserved in liquid nitrogen for long term storage. Cells were cultured to confluency, detached by 0.25% trypsin-EDTA and resuspended in freezing medium (80% FBS, 10% dimethyl sulfoxide and 10% DMEM or M199) in cryovials at a concertation of 1X 10^7 cells/ml. To prevent cell death during freezing, cells was preserved in a freezing container (Nalgene® Mr. Frosty) filled with 100% isopropyl alcohol for gradually cooling to -80 °C by -1°C/minute, then was transferred to liquid nitrogen for long term storage.

During the recovery, cells were taken out from liquid nitrogen and transported on dry ice, quickly thawed in a 37°C water bath. Cell pellets was harvested by centrifuging at 1,000g for 5 min at room temperature and suspended into pre-warmed growth medium in new 0.04% gelatine-coated flasks. After incubation at in a humid incubator of 5 % CO_2 at 37^0C overnight, medium was removed and replaced with fresh growth medium.

2.2 Bioinformatics analysis

To explore characteristics of BP-associated SNPs and potential transcriptional factor binding sites (TFBS) or micro RNA interactions, a series of programs and tools were used. The SNAP (SNP Annotation and Proxy Search; http://www.broadinstitute.org/mpg/snap/) based on data from the International HapMap Project was used for exploring BP associated SNPs in high LD in different populations. The UCSC Genomic Bioinformatics database (http://genome-euro.ucsc.edu/; GRCh37/hg19 produced by Genome Reference Consortium), Gene Regulation (http://www.gene-regulation.com/pub/programs.html), were used to investigate potential transcriptional factor binding sites (TFBS) or histone-modification associated with BP-associated variants at *NPR3* locus.

Databases or programs such as TargetScan (http://www.targetscan.org/vert_61/) Micro RNA (http://www.microrna.org/microrna/home.do) and micRWalk v3.0 (http://www.umm.uni-heidelberg.de/apps/zmf/mirwalk/) were used for searching possible micRNA associated with BP associated SNPs at *NPR3* locus. As shown in Table 2.1, the potential transcription factors or histone modifications as well as miRNA were predicated to be associating to BP-associated SNPs in rs1173771 LD block at *NPR3* locus.

Table 2.1 Bioinformatics update about BP-associated SNPs in rs1173771 LD block.

	ENCODE		Other tools
SNP	Cell lines	TFBS/HM	TFBS
rs1173771	HUMM	H3K27AC;H3K27M3	
	HUMM tube	H3K4M1	
	HuVEC	H3K9M3	
rs1173743	HUMM	H3K9M3;EZH2	PAI-2
	HUMM tube	H3K9M3;H3K27M3	P53.05
	HuVEC	H3K9M3	
rs1173747	HUMM		GATA-1
	HUMM tube	H3K27AC;H3K27M3	GR,GR-alpha, GR-beta
	HuVEC	H3K9M3	Y-box binding factor; TCF3
rs1173756	HUMM	H3K9M3; H3K4M1	
	HUMM tube	H3K27AC;H3K27M3;EZH2	
	HuVEC	H3K9M3	

TFBS: transcription factor binding sites; HM: histone modification; HUMM: skeletal muscle myoblasts; HUMM tube: skeletal muscle myotubes differentiated from the HSMM cell line.

2.3 Genotyping (KASPar SNP Genotyping system)

The Kbiosciences Competitive Allelic-specific PCR SNP genotyping system (KASPar) is a fluorescent genotyping system that is cost-effective and widely used. This technique involves two 5'-fluro-labelled oligos, one labelled with FAM, the other with VIC/HEX, and sequences of oligos are designed to interact with the sequences of the tails of allele specific primers. Once dsDNA denature, allele specific primers bind to ssDNA with target SNP and amplify the target region with the common reverse primer,

generating a complimentary copy of target allele tail. New allele-specific tail sequences increase with more cycles, and bind the complementary fluoro-labelled part of FRET cassette, releasing the fluorescence label from its quencher to generate a fluorescent signal.

This method was used investigating genotypes of blood-pressure associated SNPs (rs1173771 LD block and rs1421811 LD block) at *NPR3* gene locus in HUASMCs and HUVECs.

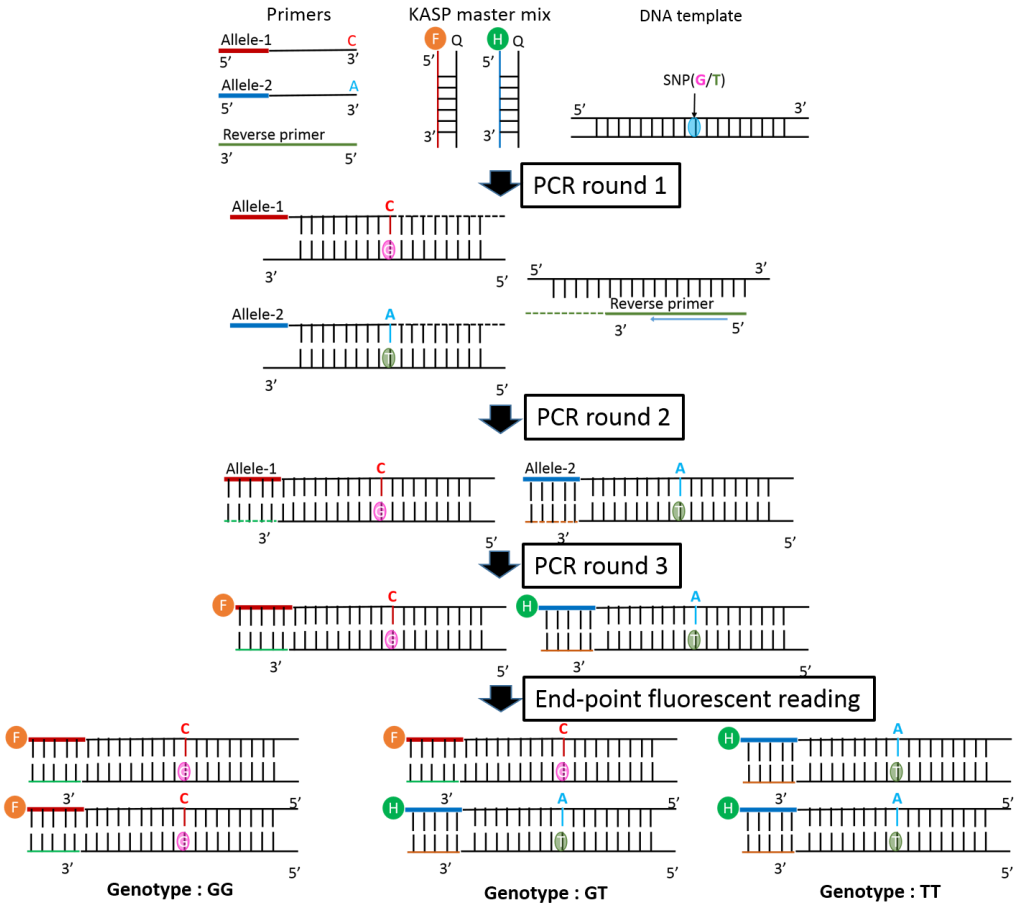

Figure 2.3 Systemic principles of KASPar genotyping system.

KASPar genotyping is a fluorescent genotyping system involving two 5'-fluro-oligos/primers labelled with FAM, or VIC/HEX targeting each allele. After amplification by PCR, clusters representing different genotypes are separated by end-point fluorescent reading. (Modified from: http://www.lgcgenomics.com/genotyping/kasp-genotyping-chemistry/how-does-kasp-work/)

2.3.1 DNA extraction

HUASMCs and HUVECs were harvested from flasks and suspended in 500µl lysis buffer (10 mM Tris pH 8.0, 10 mM EDTA, 100 mM NaCl, 0.5 % SDS), and then 250µl of 5 M NaCl. The samples were mixed until the cells were totally dissolved. The mixture was centrifuged at room temperature for 5 min at 13,000g and the supernatant was removed to a fresh microcentrifuge tube. Following this, 500µl isopropanol was added, then mixed gently for 2 min. After the samples were centrifuged again and the supernatant discarded, the DNA pellet left in the tubes was washed with 500µl 70% ethanol, then the mixture was centrifuged at 13,000g at room temperature and the majority of supernatant was carefully removed. The DNA was allowed for air dry for approx. 30 min and was eluted with 40µl nuclease-free water with gentle mixing. In the end, the concentration of DNA was quantified by NanoDrop (Thermo Scientific) and adjusted to 5 ng/µl for further use. The ratio of absorbance at 260 nm (A260) and 280 nm (A280) is used to assess the purity of DNA, and a ratio of ~1.8 is generally accepted as “pure” for DNA. Lower than 1.8 indicates protein contamination in the samples. Ratio of A260/A230 is used as a secondary measure of nucleic acid purity with an expected 260/230 values in the range of 2.0-2.2. Values lower than 1.5 indicates the presence of contaminants which absorb at 230 nm.

2.3.2 KASPar genotyping

Prior to commencing the technique, all the allelic-specific PCR primers (Table 2.2+2.3) were designed using the Primer Picker software. DNA samples of HUASMCs (10ng/2µl) were arrayed in micro PCR 384-well plates and at least 3 wells without DNA acted as no template controls (NTC). The plate was then oven dried. The assay mix and the master mix were prepared according to the KASPar genotyping manual. The master mix (2 µl / well) was then added in the plate and briefly spun down to

eliminate the bubbles. Once arraying was done, the plate was covered with optical transparent seal. Then the amplifications of samples were performed in a PTC-225 DNA Engine Tetrad thermal cycler (MJ Research, USA) under the following conditions:

Step 1: 94 ^{O}C for 15 min		hot start activation
Step 2: 94 ^{O}C for 10 seconds	}	19 cycles
Step 3: 57 ^{O}C for 5 seconds	}	
Step 4: 72 ^{O}C for 10 min	}	
Step 5: 94 ^{O}C for 10 seconds	}	14 cycles
Step 6: 57 ^{O}C for 20 seconds	}	
Step 7: 72 ^{O}C for 40 seconds	}	

After the PCR cycles were completed, the plate was placed into the ABI 7900HT instrument which reads the fluorescence signal generated during the amplification process. The fluorescent data was presented as a scatter plot by the SDS 2.3 software, where each sample was indicated as a point on the graph. The plot should contain four separate clusters (Figure 2.4), three of which are the possible genotypes (2 homozygotes and 1 heterozygotes) and the fourth are the NTC or undetermined samples. The amplification process could be continued by adding 3 cycles each time until a proper plot was got.

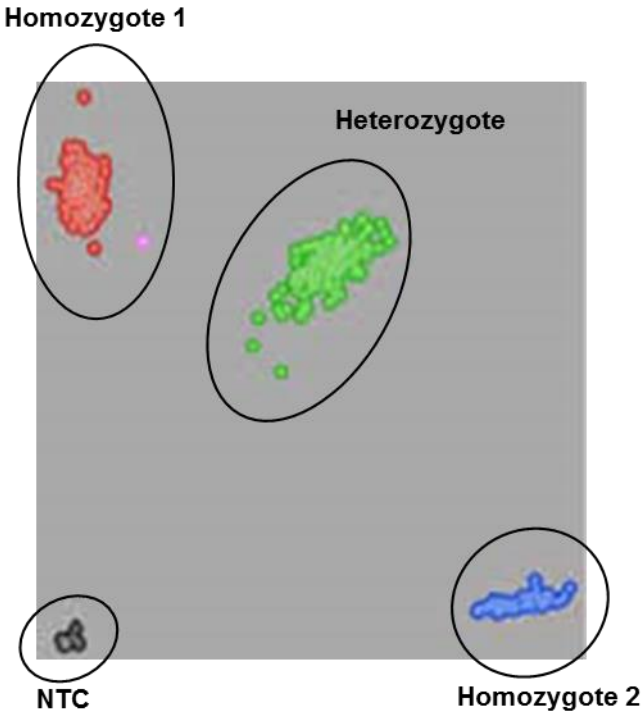

Figure 2.4 KASPar genotyping data plotted showing the four separate clusters.

Table 2.2 Primers sequence information for KASPar genotyping for variants in rs1173771 LD block.

SNP	Primers	Sequence
rs1173771	Allele_T_FAM	5'-GAAGGTGACCAAGTTCATGCT GGCTGCTGGTGCTTTGTGAATAAA-3'
	Allele_C_VIC	5'-GAAGGTCGGAGTCAACGGATTGC TGCTGGTGCTTTGTGAATAAG-3'
	Common Reverse	5'-AGCCAACCATATGATGATCTCATACCAA-3'
rs1173743	Allele_T_VIC	5'-GAAGGTCGGAGTCAACGGATTGCT TAGAGCTGAGAAAAGCAAGAA-3'
	Allele_G_FAM	5'-GAAGGTGACCAAGTTCATGCT TTAGAGCTGAGAAAAGCAAGAC-3'
	Common Reverse	5'-CAGTTGCAGCTGTGGGGCCTTT-3'
rs1173747	Allele_A_FAM	5'-GAAGGTGACCAAGTTCATGCT CCTCAGTTTCTGGTTAAAATGATTGTTT-3'
	Allele_C_VIC	5'-GAAGGTCGGAGTCAACGGATT CCTCAGTTTCTGGTTAAAATGATTGTTG-3'
	Common Reverse	5'-GACTGGGGCTTAGGGAGCTGAT-3'
rs1173756	Allele_T_FAM	5'-GAAGGTGACCAAGTTCATGCT GATCTATGCAATGGCCTTCATCTCA-3'
	Allele_C_VIC	5'-GAAGGTCGGAGTCAACGGATT ATCTATGCAATGGCCTTCATCTCG-3'
	Common Reverse	5'-GCATCACTTTCCTTTTAGTTATGGCTGAT-3'

Table 2.3 Primers sequence information for KASPar genotyping for variants in rs1421811 LD block.

SNP	Primers	Sequence
rs1421811	Allele_C_FAM	5'-GAAGGTCGGAGTCAACGGATTAAGT CAGAGACTTCCCAAGGCG-3'
	Allele_G_VIC	5'-GAAGGTGACCAAGTTCATGCTAAGT CAGAGACTTCCCAGGCC-3'
	Common Reverse	5'-CAAACCGCGGATCTCGCCCATA-3'
rs3828591	Allele_G_VIC	5'GAAGGTGACCAAGTTCATGCTGAGC TAAGTGGCGACGCCTG-3'
	Allele_C_FAM	5'-GAAGGTCGGAGTCAACGGATTGA GCTAAGTGGCGACGCCTC-3'
	Common Reverse	5'-GAAGCGTCCGCGGACGCCT-3'
rs3762988	Allele_C_FAM	5'-GAAGGTCGGAGTCAACGGAT TAACCAGGAGCAAAAGAGACATCT-3'
	Allele_T_VIC	5'-GAAGGTGACCAAGTTCATGCT AACCAGGAGCAAAAGAGACATCT-3'
	Common Reverse	5'-GTGTGGATTACCCTGTTTGTGGAATTAAA-3'
rs7729447	Allele_G_FAM	5'-GAAGGTCGGAGTCAACGGATTGC ACCACTTATACCCCCTCCG-3'
	Allele_A_VIC	5'-GAAGGTGACCAAGTTCATGCTGCA CCACTTATACCCCCTCCA-3'
	Common Reverse	5'-GAAGATGTAGGAGTATCCAAAAGAGGATA-3'

2.4 Quantitative Real-Time Reverse Transcription PCR (q RT-PCR)

Quantitative reverse transcriptase polymerase chain reaction (q RT-PCR) was conducted to quantify *NPR3* mRNA level in HUASMCs and HUVECs to test if the BP-associated SNPs influence *NPR3* gene expression. Real time qRT-PCR is a technique could detect the reaction progress in real time, by labelling the new synthesized cDNA during the reaction. The detected quantity of cDNA could be normalized relative to housekeeping genes (e.g. 18S rRNA, GADPH, β-actin), which is required for maintenance of basal cellular functions and are expected to maintain constant expression levels in all cells and conditions. Technologically, all qPCR

involves the use of fluorescence to detect the threshold cycle (C_t) during PCR when the level of fluorescence gives signal over the background and is in the linear portion of the amplified curve (Figure 2.5). Two common methods in quantitative PCR are: (1) non-specific fluorescent dyes such as SYBR-Green, which intercalate with any double-stranded cDNA. The overall fluorescence increase proportionally to the DNA concentrations and reflects the amount of cDNA templates in PCR reaction. (2) sequence-specific DNA probes consisting of oligos that are labelled with a fluorescent reporter such as TaqMan probes. TaqMan probes have a fluorophore (reporter) attached to 5'-end of the oligonucleotide probe and a quencher at 3'-end. Fluorescence detected in the real-time PCR process is directly proportional to the released fluorophore and the amount of DNA templates present in the PCR.

SYBR Green quantitative PCR technique was used in this subject.

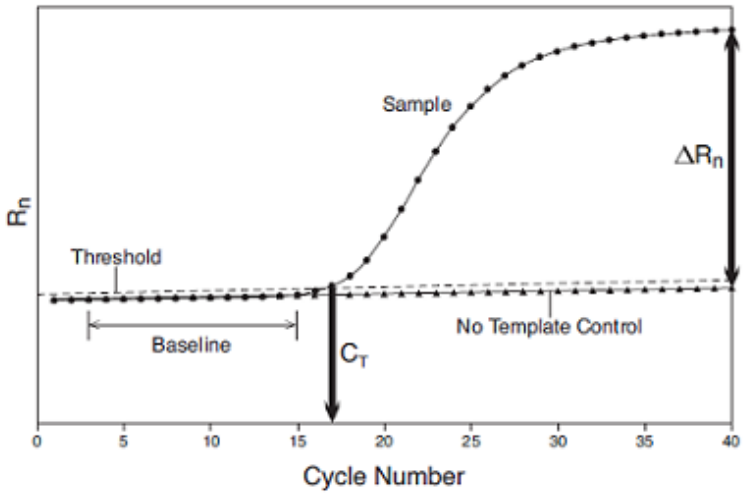

Figure 2.5 Representative amplification curve of RT-PCR.

Ct (Threshold cycle): the cycle number at which the fluorescence signal crosses threshold; ΔRn: Fluorescence signal with baseline subtracted; Baseline: background noise level before a significant amplification occurs (3-15 cycles)

2.4.1 RNA extraction

The total RNA was extracted from HUASMCs and HUVECs using the commercially available SV total RNA isolation system (Promega). Briefly, cells from flasks were harvested in sterile 1.5ml Eppendorf tubes by centrifuged at 13,000g for 5 min, were then washed with ice-cold sterile phosphate buffered saline (PBS) and centrifuged at 13,000g for another 5 min to collect the cell pellet. The extraction was then conducted according to the instructions of the kit. After extraction, purified RNA was determined using NanoDrop Spectrophotometer ND-1000 instrument and stored at -80^{o}C until further use. The ratio of A260/A280 nm and A260/A230 are used to assess the purity of RNA, and ratios of ~2.0 for A260/A280, 2.0-2.2 for A260/A230 are generally accepted as “pure” for RNA.

2.4.2 Conversion of RNA to complementary DNA

To perform qRT-PCR on the total RNA, it firstly has to be converted to complementary DNA (cDNA). This involves the use of RNA as a template in a reaction catalysed by the enzyme reverse transcriptase, which operates on a single strand of RNA, generating its complementary DNA. The conversion was performed using ImProm-II^{TM} Reverse Transcription System (Promega) as follows:

2 µl of total RNA were transferred into a 1.5 ml Eppendorf tube and incubated in water bath at 70^{0}C for 5 min. The samples were centrifuged briefly and then placed on ice. The following reagents were then added to the tube containing the 2 µl of total RNA:

- $MgCl_2$, (25mM) - 4 µl with a final concentration of 5mM
- Reverse transcription 10x Buffer - 2 µl.
- dNTP mixture, 10mM - 2 µl with a final concentration of 1mM
- Recombinant RNasin® Ribonculease Inhibitor - 0.5 µl.
- AMV reverse transcriptase - 15 units.
- Random primers - 0.5 µl.
- ddH_2O - Up to 20 µl.

The reactions were incubated for 10 min at room temperature, and then at 42°C for a further 60 min. The samples were heated at 95°C for 5 min, and quickly chilled at 4°C for another 5 min. 80 µl of ddH_2O was added to the cDNA reaction and the samples were stored at -20°C until next step.

2.4.3 SYBR-Green quantitative PCR

SYBR Green quantitative PCR technique was used to conduct qRT-PCR with 18S rRNA as the internal reference gene for normalization of *NPR3* gene expression. SYBR-Green qPCR was carried out using commercially available kit (SYBR® Select Master Mix kit) from Life Technologies as follows:

2µl (10ng) of each cDNA sample was arrayed in a PCR 384-well plate and the appropriate volume of reaction mix was prepared according to Table 2.5. 8 µl of reaction mix was then transferred into each well of the plate. Each reaction was conducted in duplicate. After arraying samples, the plate was sealed with an optical transparent cover and centrifuged briefly to spin down the contents and eliminate any air bubbles. The reaction plate was then placed in the real-time quantitative PCR instrument (ABI 7900HT machine) and the thermal cycling condition was set as Figure

2.4. The fluorescence signal generated during the amplification process was read by the machine ABI 7900HT and analysed by software SDS 2.3 to get the amplification curve. The threshold cycle (C_t) value which represents the quantification of gene expression of each sample was calculated by the program and obtained after analysis.

Table 2.4 The reagents used in SYBR Green method.

Reagents	Volume
SYBR Green ROX (2X)	5.0μl
Forward Primer (10μM)	0.1μl
Reverse Primer (10μM)	0.1μl
Nuclear free water	3.8μl
Template	2.0μl(10ng)
Total volume	10.0μl

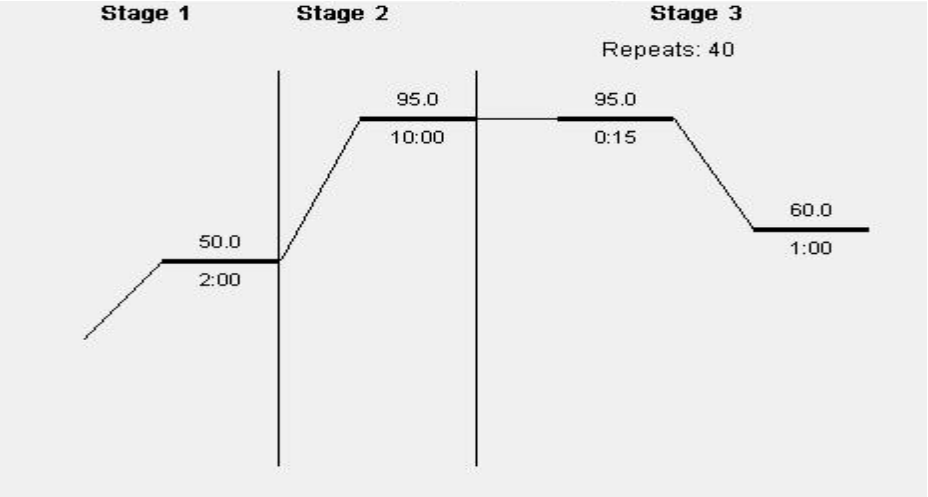

Figure 2.6 Thermal cycling conditions for qRT-PCR.

2.4.3.1 Primers design and variants expression detection

Before starting the assay, all primers of 18S rRNA, *NPR3* were designed using Primer_BLAST (http://www.ncbi.nlm.nih.gov/tools/primerblast/index.cgi?LINK_LOC=BlastHome).

It was noticed that there are three transcript variants of human *NPR3* mRNA indicated by NCBI nucleotide database (http://www.ncbi.nlm.nih.gov/nuccore/). Their NCBI Reference Sequences are NM_001204375.1 for transcript variant 1, NM_000908.3 for transcript 2 and NM_001204376.1 for transcript variant 3. They were subjected to alignment by BLAST as shown in Figure 2.6. Common sequence among these three variants was utilised for primer design of total mRNA, and primers targeting each variant mRNA were designed using their specific sequences of each variant respectively.

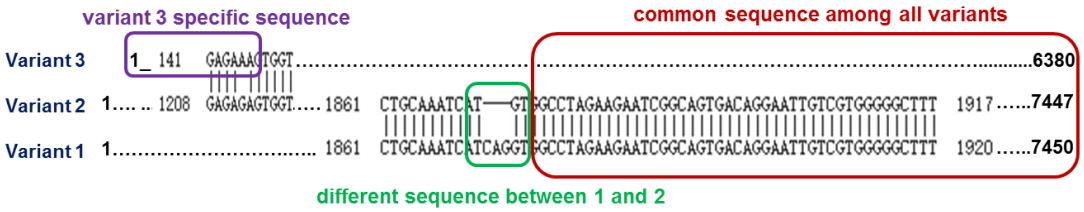

Figure 2.7 Alignment of three variants of *NPR3* mRNA sequences to show the common sequences and specific sequences for each variant.

For each target, three pairs of primers with product size around 150bp were designed and tested for specificity and sensitivity by end-point PCR. The primers pairs that had a good specificity and amplification efficiency were utilised in this assay.

Correlation analysis was also conducted for the variants mRNA expression and total mRNA expression in HUASMCs (Figure 2.8). It is manifested a strong positive correlation, reflecting a very dependent pattern among variants and total mRNA in samples. Therefore, the total mRNA expression detection was utilised in subsequent

genetic analysis. Primers targeting 18S and total *NPR3* mRNA are listed in the Table 2.5.

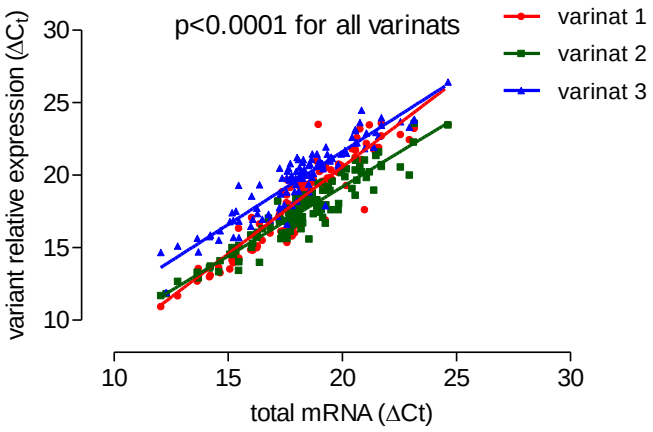

Figure 2.8 Correlation plots between variants mRNA expression and total mRNA expression of *NPR3* (N=112).

Table 2.5 Primers of 18s and *NPR3* cDNA for q RT-PCR.

Gene	Forward primer	Reverse primer
18S	5' CCCAGTAAGTGCGGGTCATAA 3'	5' CCGAGGGCCTCACTAAACC 3'
NPR3	5' GCCGCATTTCAAAACGACCT 3'	5' TGCCAACGGAGACCGATATG 3'

2.5. Allelic expression imbalance (AEI)

Regulatory polymorphisms (rSNPs) and some structural RNA SNPs (srSNPs) in the transcribed region can affect mRNA processing and turnover. Both rSNPs and srSNPs can cause allelic mRNA expression imbalance (AEI) in heterozygous individuals. AEI here was carried out to investigate the potential of BP associated SNP rs1173756 (3-UTR SNP in *NPR3*) in mRNA processing, which involving some transcriptional factors, MicRNA or other elements. This method is subjected to samples which are heterozygous at SNP rs1173756. Both genomic DNA and cDNA of each sample were

amplified by PCR in the region flanking rs1173756, and subjected to fluorescent dideoxy sequencing, the allelic ratio of cDNA after analysis was then compared with genomic DNA.

2.5.1 Preparation of DNA samples

8 HUASMCs and 7 HUVECs samples were obtained from different individuals and have been confirmed as heterozygous (C/T) genotype for rs1173756 using KASPar SNP genotyping method (section 2.3.2). Genomic DNA was extracted as described in section 2.3.1. Total RNA of these samples was extracted and reversely transcribed into cDNA as described in qRT-PCR methodology (see section 2.4). Primers for targeting rs1173756 DNA fragments in genomic DNA and cDNA were designed using Primer_BLAST (Table 2.6)

Table 2.4 Information of primers for rs1173756 DNA fragments.

rs1173756	genomic DNA	cDNA
Forward primer	5'-TTGGAATGCCCTCACTTCTC-3'	5'-TGCTTTGGAATGCCCTCACT-3'
Reverse primer	5'-GTGACGCCACTGGAACCTAC-3'	5'-ACGCCACTGGAACCTACTTT-3'
Product size	220bp	221bp

2.5.2 Polymerase chain reaction (PCR)

PCR for genomic DNA and cDNA of rs1173756 fragments was performed using commercially available kit (Novagen): A number of 0.2ml nuclear free Eppendorf tubes were prepared and added into with the reagents shown in Table 2.7. All the samples

were placed into PTC-225 DNA Engine Tetrad thermal cycler (MJ Research, USA) and amplified using the following condition.

Step 1: 94 ^{O}C for 5 min hot start activation

Step 2: 94 ^{O}C for 15 seconds

Step 3: 55 ^{O}C for 15 seconds } 35 cycles

Step 4: 72 ^{O}C for 30 seconds

Step 5: 72 ^{O}C for 2 min

Step 6: 4 ^{O}C

Table 2.5 Constitute reagents volume in PCR system.

Reagents	**Volume (μl)**
10X PCR buffer	2.5
$MgCl_2$ (25mM)	1.5 (final concertation: 1.5mM)
dNTP(2mM)	2.5 (final concertation: 0.2mM)
Primer-mix (10μM)	1.0
Taq polymerase	0.13
DNA(10ng/μl)	2.0
Nuclear free water	15.67
In total	25

2.5.3 Agarose gel electrophoresis

Agarose gel electrophoresis is a technique used to separate nucleic acids according to their size under the influence of an electric current. The shorter fragments will migrate at a faster rate than the longer fragments. An agarose gel was prepared as follows:

1.2 g of agarose powder (Sigma, UK) was dissolved in 60 ml of 1x Tris-borate-EDTA (TBE; Bioline Ltd, UK) buffer for a 2% w/v agarose gel. The solution was left to cool down and 6 µl of Gel Red (x10, 000: Biotium, USA) was added. The solution was poured into a medium-sized casting tray containing a sample comb and allowed to solidify for 40 min at room temperature. The gel was then placed horizontally into an electrophoresis chamber containing sufficient amount of 1x TBE buffer to cover the gel. 25 µl of the amplified fragments were mixed with 2.7 µl of 10X bromophenol blue dye (Sigma, UK) and then pipetted into the wells. A 100bp molecular ladder (ABgene, UK) was run alongside all samples. After 40 min at 100 volts, the DNA fragments were visualized by using a UV transilluminator (UVP, Canada) as shown in Figure 2.7.

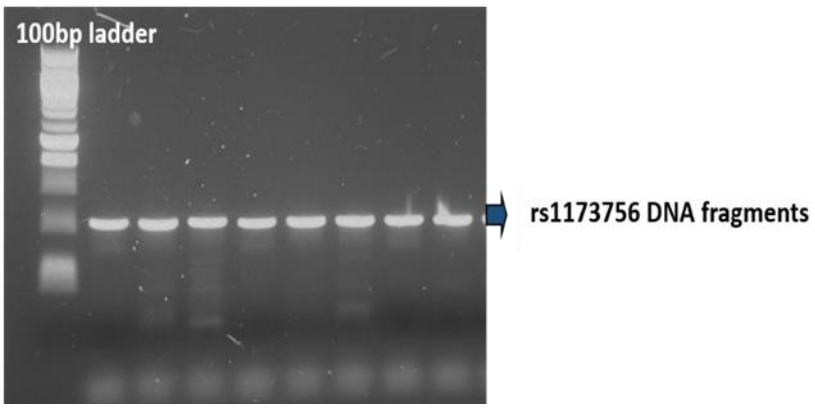

Figure 2.6 The DNA fragments under a UV transilluminator.

.

2.5.4 DNA purification from gel and quantification

Kit from Promega were used for DNA purification from gel and the main procedure according to manufacture is as follows: After electrophoresis, DNA band was carefully cut from gel and the gel slices was placed in pre-labelled 1.5ml micro centrifuge tubes. The purification was done according to the instruction. Once DNA was purified, it was quantified using NanoDrop and stored at 4°C or –20°C until further use.

2.5.5 Sanger sequencing

Chain termination method (Sanger dideoxy method) is one of the most widely used technique for sequencing DNA. All sequencing studies were done by Barts and The London Genome Centre using Big Dye 3.1 chemistry with visualization on the ABI 3730 capillary sequencer. The following figure (Figure 2.8) shows an example of the sequencing result analysed by Bio Edit.

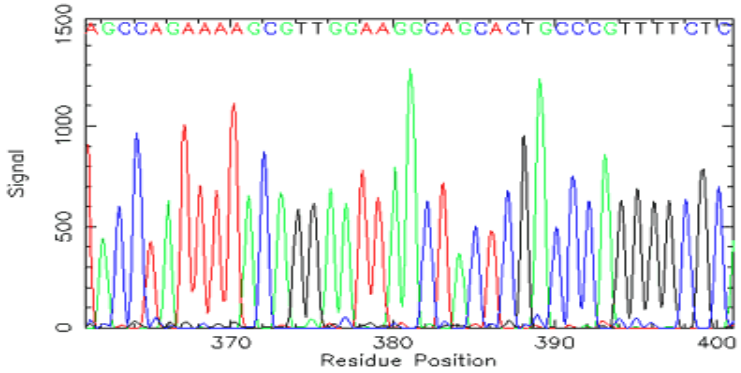

Figure 2.7 A representative sequencing result.

Sanger sequencing technique is mainly based on fluorescently labelled dideoxyribonucleotide terminators (ddNTPs). When ddNTP is added to the growing chain during DNA synthesis, the chain is terminated ending with the ddNTP with different colours. As shown in the figure, the color can tell which of the four DNA bases, A, C, T, or G are present at that position. The whole DNA sequence is inferred by reading the colours of all the different shortened products.

2.6 Western Blot Analysis

Western blot analysis is a technique that identifies specific proteins from a protein mixture extracted from cells. It was performed here to explore whether BP-associated SNPs affect NPR-C protein expression in HUASMCs and HUVECs.

2.6.1 Preparation of lysate from cell culture

HUASMCs or HUVECs cultured in a T75 flask was washed twice with ice-cold PBS and placed on ice. 1ml of ice-cold PBS with protease inhibitor (PI) (Table 2.8) was added into the flask, the cells were then scraped from flasks using a cold plastic cell scraper. After that, the cell suspension was gently transferred into a pre-cooled microcentrifuge tube and centrifuged at 13,000g at 4 ºC. The supernatant was discarded after centrifugation and cell pellet was harvested. 200µl of ice-cold radio-immuno precipitation assay (RIPA) lysis buffer (150 mM NaCl, 0.1% Triton-X 100, 0.5% sodium deoxycholate,0.1% sodium dodecyl sulphate, 50mM Tris-HCl pH 8.0, 1X protease inhibitor) was added into each pellet and disrupted by pipette mixing, followed by sonication for 1-2 min. The lysate was placed on ice for an hour with pipetted mixing every 10 min. After being centrifuged at 13,000 x g for 20 min in a 4°C pre-cooled centrifuge, the supernatant was carefully collected into a fresh chilled tube without disrupting pelleted debris at the bottom. The protein was finally stored at -80°C until further use.

Table 2.6 Components in protease inhibitor cocktail.

Components	Company	Working concentrations
Phenylmethylsulfonyl flouride (PMSF)	SLS, P7626	1mM
Leupeptin hemisulfate	SLS, L2884	1μg/ml
Aprotinin from bovine lung	SLS, A1153	1μg/ml
Pepstatin A	SLS, P4265	1μg/ml

2.6.2 Quantification of protein using bicinchoninic acid assay (BCA) kit

The quantification of protein was carried out with commercially available BCA kit from Pierce as follows: A series of bovine serum albumin (BSA) standards (0, 0.25, 0.5, 0.75, 1.0, 1.5, and 2.0 μg/ml) were prepared before quantification. The BCA working solution was also prepared by a ratio of reagent A: B= 50:1 and mixed well by inverting. The protein samples to be quantified were diluted by 10 (1:9) and 5 (2:8) with lysis buffer used in section 2.5.1. Once the preparation work done, 10 μl of diluted samples and standards were added into a 96-well microplate (Thermo Scientific™ Pierce™ 96-Well Plates) in duplicate. 200μl of working solution was then pipetted into each well, with following incubation at 37°C for 30 min.

The plate was then allowed to cool down to room temperature and placed into a plate reader (MRX-TC Revelation, Dynex Technologies, UK) and the absorbance of each reaction at the wavelength of 570 nm was read. The value of each sample was corrected with the average absorbance of 0 μg/ml, then the standard curve was based on the light absorbance of standards as following Figure 2.9. Each sample was adjusted to the desired concentration with RIPA buffer. 20 μl aliquots of each sample were stored in -80°C until further use.

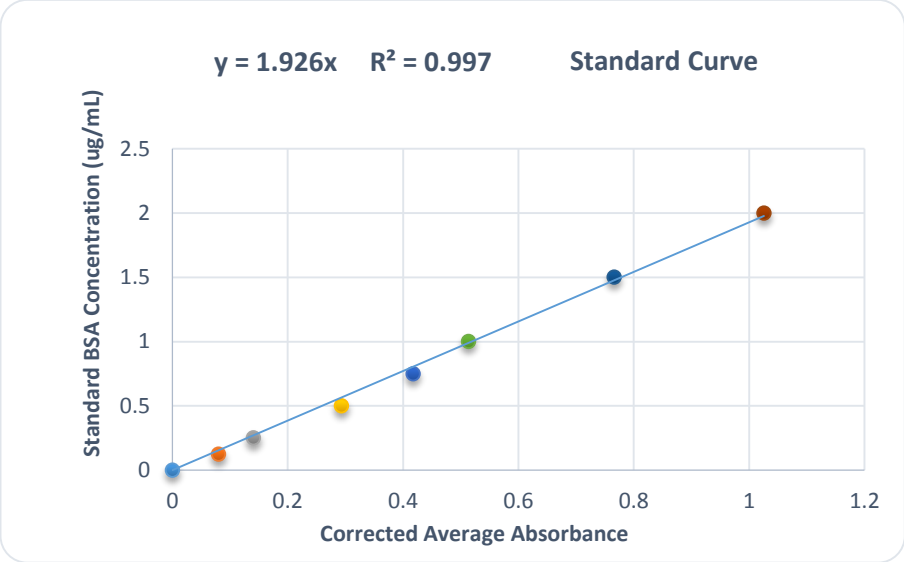

Figure 2.8 Standard curve for protein concentration quantification in bicinchoninic acid assay (BCA) assay.

Eight concentrations (0-2.0μg/ml) of bovine serum albumin (BSA) were assayed. The response values (absorbances) were plotted and a best-fit line drawn through the points. If unknown samples were tested at the same time, their concentrations could be determined by reference to the standard curve.

2.6.3 Sodium-dodecyl-sulfate polyacrylamide gel electrophoresis

Sodium-dodecyl-sulfate polyacrylamide gel electrophoresis (SDS-PAGE) is a technique utilised to separate proteins based on their molecular weight upon application of an electric field across the gel. The binding of SDS to polypeptide chain imparts in most proteins charge per unit mass, thus resulting in a fractionation by approximate size during electrophoresis via different mobility. Briefly, 10% separating SDS-PAGE gel and 5% stacking SDS-PAGE gel were prepared as Table 2.9 and stored at 4°C before use. Equal amount protein of each samples were defrosted at 37°C, and added with 5X protein loading buffer (312.5 mM Tris pH 6.8, 10% w/v SDS,

50% v/v glycerol, 0.5% w/v bromophenol blue, 5% v/v β-mercaptoethanol), they were then boiled at 95°C for 5 min, followed by centrifugation at 13,000 x g for 5 min. 30 µl of protein samples (20 ng protein in each), along with 6µl of molecular weight markers (7-175 kDa, NEB, p7709s) were carefully loaded onto the wells of the SDS-PAGE gel filling with running buffer (SDS: 0.1% w/v, Tris base: 25mM,Glycine: 192mM), the gel was then run at 90 V for 30min in the stacking gel, then 160 V for another approximately 90min until appropriate separation of achieved.

Table 2.7 Constitute reagents volume in separating gel and stacking gel.

Separating (10%)	Volume(ml)	Stacking (5%)	Volume(ml)
30% Polyacrylamide	3.33	30% Polyacrylamide	0.68
1.5M Tris (pH8.8)	2.5	1.0M Tris (pH6.8)	0.5
10% Ammonium persulfate	0.1	10% Ammonium persulfate	0.04
10% SDS	0.1	10% SDS	0.04
TEMED	0.004	TEMED	0.004
H_2O	3.97	H_2O	2.72
Total volume (mL)	10	Total volume	4

2.6.4 Electro transfer

Before transfer, a piece of 7.5cm×9.0cm polyvinylidene fluoride (PVDF) membrane (Hybond ECL, GE Healthcare) was pre-activated in methanol for 2 min, and washed with cold Tris-buffered saline with Tween (TBST) buffer (Tris HCI: 50mM,Tris base: 50mM, NaCI: 150 mM, Tween-20: 0.1%v/v). The filter papers and sponge were also pre-chilled in cold TBST before making stack. The gel was carefully removed from running unit, the transfer “Sandwich” was then prepared as following Figure 2.10, and

put into transfer unit filling with transfer buffer (Tris base: 25mM, glycine: 192mM, methanol: 20% v/v), and was run at 60 V for 2.5 hours at 4°C.

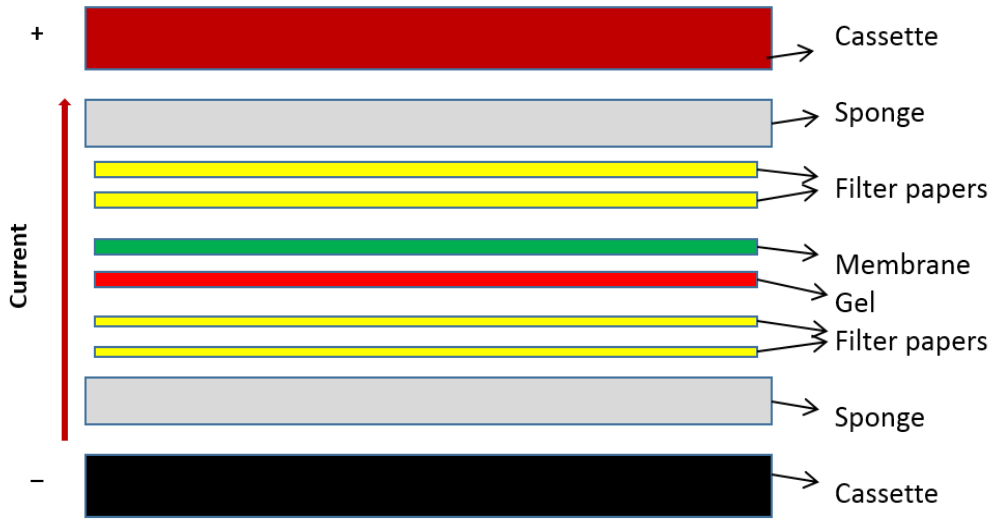

Figure 2.9 Assembly of a transfer 'sandwich' in western Blot

In the presence of transfer buffer, 'Sandwich' is assembled by placing two pieces of filter papers (yellow) soaked in transfer buffer followed by the gel (red) with separated proteins, the PVDF membrane (green), then two more pieces (yellow). Current arrow shows the direction of protein transfer from gel to membrane.

2.6.5 Antibody staining and detection

After transfer, the membrane was incubated for 1 hour at room temperature with 5% blocking solution (5% non-fat milk in TBST), then incubated with 1:1000 dilution of anti-NPR-C antibody (Table 2.10) in 5% blocking solution overnight at 4°C. The membrane was washed with TBST three times with gentle agitation, 10 min each at room temperature. This is followed by incubation with 1:3000 horseradish peroxidase (HRP)-conjugated anti-mouse IgG (Table 2.10) at room temperature for 1 hour. The membrane was washed again with TBST and rinsed in Tris-buffered saline (TBS).

While waiting for the last wash, appropriate volume of enhanced chemiluminescence (ECL) 1 and 2 reagents (Table 2.11) were prepared with ratio of 1:1 before mixing. The membrane was taken out from washing buffer and placed into a new container. The ECL mix was poured to cover the membrane and incubated for 5 min in dark room. The membrane after incubation with ECL was covered in transparent plastic wrap and put into a cassette. A piece of autoradiography film (Thermo scientific) was exposed to the membrane for 1 to 5 min until a desired signal was achieved. The film then developed (SRX-101A, KONICA MINOTA)

Table 2.8 Information on the antibodies used in Western Blot analysis.

Antibody	Description	Company	Product No
Anti-NPR-C antibody	mouse monoclonal	Abcam	ab123957
Anti-β-actin antibody	mouse monoclonal	Abcam	ab 8226
Anti-mouse IgG ,HRP-linked antibody		Cell Signalling	#7076S

Table 2.9 Components in ECL solutions.

Reagents in ECL-1	Working concentration	Reagents in ECL-2	Working concentration
Tris-HCl, pH 8.5	100mM	Tris-HCl, pH 8.5	100mM
Coumaric acid	0.405mM	Hydrogen Peroxide	0.018%
Luminol	2.5mM		

2.6.6 Blocking peptide competition

Two copies of PVDF membranes with identical HUASMC samples were collected after electro transfer. After 1h blocking, membrane 1 was put in “control” tube with 1:1000 dilution anti-NPR-C antibody buffer, while membrane 2 was put into “blocked”

tube with 1:1000 dilution NPR-C antibody buffer with additional 1:333 dilution NPR-C peptide (ab42266, Abcam). Both were incubated with gentle agitation at 4 ^{o}C overnight, and staining detection was performed subsequently with ECL and film. Signals that were present on the “control” film but no in the “blocked” film were regarded as specific NPR-C fragments (Figure 2.11).

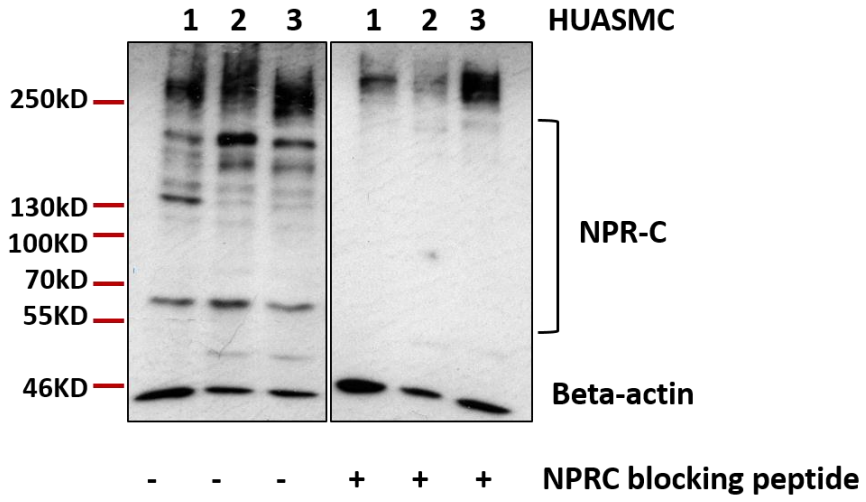

Figure 2.10 Blocking competition with NPR-C blocking peptide in HUASMCs.

Western blot analysis of extracts from HUASMCs (samples 1, 2, and 3) using anti-NPR-C antibody (control) or the same antibody pre-incubated with NPR-C blocking peptide (blocked). Signals that were present on the “control” film but no in the “blocked” film were regarded as specific NPR-C fragments.

2.7 Electrophoretic mobility shift assay (EMSA)

The interaction of transcriptional or co-transcriptional factors with DNA is crucial for gene expression. The electrophoretic mobility shift assay (EMSA) is a technique that studies *in vitro* protein/DNA interaction. This technique is based on the observation that protein-DNA complexes migrate more slowly than the corresponding free nucleic

acids when subjected to non-denaturing polyacrylamide gel electrophoresis. During electrophoresis, the protein-DNA complexes are quickly resolved from free DNA, providing a "snapshot" of the equilibrium between bound and free DNA in the original sample. After electrophoresis, the distribution of species containing nucleic acid is determined, usually by autoradiography of ^{32}P-labelled nucleic acids or covalent labelling of nucleic acids with a flurophore such as biotin. EMSA was conducted here to find the possible proteins in regulating *NPR3* associated with BP associated variants (rs1173771, rs1173743, rs1173747, rs1173756) using biotin-labelled probes.

2.7.1 Preparation of probes

The allele specific probes were labelled with biotin by IDT and sequences of biotin-labelled and non-labelled probes are shown in Table 2.12. To anneal the oligos to double-stranded probes, each oligo pair of labelled or unlabelled allele specific oligos of each SNP were mixed to certain concentrations (labelled oligos: 0.01μM; unlabelled oligos: 0.1 - 1μM) with annealing buffer (10mM Tris, pH8.0, 50mM NaCl, 1mM EDTA) and heated at 95°C for 2 min, then allowed for cooling down to room temperature for 30min.

Table 2.10 Information of oligos in EMSA.

SNP	Oligos	Sequence (forward oligos)*	Sequence (reverse oligos)
rs1173771	EMSA_C alelle_F/R	CTCATACCAACTTATTCACAA	TTGTGAATAAGTTGGTATGAG
	EMSA_T allele_F/R	CTCATACCAATTTATTCACAA	TTGTGAATAAATTGGTATGAG
rs1173743	EMSA_T alelle_F/R	CCTTTCCAGCTTCTTGCTTTT	AAAAGCAAGAAGCTGGAAAGG
	EMSA_G allele_F/R	CCTTTCCAGCGTCTTGCTTTT	AAAAGCAAGACGCTGGAAAGG
rs1173747	EMSA_A alelle_F/R	GGAGCTGATCAAACAATCATT	AATGATTGTTTGATCAGCTCC
	EMSA_C allele_F/R	GGAGCTGATCCAACAATCATT	AATGATTGTTGGATCAGCTCC
rs1173756	EMSA_C alelle_F/R	CAGTCAACAACGAGATGAAGG	CCTTCATCTCGTTGTTGACTG
	EMSA_T allele_F/R	CAGTCAACAATGAGATGAAGG	CCTTCATCTCATTGTTGACTG

Forward oligos * of each allele in each SNP were also prepared labelled ones with biotin in 5' tail. SNP of interest indicated in red and underlined

2.7.2 Cytosolic and nuclear protein extraction

Buffer A and B involved in the extraction were prepared as Table 2.13. HUASMCs or HUVECs in a T75 flask was washed with ice-cold PBS twice. 1ml of buffer A was added directly to each flask, and incubated for 10 min at room temperature. Cells were scraped from flasks into a 1.5 ml microfuge tube, with pipette mixing to disrupt cell clumps. Then the cell lysate was centrifuged at 4°C at about 15,000g for 3min. The supernatant was collected as cytoplasmic extract. The pellet containing unlysed nuclei was resuspended in 125µl buffer B, also mixing by pipetting up and down, and placed on ice for 10min. The supernatant (nuclear extract) was collected centrifugation at 4°C at 15,000g for 5 min and quantified with BCA (section 2.5.2) using buffer B standards, then stored at -80°C until further use.

Table 2.11 Constitute in buffer A and buffer B.

Reagents in buffer A	Working solution	Reagents in buffer B	Working solution
HEPES, PH 7.9	10mM	HEPES, PH 7.9	10mM
KCl	10mM	NaCl	0.4M
EDTA	0.1mM	EDTA	1mM
PI	X1	PI	X1
IGEPAL	0.004%	Glycerol	10%

2.7.3 Pre-running

6% non-denaturing polyacrylamide gel was made as Table 2.14. The gel was placed in the electrophoresis unit filled with 0.5X TBE (40 mM Tris-Cl pH 8.3, 45 mM boric acid, 1 mM EDTA). Loading buffer was pipetted into each well and the gel was pre-electrophoresed for about 90 min at 100V until bromophenol blue run off.

Table 2.12 Components in 6% non-denaturing polyacrylamide gel.

Gel components	12ml 6% gel
Acrylamide 30%	2.43ml
1x TBE	0.6ml
10% APS	120µl
TEMED	12µl
H_2O	8.89ml

2.7.4 Electrophoretic binding reaction

The reaction mix was prepared as Table 2.15 and incubated at room temperature for 20 min. When specific antibody super shift is performed, the mixture with protein and oligos was incubated for 20 min first, then with antibody for further 20 min. 2μl of 10x DNA loading buffer (10mM Tris pH7.5, 1mM EDTA, 50%v/v glycerol, 1% bromophenol blue) was added into each sample (20μl in total), with pipetting the mix up and down several times. The samples were loaded into the wells of gel and run at 100 V at 4°C until the bromophenol blue dye went down 3 cm to the bottom.

Table 2.13 Preparation of reaction mix.

1x Reaction Mix	Working solution	Per reaction (18ul)
1M Tris pH 7.5	10mM	0.18μl
5M NaCl	50mM	0.18μl
0.5M EDTA	1mM	0.036μl
Glycerol	5%	0.9ul
Protease Inhibitors	1x	0.72μl
Labelled oligo (0.01μM stock)	10^{-14}moles	1μl
Poly (dI.dC)0.5mg/1ml	0.125mcg	0.225μl
Nuclear extract	2ng/μl	Up to 5μl (in each sample)
(when doing competing assay) Competitor oligo(0.1μM stock)	$5x10^{-13}$ moles (50x)	1μl
H_2O		up to 18μl

2.7.5 Electrophoretic transferring and crosslinking.

Nylon membrane (Amersham) was soaked in 0.5X TBE for 15 min before transfer. After electrophoresis, the gel was carefully removed into a cassette and was made a "sandwich" with nylon membrane and blotting papers in a lean electrophoretic transfer unit as Figure 2.6 then, transferred at 380mA (~100 V) for 30 min. When the transfer was complete, the oligonucleotides were crosslinked to the membrane using a 245nm UV-light cross linker at 120 mJ/cm^2 for 45-60 seconds.

2.7.6 Detection with Pierce kit

Signal detection was conducted according to the instruction of Chemiluminescent Nucleic Acid Detection Module (89880, Pierce). After 5-min incubation of substrate working solution, the membrane was removed from the buffer and allowed to remove excess liquid. The moist membrane was then quickly wrapped in plastic wrap and placed into a film cassette, with eliminating bubbles and wrinkles. An autoradiography film (Thermo scientific) was immediately exposed to the membrane for 1 to 5 min until a desired signal was achieved. The film was then developed (SRX-101A, KONICA MINOTA).

2.7.7 Efficiency test of biotin-labelled probes by dot blot assay

A serial dilution (10^{-6}, 10^{-7}, and 10^{-8} M) of biotin-labelled probes were prepared with annealing buffer. 1µl of each test sample was dotted on the nylon membrane pre-soaked in 0.5X TBE and allowed to air dry for 3-5 min. The membrane was then UV-cross-linked immediately followed by the detection step as described in section 2.7.6. As is shown in Figure 2.12, the efficiency of biotin-labelled is high and there were very

bright dots for 1μl of 10^{-8}M (10^{-14}mole) of each probe, thus 10^{-8}M (10^{-14}mole) was chosen for the reaction amount of biotin-labelled probes in EMSA.

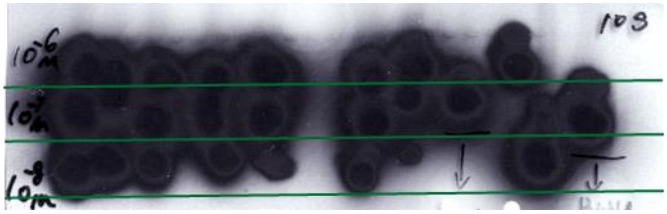

Figure 2.11 The diagram of biotin-labelled probes after dot blot assay.

2.7.8 Annealing efficiency test

The biotin-labelled and unlabelled probes (as control) were prepared as section 2.7.1, and then were quantificated by NanoDrop (10ng/μl). 20μl of annealed oligos (double-stranded DNA) and unannealed oligos (single-stranded DNA) were added into 0.5 ml Eppendorf tubes, mixed with 5μl 5X DNA loading buffer. They were run at 120 V in a 2% agarose gel for 50 min, the DNA fragments were then visualized by using a UV transilluminator. As shown in Figure 2.13, the annealed oligos on gel run much slowly than unannealed oligos and this validated they were double-stranded DNA fragments with a successful annealing.

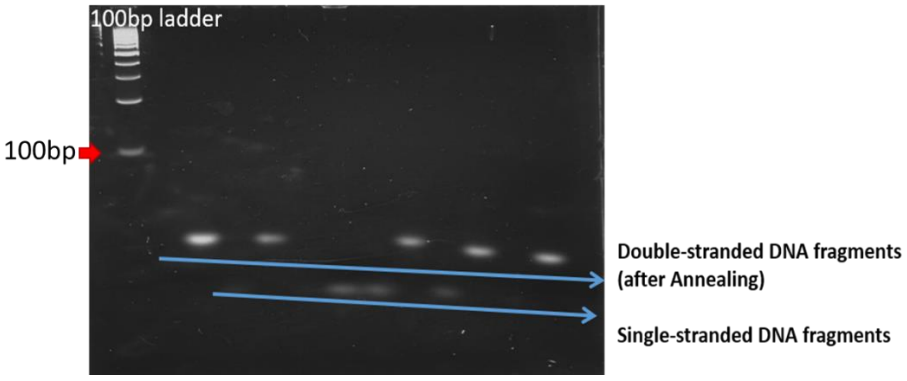

Figure 2.12 The annealed oligos under a UV transilluminator.

2.8 Cross-linked chromatin immune-precipitation (X-ChIP)

Cross-linked ChIP is suitable for mapping the DNA targets of transcription factors or other chromatin-associated proteins. This study uses cross-linked chromatin as starting material, with reversible cross-linking achieved by formaldehyde. Cross-linked ChIP was performed to investigate the potential transcription factors or other chromatin-associated proteins associated with BP-associated SNPs. ChIP assay was carried out with four basic steps.

2.8.1 Cross-linking and sonication.

When performing the ChIP, a final concentration of 1% of formaldehyde was added into a T75 cell flask and incubated for 10 min at room temperature. Then 1ml of glycine was added to quench excess formaldehyde. The cells were subsequently washed with ice cold PBS and scraped into tubes. The cells were resuspended in ChIP lysis buffer (1% SDS, 10mM EDTA, 50mM Tris-HCl) and incubated on ice for 10 min and then sonicated to shear DNA to length between 200bp and 500bp (40 seconds sonication for HUASMC). The sonicated samples were centrifuged, and the supernatants, containing the sonicated DNA fragments, were kept.

2.8.2 Immunoselection with specific antibody

Sonicated lysates were diluted with ChIP dilution buffer (1% Triton X-100, 1mM EDTA, 15mM Tris-Cl pH 7.5, 150mM NaCl)(1:100) and added into pre-blocked G-agarose beads and the solution mixed by rotating the tube at 4 ^{o}C for 60 min. The agarose beads were pelleted by centrifuge at 13,000g at 4 ^{o}C and the supernatant containing chromatin was collected. Specific anti-RNA polymerase II (5µg) was added into the

supernatant fraction and incubated overnight at 4°C with rotation. 10ng protein agarose G was added and the solution incubated for 3-hour then centrifuged. The supernatant was removed and the agarose/antibody/protein/DNA complex was kept.

2.8.3 Reversing of the cross-linking

The protein G agarose antibody / chromatin complex was washed with cold washing buffers, and the complex separated from the antibody by adding an elution buffer (1%SDS, 0.1M $NaHCO_3$). The agarose was spun down and the supernatant fraction containing DNA-protein complex collected. 5M NaCl solution (final concentration: 200mM) was added and the sample was incubated at 65 °C overnight to reverse histone-DNA crosslinking. Then a solution containing 0.5 M EDTA, 1M Tris-HCl and 1ul 10mg/ml proteinase K was added and the sample incubated for 1 hour at 45 °C.

2.8.4 Purification of DNA and detection of DNA sequence

DNA purification was performed using a DNA purification kit (Wizard R SV genomic DNA purification system, Promega). The concentration of the purified DNA was determined using a NanoDrop. An aliquot of 20ng DNA per sample was used as a template in a standard end-point PCR.

2.8.5 Optimization of sonication time

After cross- linking and lysis as described in 2.8.1, each 200 µl of the lysates was sonicated with a series of times (25s, 30s, 35s, 40s, and 45s) separately and were centrifuged at 13,000g at 4 °C. The supernatant was collected and then processed as section 2.8.3 and section 2.8.4. 200 ng of sonicated DNA samples were run on a 2% agarose gel. The result was as Figure 2.14. A range of DNA fragments from 100bp

to about 800bp could be observed and 40s was the optimal sonication time to get fragments from 200bp to 500bp.

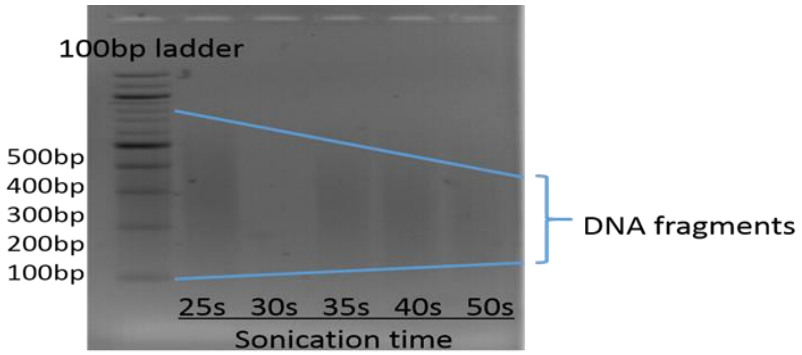

Figure 2.13 The DNA fragments range under different sonication times.

2.9 Formaldehyde-assisted isolation of regulatory elements (FAIRE)

Destabilization of nucleosomes from chromatin is a hallmark of functional regulatory elements of the eukaryotic genome. Historically identified by nuclease hypersensitivity, these regulatory elements are typically bound by transcription factors or other regulatory proteins (enhancers, silencer, insulator et al). FAIRE (Formaldehyde-Assisted Isolation of Regulatory Elements) is an approach to identify these genomic regions and has proven successful in a multitude of eukaryotic cell and tissue types. Cells or dissociated tissues are cross-linked briefly with formaldehyde, lysed, and sonicated. Sheared chromatin is subjected to phenol-chloroform extraction and the isolated open DNA is purified and conducted to quantitative PCR or sequencing to detect the open chromatin state or hypersensitive sits in DNA fragments of interest.

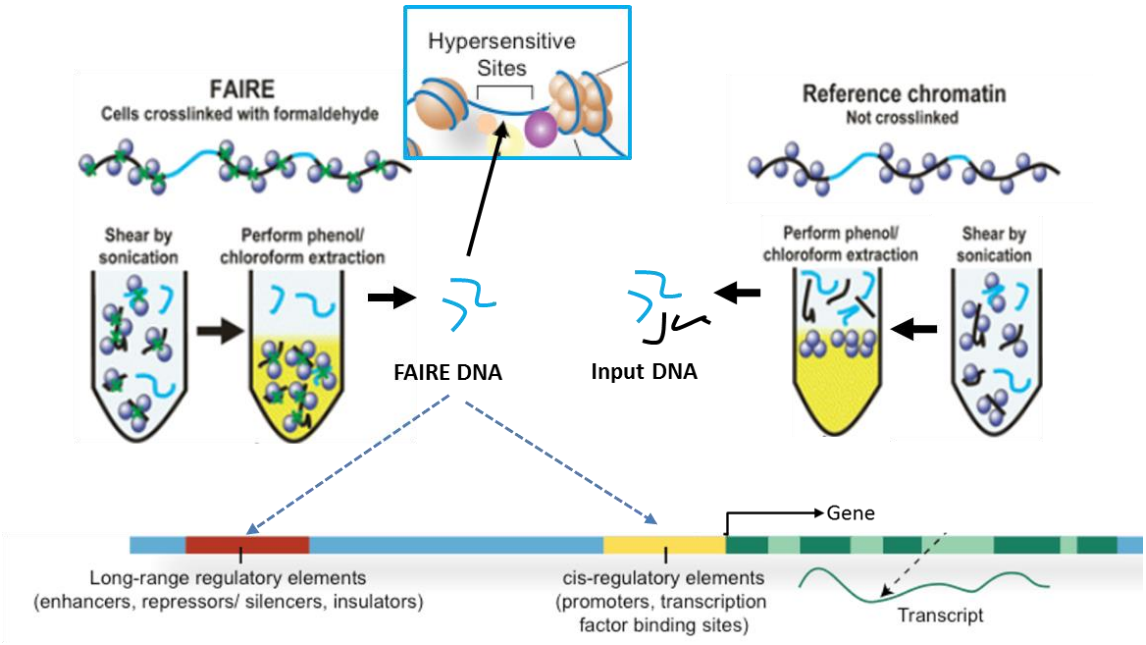

Figure 2.14 Principles of formaldehyde-assisted isolation of regulatory elements (FAIRE).

Cells was crosslinked with formaldehyde and sheared by sonication. DNA lysis was subjected to phenol/chloroform extraction to harvest the open chromatin (FAIRE DNA), which is hypersensitive sites interacting with regulatory factors during transcription. Reference chromatin (Input DNA) was also obtained from cells without formaldehyde-crosslinking. Modified from http://www.encode.com and published literature.[140]

2.9.1 Cross-linking and sonication

Cells in a T75 flask was cultured with growth medium until reaching up 90% confluence and a final concentration of 1% of formaldehyde was added into and incubated for 5 min while rocking at room temperature. A final concentration of 125mM of glycine was added to quench the formaldehyde. The cells were then washed with ice cold PBS and scraped into fresh 1.5ml tubes. The cells were resuspended in lysis buffer (10mM Tris-HCl pH8.0, 2% v/v Triton X-100, 1% w/v SDS, 100mM NaCl, 1mM EDTA) and incubated on ice for 10 min and then sonicated to shear DNA to length between 200bp and 500bp (40 seconds sonication for HUASMC). The sonicated

samples were centrifuged, the supernatants, which contained the sonicated DNA fragments, were kept in -80 °C until next step.

2.9.2 Preparation of DNA

400µl cell lysate was added into fresh 1.5ml tubes and centrifuged at 15,000g for 5 min at 4 °C to pellet cell debris. Supernatants containing chromatin was transferred into 1.5ml tubes and 1 volume of phenol/chloroform/isoamyl alcohol was added into each tube. The samples were then mixed by vortex and centrifuged at 15,000g at 4 °C for 5 min. The aqueous (top) layer was removed into fresh 1.5ml tubes. 150µl 10mM Tris-HCl pH7.4 was added into the tubes containing the interphase and organic layers, centrifuged and the top layer was transferred into previous aqueous material tubes. Extraction of open DNA fragments by phenol/chloroform/isoamyl alcohol as described above was repeated. 200µl chloroform/isoamyl alcohol was added into tubes and centrifuged at 12,000g for 5min to remove then trace of phenol. The aqueous layer was collected, with the addition of 2 volumes of 95% ethanol, 1/10 volume of 3M Sodium Acetate (pH 5.2) and 1µl 20mg/mL glycogen (Thermo Scientific) was added into the materials. This was incubated at -80 °C for 2 hours. Samples were taken out and centrifuged at 12,000g for 15min to obtain a DNA pellet. The supernatant was carefully removed and DNA pellets were washed with 500µl ice cold 70% ethanol. The DNA pellets were then dried by leaving tubes open for 60min and then eluted in 50µl 10mM Tris-HCl pH7.4. Samples with 1µl proteinase K were incubated at 55 °C for 1h, with following heating at 65 °C overnight to reverse DNA-DNA crosslinks.

2.9.3 Purification of DNA

Samples were purified using the Wizard® SV Gel and PCR Clean-Up System (Promega, A9281) according to introduction. DNA was eluted twice with 15μl 10mM Tris-HCl pH7.4, then quantified by NanoDrop and stored at -80 ^{o}C until use in downstream processes.

2.9.4 Detection of FAIRE enrichment by sequencing

PCR for FAIRE DNA and input DNA flanking SNPs of interest were performed, and DNA purification from gel and following Sanger sequencing were carried out to detect allelic enrichment (technique details see section 2.5.2-2.5.5.)

2.10 Cell proliferation assay

Proliferation of VSMCs and ECs play an important role in the development of hypertension. NPR-C has been shown that, as a Gi protein coupled receptor, it could regulate cell proliferation via NPR-C related signalling pathway [133]. Therefore, cell proliferation assay was carried out to explore whether BP-associated SNPs at *NPR3* gene locus influence the proliferation of HUASMCs and HUVECs using CCK-8 kit (Sigma, UK).

This method is based on a chemical, WST-8 (2-(2-methoxy-4-nitrophenyl)-3-(4-nitrophenyl)-5-(2, 4-disulfophenyl)-2H-tetrazolium, monosodium salt), which produces a water-soluble formazan dye upon bio- reduction in the presence of an

electron carrier. The amount of the formazan dye generated by dehydrogenases in cells is directly proportional to the number of living cells.

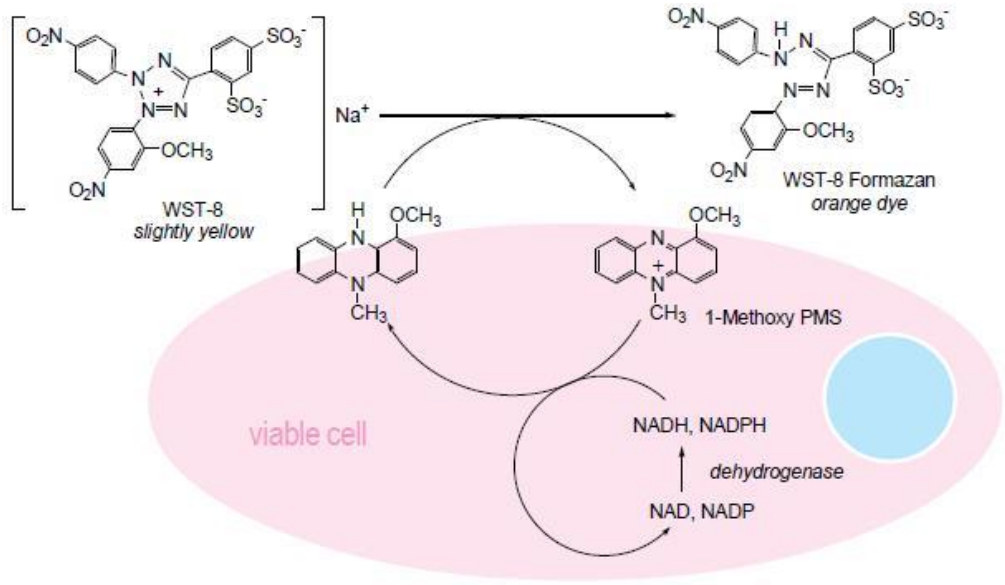

Figure 2.15 Principle of the cell viability detection with Cell Counting Kit-8.

The soluble tetrazolium salt in this assay, WST-8, is reduced by dehydrogenase activities in viable cells to give an orange-color formazan dye, which can be detected under the wavelength of 450nm. (http://www.dojindo.com/store/p/456-Cell-Counting-Kit-8.html)

In brief, cells were cultured in growth medium (see section 2.1.1). When the cells grew up to 80% confluence, they were detached with 0.25% trypsin-EDTA and sub-cultured into a new 0.04% gelatine-coated clear 96-well plate at a density (4,000 cells/ well for HUASMCs and 3,000cells/well for HUVECs) in triplicate, with fresh growth medium.

After incubation in a humid incubator with 5% CO_2 at 37^0C overnight, cell medium for HUASMCs was replaced with 100µl/well low-serum medium (DMEM with 0.5% FBS, 2mM L-glutamine, 100 U/mL penicillin and 100 mg/mL streptomycin) and cells was then starved for 24 hours. Subsequently, cells was cultured in 100µl/well growth

medium (formations see section 2.1.1) or with CNP /C-ANF$_{4-23}$ at the concentration of 100nM.). For HUVECs, cells was starved for 4h with 0.2% BSA in M199 then cultured in 100µl/well growth medium (see section 2.1.2.), with or without CNP/ C-ANF$_{4-23}$ at the concentration of 1nM. Cells were then incubated for 24 hours. 10µl/well of CCK-8 solution was added into each well of the plate, and was incubated for 2 hour at 37^{0}C, then the absorbance at baseline and 24 hours in each group was measured at 450nm using a microplate reader (Dynex MRX TC Revelation Microplate Reader).

2.10.1 Optimization of CNP concentration in HUASMCs

As described above, HUASMCs were plated into 96-well microplate overnight and starved, then treated with a serial concentrations of CNP. After incubation of 24h, proliferation in control and CNP groups were assayed by CCK-8. As indicated in Figure 2.17, higher doses of CNP (100nM and 1µM) significantly inhibited HUASMCs proliferation compared with control group. 100nM CNP was chosen here for the subsequent HUASMC proliferation assay (Figure 2.17).

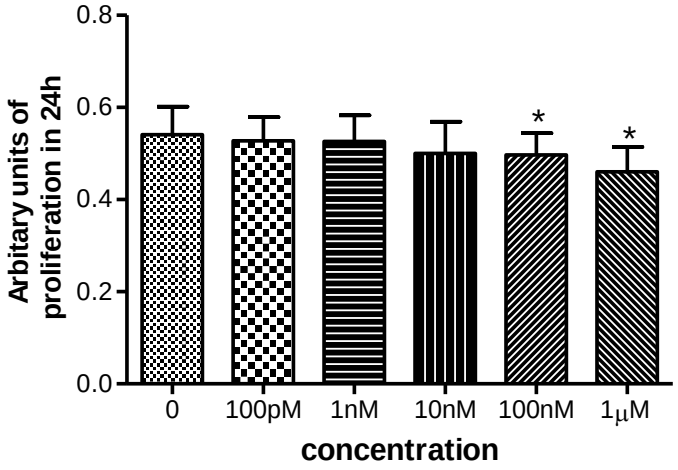

Figure 2.16 Optimization of CNP concentration in HUASMC proliferation.

HUASMCs were treated by a range of CNP (100pM to 1μM) for 24h, and proliferation was detected by cell counting assay. It was observed higher doses of CNP (100nM and 1μM) diminished the HUASMCs proliferation. N=5, * $P < 0.05$ by paired t test when CNP group compared with control.

2.11 *In vitro* scratch assay

To investigate whether these BP-associated SNPs affect the VSMCs ability of migration, the *in vitro* scratch assay was performed. The scratch assay is a convenient and cost-effective method to study cell migration which is based on the observation upon creation of a new artificial gap, so called 'scratch', on a confluent cell monolayer. The cells on the edge of the newly created gap will move toward the opening to close the 'scratch' until new cell-cell contacts are established again. This assay was conducted according to a previously published method with a small modification.[141]

Briefly, VSMCs were plated in a 24-well plate at a density of $1X10^5$ cells/well to reach a confluent cell monolayer overnight before the assay. Parallel lines were drawn using a marker pen on the back of each well and then a straight-line wound was made vertical to them by scratching the cell monolayer with a p200 sterile tip. The debris

was washed away with pre-warmed PBS twice and growth medium once, followed by adding a serial of working mediums as shown in the Table 2.16 below.

Table 2.14 Working media for *in vitro* scratch assay.

Working media	**Compositions**
Complete medium	DMEM with 15% FBS
CNP-complete medium	100nM CNP in complete medium
C-ANF$_{4-23}$ complete medium	100nM C-ANF$_{4-23}$ in complete medium
Low serum medium	DMEM with 0.5% FBS
CNP-low serum medium	100nM CNP in low serum medium
C-ANF$_{4-23}$ low serum medium	100nM C-ANF$_{4-23}$ in low serum medium

Images of the wound in each well were taken from some proper plots close to the parallel lines. Cells were then incubated in a humidified incubator with 5 % CO_2 at 37^0C and gap of the cell monolayer of each well was captured again after 6 hours and 12 hours respectively. Image J software was used to measure the distances between two edges of the wound.

2.12 Fluorescent imaging plate reader (FLIPR) calcium flux assay

Calcium flux was to detect changes in intracellular calcium using some sensitive, reliable fluorescent calcium indicators or dyes. Cells are incubated with loading dye in assay buffer and indicators passes through the cell membrane and esterase in the

cytoplasm cleave the acetoxymethyl ester (AM) portion of the molecular during the incubation (Figure 2.19). Once the target is activated, intracellular fluorescence change due to increased calcium concentration can be detected by fluorescent imaging plate reader (FLIPR) or FlexStation microplate readers.

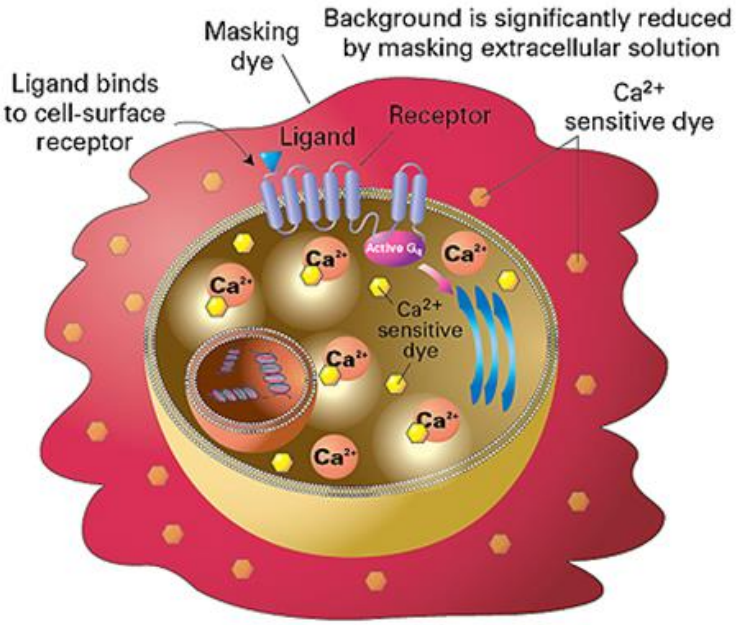

Figure 2.17 Calcium flux assay principle

Calcium sensitive dye ester is loaded into the cell and is cleaved by cell esterases to active dye. Ca^{2+} entering the cells bind to intra-cellular dye and results in increased fluorescent emission. (http://www.moleculardevices.com).

HUASMCs or HUVECs were plated into a gelatine-coated 96-well plate (clear bottom, black wall) at a density of 5,000 cells/well in triplicate with growth medium to get a confluence of around 80%, and incubated at 37^0C, 5 % CO_2 overnight. Cell medium in plate was replaced with 50µl fresh growth medium before loading. Loading buffer for each plate was prepared with fluorescent dye calcium 6, assay buffer with 20mM HEPES (Gibco,15630-106) in 1X Hanks' balanced salt solution (HBSS)

(Gibco,14065-056), and a final concentration of 2.5mM Probenicid (Thermo Scientific, P36400) according to the introduction of the FLIPR Calcium 6 assay Kit (Molecular Devices). Equal volume (50 µl) of loading buffer was added into each well, then the cell plate was incubated for two hours at 37^0C, 5 % CO2. Compounds plate 1 (96-well microplate, V-shaped bottom) with Losartan (Sigma, UK), Isoprothenol (ISO) (Sigma, UK), CNP and C-ANF_{4-23}, and compound plate 2 with Carbachol (Sigma, UK), angiotensin (Ang II) (Sigma, UK) were prepared freshly before reading (Table 2.17). All compounds were dissolved in ddH_2O filtered with 0.22µm filter units (Millipore, SLGP033RS) at a stock concertation of 1mM and 100mM (only for carbachol).

Table 2.15 The working concentrations of compounds used in FLIPR assay.

Compounds in plate 1	**Working concentrations**
Losartan	1µM
ISO	50mM, 1µM
CNP	1pM to 1µM
C-ANF_{4-23}	1pM to 1µM
Compounds in plate 2	**Working concentrations**
Carbachol	10mM
Ang II	1pM to 10µM

FLIPR machine programme was set up to 37^0C. 11µl of compounds in plate 1 were automatically dispensed into wells and incubated for 10min. 12µl of Ang II or Carbachol was then dispensed inside to stimulate the calcium flux. Once stimulation by agonists, Calcium flux signal was detected for 3min by every 1 second with the first 15 seconds as baseline reading (F0). The peak response signal during the reading is regarded as Fmax, then the relative signal was calculated by the formula of (Fmax-F0)/F0 (Figure 2.20). More than two independent experiments were run for each sample.

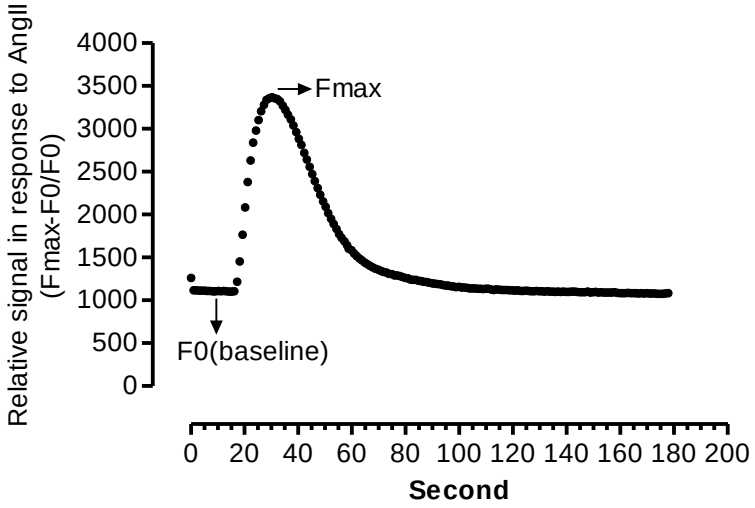

Figure 2.18 Representative trace of intracellular calcium changes in response to Ang II in HUASMCs.

Calcium flux signal under stimulation of Ang II was detected for 3 min. Baseline reading in the first 15 seconds is F0, and the peak response signal during the reading is regarded as Fmax, then the relative signal was calculated by the formula of (Fmax-F0)/F0.

2.12.1 Optimization of loading dyes and Ang II concentrations in HUASMCs

As described above, cells plates were incubated with three different loading dyes of Calcium 6 (Molecular Device), Fluo-4 (Invitrogen) and Calcium direct (Invitrogen) respectively and subjected to FLIPR reading with stimulation by 100μM pyrimidine nucleoside triphosphate (UTP) (Sigma), 10mM Carbachol as positive controls, PBS as negative control and a serial of Ang II from 1pM to 10μM. It is shown as Figure 2.20-A, Calcium 6 has a more sensitive response in positive controls groups compared with other two loading dyes. It was observed Ang II EC_{50} and $EC_{80/90}$ in HUASMCs using calcium 6 are around 10nM, 100nM respectively (Figure 2.20-B).

Except 10nM (EC_{50}) Ang II, 100nM Ang II was also chosen to utilised to detect the possible counteracting effect of compounds CNP/C-ANF_{4-23} on Ang II-induced intracellular calcium changes in subsequent experiments.

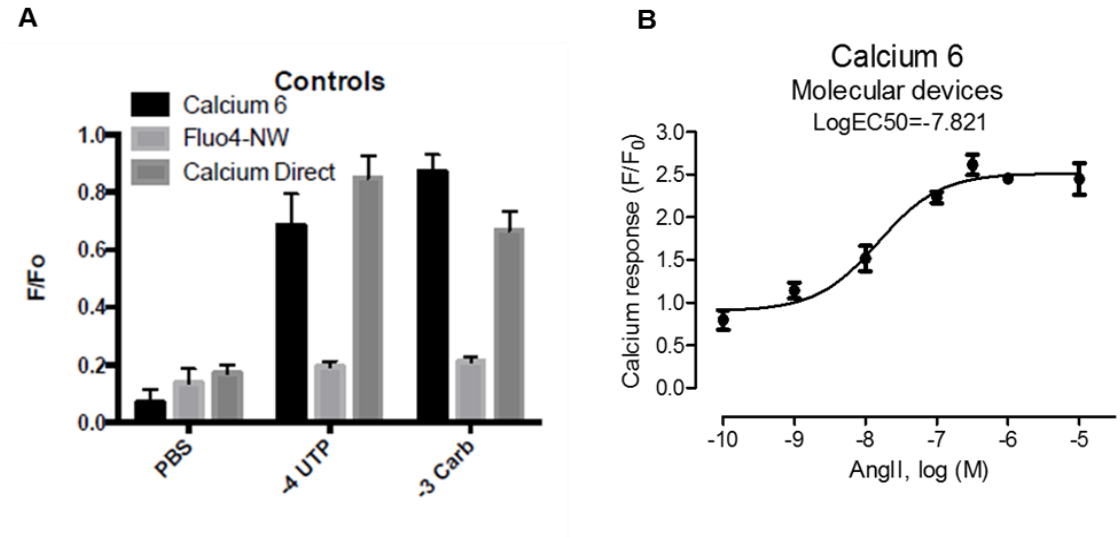

Figure 2.19 Optimization of three different loading dyes (A) and Ang II concentration with calcium 6 (B) in HUASMCs.

A, HUASMCs were incubated with three different loading dyes of Calcium 6, Fluo-4 and Calcium direct respectively under stimulation by UTP and carbachol with PBS as negative control. **B**, A serial of Ang II from 1pM to 10μM were utilised to induce HUASMCs calcium flux and the concentration curve showed the EC_{50} of Ang II in HUASMCs was $10^{-7.8}$ M.

2.12.2 Optimization of CNP/C-ANF_{4-23} concentrations in calcium flux in HUASMCs

As described in section 2.12, HUASMCs were incubated with calcium 6 loading buffer for 2 hours at 37^0C, 5 % CO_2, then pre-incubated with a range of CNP/C-ANF_{4-23} (1pM to 1μM), and Losartan (1μM) as antagonist control for 10 min. Ang II with a working concentration of 1nM was then dispensed into wells to stimulate the calcium flux. Fluorescent signal which presents the intercellular calcium changes was detected for 3 min and calculated by the formula of (Fmax-F0)/F0. Three independent experiments

were run for each sample. As shown in Figure 2.21, a dose-dependent inhibition was observed in Ang II-induced calcium flux when pre-treated with CNP/ C-ANF$_{4-23}$, and 1μM CNP/ C-ANF$_{4-23}$ could significantly counteract the intracellular calcium changes in response to 10nM Ang II.

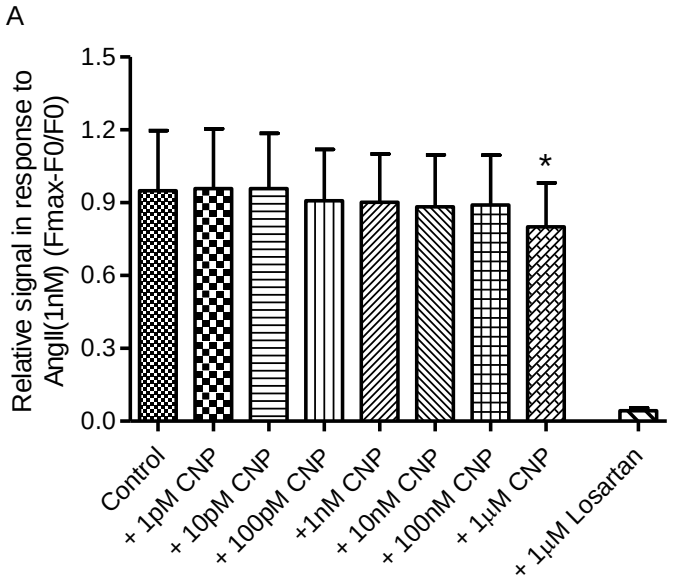

*p=0.019 when control vs 1μM CNP (N=9 running in triplicate)

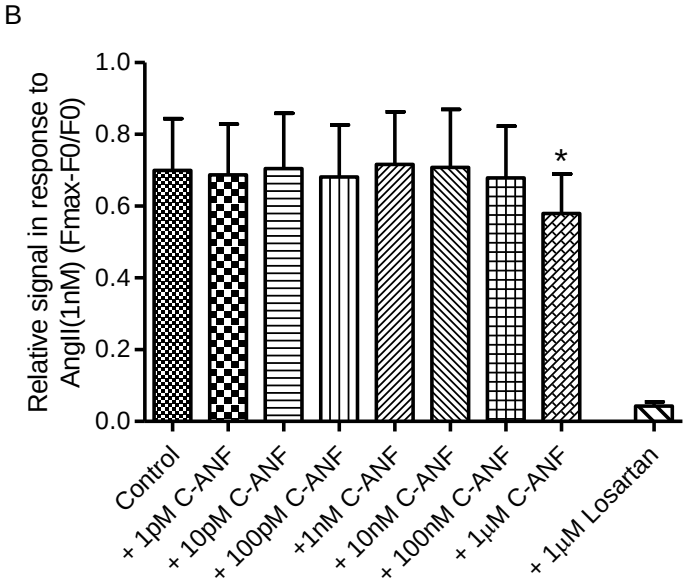

*p=0.015 when control vs 1μM C-ANP$_{4-23}$ (N=7 running in triplicate)

Figure 2.20 Optimization of concentrations of CNP (1pM to 1μM) (A) and C-ANF$_{4-23}$ (1pM to 1μM) (B) with Losartan (1μM) as antagonist control in Ang II (10nM) - induced intracellular calcium changes in HUASMCs.

Values are presented as mean ±SEM, *p<0.05 when control vs CNP/ C-ANF4-23, N≥ 7 running in triplicate.

2.12.3 Preliminary test for agonists of calcium flux in HUVECs

As described in section 2.12, HUVECs were incubated with Calcium 6 for 2 hours and subjected to FLIPR reading under stimulation by a range of agonists as listed in the Table 2.18 below and PBS as negative control. As compared with calcium signal of HUASMCs under 100nM Ang II, the response to Ang II as well as the other agonists in HUVECs were very low (Figure 2.23). This small signal window is probably not very proper to detect the potential genetic difference among genotypes in HUVECs. Thus, calcium flux for HUVECs was not conducted in this subject.

Table 2.16 Agonists used in HUVECs calcium flux.

Agonists	Working concentrations
UTP	1mM
bzUTP	1mM
Carbachol	10mM
Ang II	100nM

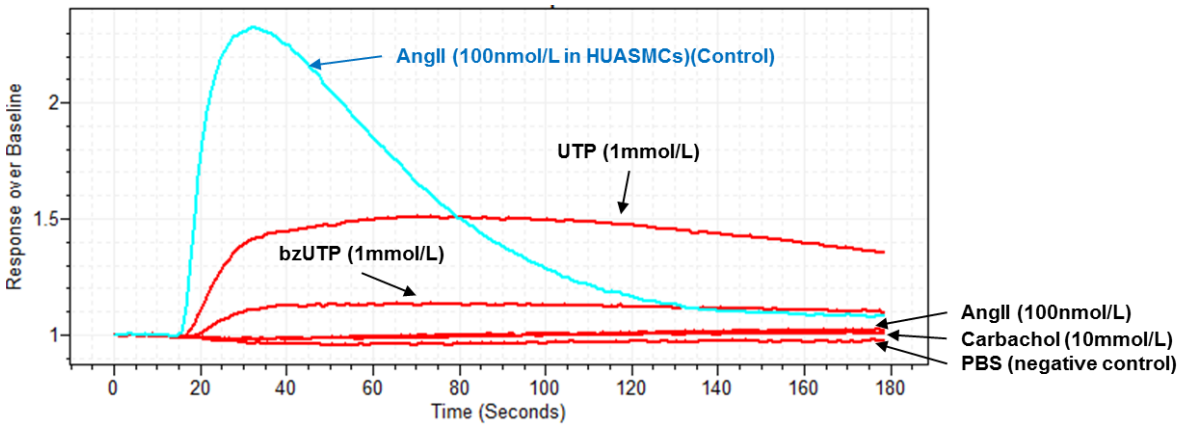

Figure 2.21 Optimization for agonist of calcium flux in HUVECs.

HUVECs were subjected to FLIPR reading under stimulation by UTP, bzUTP, Ang II, carbachol and PBS as negative control. However, the calcium signals in HUVECs were all very low compared with HUASMCs under Ang II.

2.13 Data and statistical analysis.

Statistical analyses were performed using Graph Pad Prism version 5 (Graph Pad Software, California, USA). Results are expressed as mean ± SEM. Comparisons between two groups were made with paired, unpaired student t test (two tailed) or Wilcoxon signed-rank test. Differences among three or more than three groups were analysed with one-way ANOVA in conjunction with a post-test of Bonferroni's Multiple Comparison Test. Results were considered significant at a value of $p < 0.05$.

3. Result of Functional study of BP-associated variants at the *NPR3* gene locus in HUASMCs

3.1 Genotyping results of BP- associated SNPs at the *NPR3* locus in HUASMCs.

Genomic DNA from HUASMCs was extracted and genotyped using the KASPar genotyping technique described in section 2.3. Genotyping results for the BP-associated SNPs were obtained by at least 2 replicates. A presentative plot for allelic discrimination is shown in Figure 3.1. All the BP-associated SNPs genotyping results in HUASMCs are in accordance with Hardy-Weinberg equilibrium (Table 3.1).

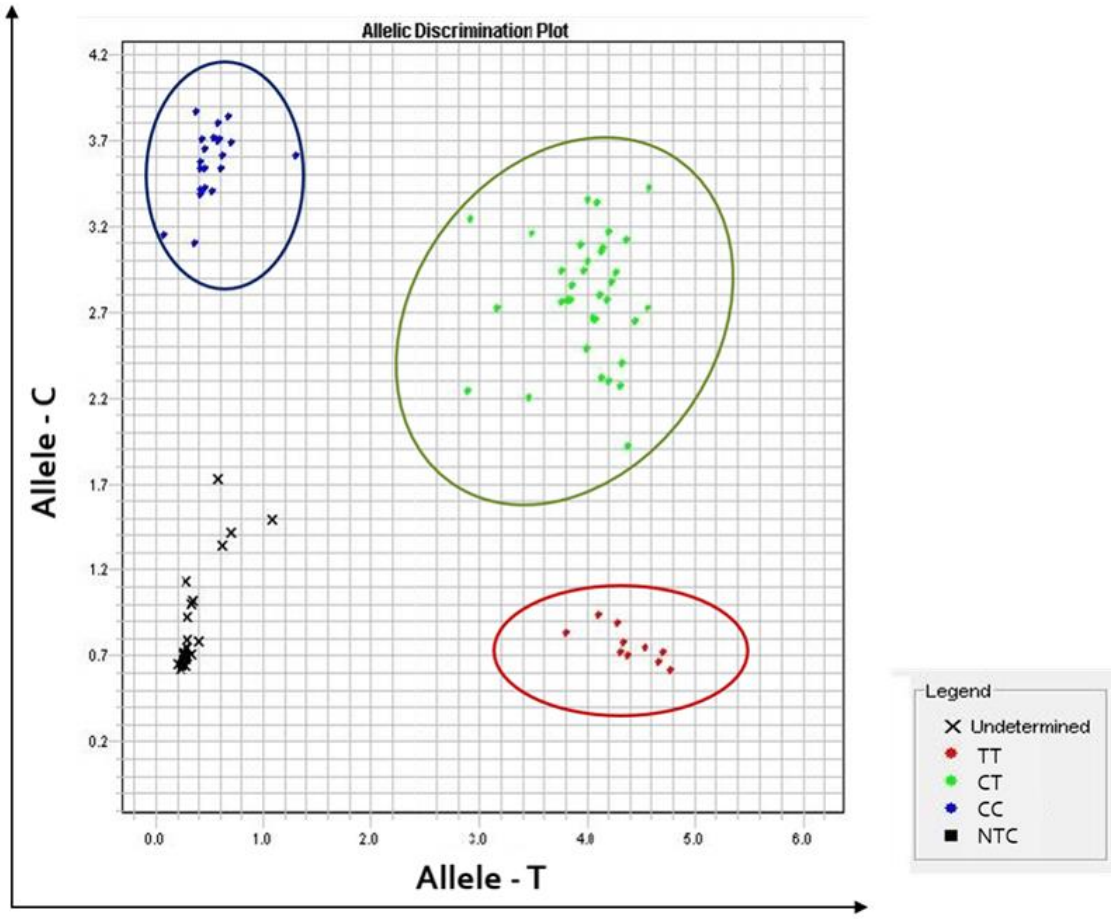

Figure 3.1 An allelic discrimination plot for SNP rs1173771 in HUASMCs analysed by SDS 2.3.

Four clusters were separated after genotyping. Blue cluster stands for the genotype of CC, green for CT, red for TT and black represents NTC and samples undetermined.

Table 3.1 BP-associated SNPs genotyping result in HUASMCs.

	Variants in block 1		
	rs1173743/ rs1173747(r^2=1)	rs1173756	rs1173771
Major allele homozygotes	85	85	89
Heterozygotes	107	112	107
Minor allele homozygotes	34	35	34
HWE calculation			
P-value by Chi-Square Test	0.9725	0.8484	0.8467
	Variants in block 2		
	rs7729447	rs3762988	rs1421811/ rs3828591(r^2=1)
Major allele homozygotes	130	101	104
Heterozygotes	70	89	86
Minor allele homozygotes	9	20	19
HWE calculation			
P-value by Chi-Square Test	0.9128	0.9511	0.8953

HWE= Hardy-Weinberg equilibrium

Moreover, the linkage disequilibrium values between these SNPs in our HUASMCs collection are very similar to those in the HapMap data set obtained using the SNAP programme (Table 3.2).

Table 3.2 Linkage disequilibrium (LD) values between *NPR3* SNPs.

Lead SNP	SNP in LD	Hap map value (CEU)	Value in current collection of HUASMCs
rs1173771	rs1173743/ rs1173747(r^2=1)	0.78	0.83
rs1173771	rs1173756	0.78	0.81
rs1173771	**rs1421811**	**0.13**	**0.15**
rs1421811	rs3828591	1.0	1.0
rs1421811	rs3762988	0.83	0.85
rs1421811	rs7729447	0.56	0.63

As predicted by HapMap and data in our collection, the LD between the two lead SNPs rs1173771 and rs1421811 is 0.13-0.15 (Table 3.2). Therefore, it appears that these two SNPs are in two separate LD blocks and thus functional studies were conducted independently for these two blocks.

3.2 Functional study of variants in the rs1173771 linkage disequilibrium block in HUASMCs

3.2.1 Effect of BP-associated SNPs on *NPR3* mRNA level in HUASMCs

Quantitative Reverse transcription PCR (qRT-PCR) was performed on mRNA extracted from HUASMCs (see section 2.5.1) to assess if the BP-associated SNPs rs1173771, rs1173743, rs1173747 and rs1173756 are associated with *NPR3* expression level. To test the *NPR3* expression levels in HUASMCs, SYBR-Green qPCR technique was used here (as described in section 2.4). After analysis by SDS 2.3, a Ct value which presents the quantitation of gene expression of samples was obtained, the delta Ct (ΔCt) of samples was then obtained by standardising to the internal reference gene 18S, and delta delta Ct (ΔΔCt) in each group by standardized

with the mean of ΔCt of BP-elevating allele homozygous group (reference group). Relative *NPR3* expression levels were transformed using $2^{-\Delta\Delta Ct}$ and plotted by each genotype of HUASMCs. The statistics was finally analysed by One-way ANOVA with a post-test of Bonferroni's Multiple Comparison Test.

In addition of real-time PCR, another method, allelic expression imbalance (AEI), was also performed to investigate whether BP-associated SNPs could influence *NPR3* mRNA level. Briefly, this assay was conducted in HUASMCs that were heterozygous for the 3-UTR SNP rs1173756 (C/T), and the ratio of the two alleles in genomic DNA and mRNA was obtained and compared by Wilcoxon signed rank test.

3.2.1.1 Association of BP-elevating allele with decreased *NPR3* mRNA level

In HUASMCs samples, there was lower relative *NPR3* mRNA level in samples with the BP-elevating allele (major allele) the intronic SNPs rs1173747 and rs1173743, and no significant difference heterozygotes and homozygotes of this allele (AA versus AC) (Figure 3.3 B). It was also demonstrated that a similarly decreased level is present in BP-elevating allele carriers of 3-UTR SNP rs1173756 (Figure 3.3 C). This difference was also noted with the down-stream SNP rs1173771, but did not reach statistical significance with the current sample size. (Figure 3.3 D). These data show that the BP-associated SNPs in rs1173771 linkage disequilibrium block is associated with *NPR3* gene mRNA expression level.

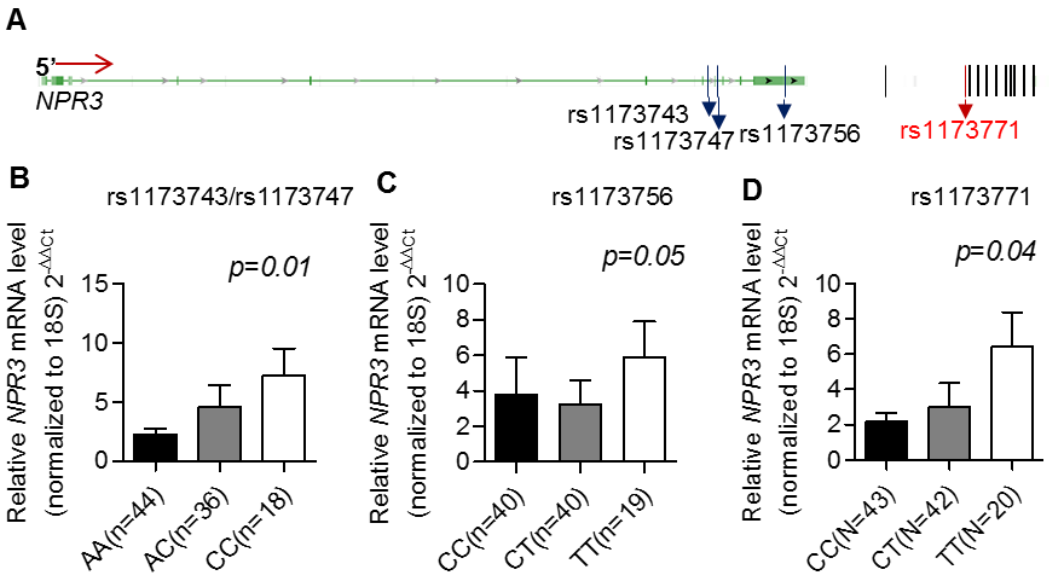

Figure 3.2 Quantitative analysis of mRNA levels of *NPR3* among BP- associated SNPs in linkage disequilibrium block of rs1173771 in HUASMCs.

A, Positions of BP-associated variants of rs1173771 linkage disequilibrium block at the *NPR3* gene locus. **B, C, D**, genotype-dependent effect on *NPR3* gene mRNA level by quantitative reverse-transcription polymerase chain reaction (qRT-PCR) assay for intronic variants rs1173743 and rs1173747 (r^2=1.0) (**B**), 3'UTR variant rs1173756 (**C**), and 3' flanking region variant rs1173771 (**D**), respectively. Values are presented as mean ± SEM, *P<0.05, **P<0.01 by Kruskal-Wallis test.

3.2.1.2 Allelic expression imbalance of *NPR3*

A further experiment, allelic expression imbalance (AEI) assay, was carried out to investigate the relative expression levels of the two alleles of the BP-associated SNPs. The 3'-UTR SNP rs1173756 was used as a maker in this assay because it is in the *NPR3* transcript whereas the other SNPs are intronic or downstream and therefore cannot been directly analysed in this assay. Genomic DNA and cDNA (mRNA) of HUASMCs from 8 heterozygotes were subjected to end-point PCR and subsequent Sanger sequencing. As shown in Figure 3.4, the peak height of the BP-elevating allele

(major allele, C) versus that of the alterative allele (minor allele, T) was significantly lower in the chromatogram from cDNA than that from the chromatogram from genomic DNA in HUASMCs, suggesting lower *NPR3* expression of the BP-elevating allele, which is in agreement with qRT-PCR data described above.

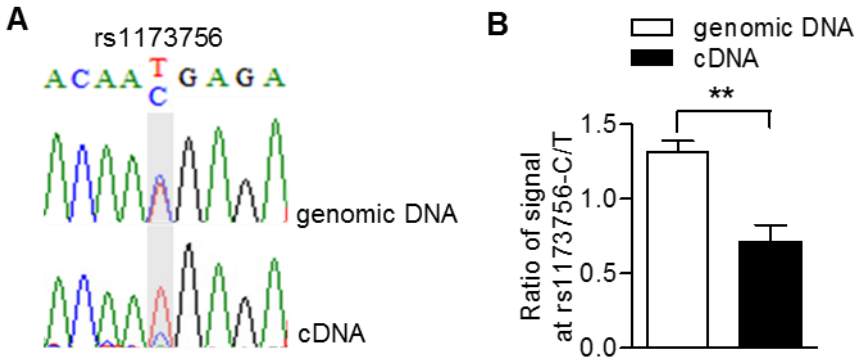

Figure 3.3 Allelic expression imbalance of 3-UTR SNP rs1173756 in the *NPR3* gene in HUASMCs.

A, Representative section of sequencing chromatogram showing the peaks of the two alleles (T and C) of rs1173756 in genomic DNA and corresponding cDNA samples from HUASMCs. **B**, The peak height of each allele was determined by the Peak Picker programme. Column chart shows means and SEM of relative peak heights of the two alleles in the chromatograms from genomic DNA and cDNA, respectively, in HUASMCs from 8 individuals, **P=0.0078 by Wilcoxon signed-rank test.

3.2.2 Effects of variants in the rs1173771 LD block on NPR-C protein level

To investigate whether the BP-associated SNPs influence NPR-C protein expression, Western blot analysis was completed with HUASMCs samples from individuals of different genotypes for rs1173747 (also for rs1173743, rs1173756 and rs1173771 due to LD). The assay revealed lower NPR-C protein levels in BP-elevating allele homozygotes than in BP-lowering allele homozygotes (Figure 3.4). These results are in line with the analyses of mRNA levels (section 3.2.1).

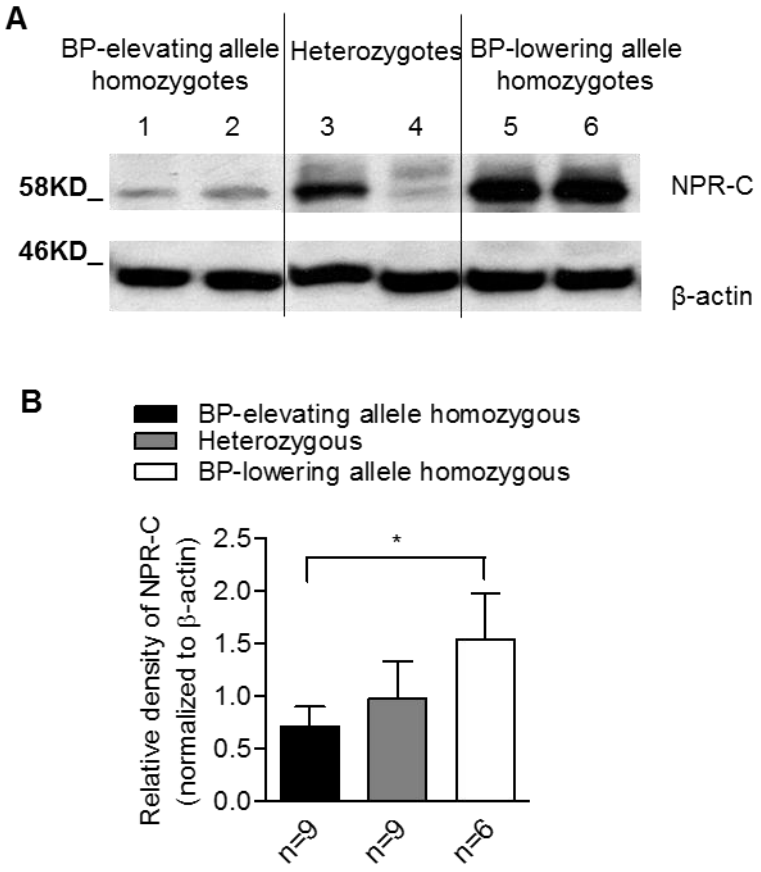

Figure 3.4 Blood pressure-associated variant in rs1173771 LD block significantly affect natriuretic peptide receptor C (NPR3) protein level in human umbilical arterial smooth muscle cells (HUASMCs).

A,B, Western blotting shows NPR-C protein level is lower in HUASMCs homozygotes of the BP-elevating genotype compared with BP-lowering allele homozygotes, *P<0.05 by unpaired t-test (N≥5 for each genotype).

3.2.3 Interaction of BP-associated SNPs in rs1173771 LD block with nuclear proteins

To investigate whether BP-associated SNPs interact with nuclear proteins, electrophoretic mobility shift assays (EMSA) were carried out. Biotin-labelled oligos representing regions around BP-associated SNPs were incubated with nuclear extracts from HUASMCs. In studies relating to the intronic SNP rs1173743, an allelic-specific DNA-protein complex was observed in this *in vitro* assay, showing a higher affinity for the rs1173743-G probe than for the rs1173743-T probe, and band for this complex was abolished by 50 fold excess specific unlabelled rs1173743-G oligo (Fig 3.6 A, lane 7) but not by an unspecific competitor (Figure 3.6 A, lane 6). Protein interaction was also detected for another intronic SNP, rs1173747, and the complex for the rs1173747-C allele was almost fully competed out by 50 fold excess unlabelled rs1173747-C oligo (lane 7 in Figure 3.6 B), whereas the complex for the rs1173747-A allele was not (lane 7 in Figure 3.6 B), suggesting a difference between two alleles in their affinity with nuclear protein. . As shown in Figure 3.7, protein interaction was also detected for rs1173771 and rs1173756, and assays with competitors suggest an allelic effect on protein interaction by rs1173756 (Figure 3.7, lanes 9 and 12) but not rs1173771 (Figure 3.7, lanes 3 and 6).

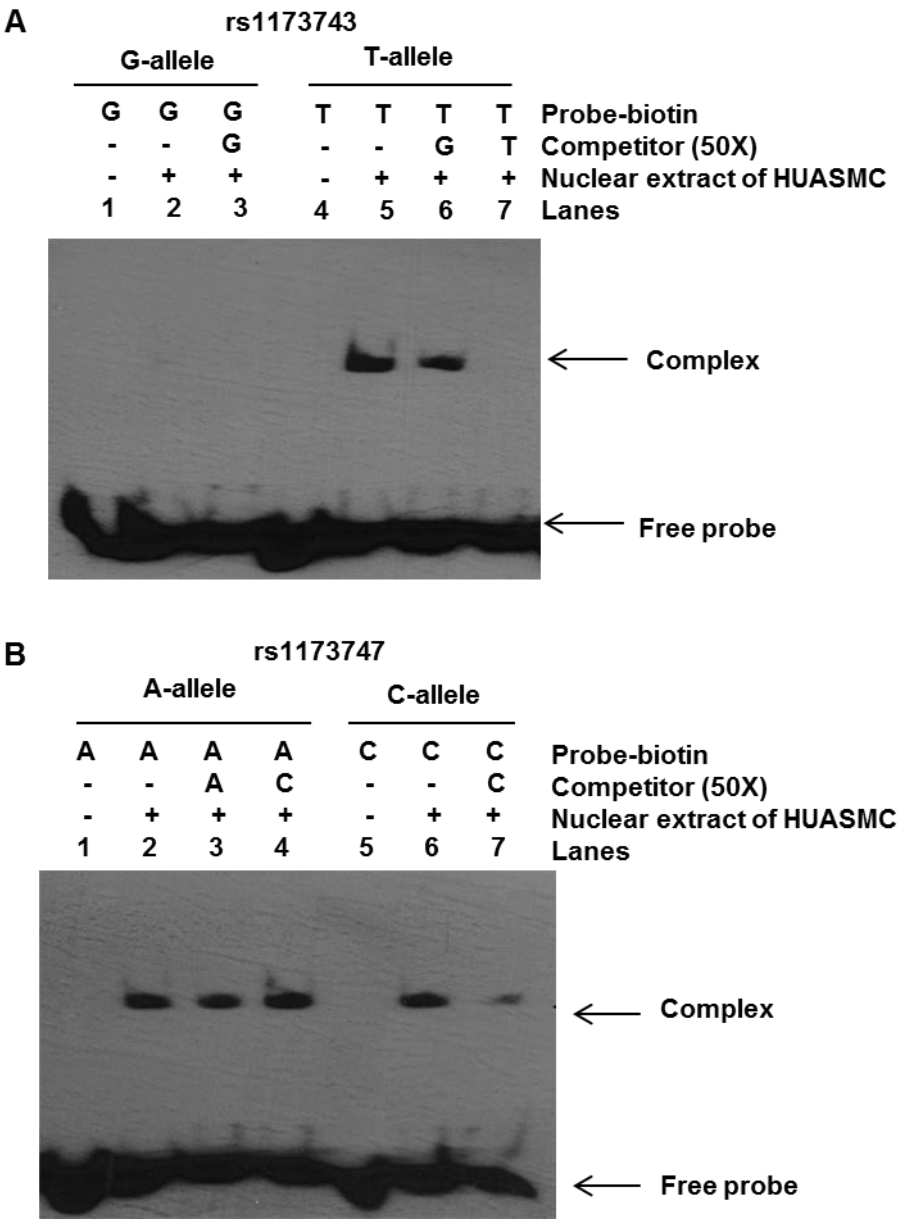

Figure 3.5 Interaction of *NPR3*-intronic SNPs rs1173743 and rs1173747with HUASMC nuclear proteins *in vitro*.

The Biotin-labelled oligonucleotide probes were incubated with HUASMC nuclear extracts, and also with or without-50 fold molar excess of unlabelled oligos as competitors. As shown in image **A** are assays of rs1173743-G and rs1173743-T probes and image **B** are assays of rs1173747-A and rs117374-C probes.

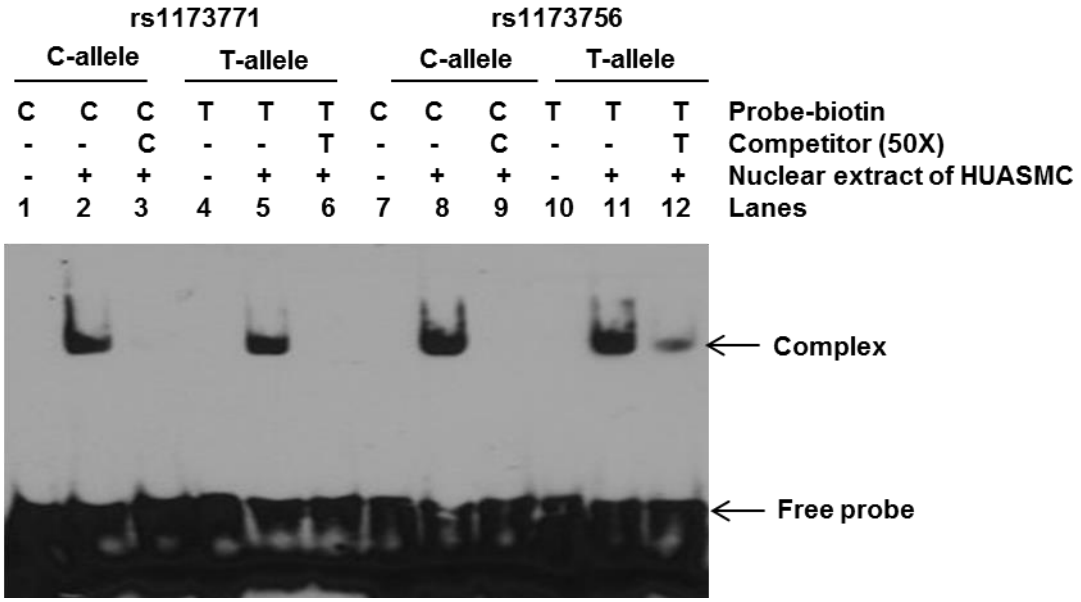

Figure 3.6 Interaction of *NPR3* SNPs rs1173771 (intergenic) and rs1173756 (located in 3'-UTR) with HUASMC nuclear proteins *in vitro*.

Biotin-labelled oligonucleotide were incubated with HUASMC nuclear extracts, and also with or without 50 fold molar excess of unlabelled oligos as competitors.

3.2.4 BP-associated variants reside in open chromatins in HUASMCs

Open chromatin (euchromatin) is widely regarded as permissible structures for transcription through binding of regulatory elements (Clapier & Cairns, 2009). FAIRE was conducted here to explore whether blood-pressure associated variants reside in the open chromatin region, to further investigate the potential molecular mechanism of genetic regulation of *NPR3* in HUASMCs.

3.2.4.1 BP-elevating allele of rs1173747 is less represented in open chromatin in HUASMCs.

To assess the potential allelic imbalance of open chromatin status, FAIRE and input DNA samples were subjected to Sanger sequencing. The sequencing signals of the rs1173747-BP-elevating allele (A) were less enriched in FAIRE DNA relative to input DNA of HUASMCs (Figure 3.8 A+B). Allelic-specific qPCR was also performed to determine the relative levels of BP-elevating allele (A) and BP-lowering allele (C) in the FAIRE DNA and corresponding input DNA, and also showed a much lower level of BP-elevating allele in FAIRE DNA (Figure 3.8 -C). These results indicate that the intronic SNP rs1173747 is located in the open chromatin in HUASMCs with an allelic imbalance pattern.

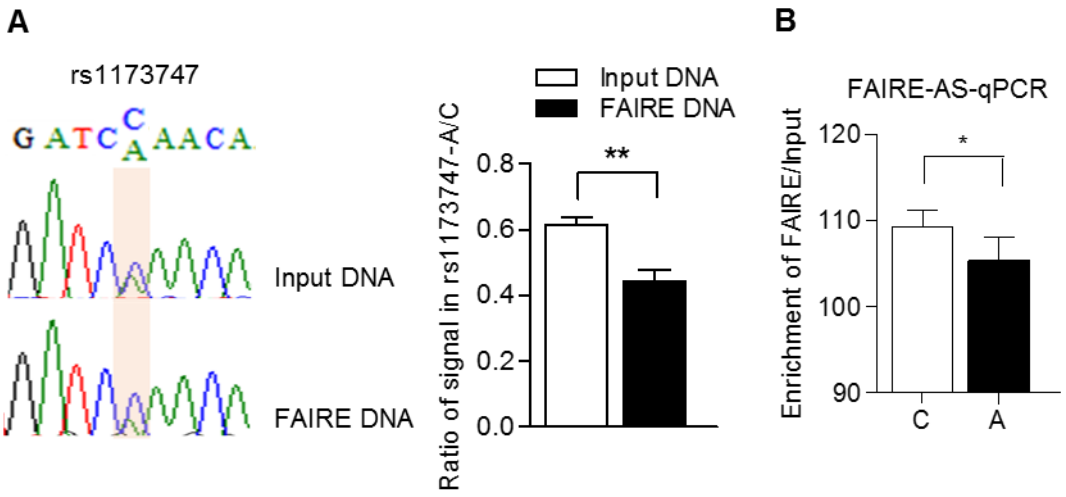

Figure 3.7 Allele-specific difference of rs1173747 in open chromatin in HUASMCs.

Sanger sequencing chromatograms of FAIRE and input DNA from the region around rs1173747 revealed that the minor allele (C) is enriched in open chromatin in HUASMCs (N=6) (**A**), and allelic-specific qPCR confirmed this finding (N=8) (**B**).

3.2.4.2 BP-elevating allele of rs1173756 is less represented in open chromatin in HUASMCs.

A similar assay was performed for rs1173756 and showed that the rs1173756-BP-elevating allele (C) was less enriched in FAIRE DNA relative to input DNA in HUASMCs (Figure 3.9-A+B).This finding suggests the 3'-UTR SNP rs1173756 is located in the open chromatin in HUASMCs with an allelic imbalance pattern, which direction is also in line with the rs1173747 data.

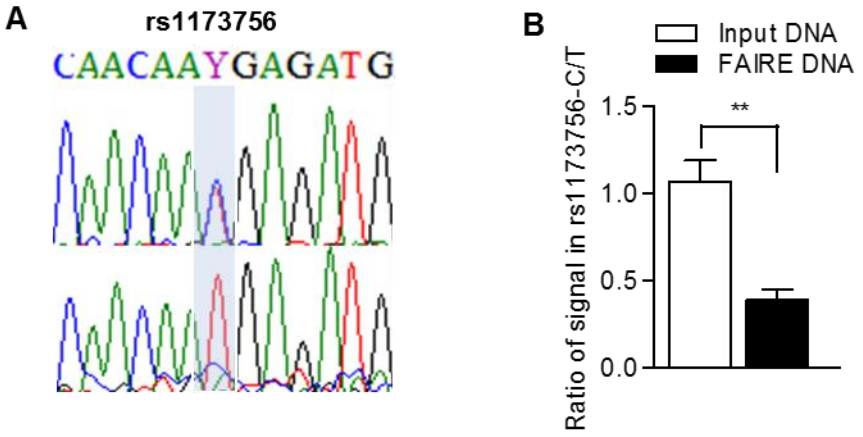

Figure 3.8 Allele-specific difference of rs1173756 in open chromatin in HUASMCs.

Sanger sequencing chromatograms of FAIRE and Input DNA from the region flanking rs1173756 revealed that the minor allele (C) is enriched in open chromatin fragments in HUASMCs (N=5).

3.2.5 BP-elevating allele of variants in the rs1173771 LD block increases HUASMC proliferation

Proliferation of VSMCs contributes to the development of hypertension. NPR-C, as a G_i protein coupled receptor, has been shown to regulate cell proliferation via NPR-C related signalling pathway [133], therefore, the primary HUASMCs proliferation was determined by cell counting assay (as described in section 2.10) to see whether there is an effect of BP-associated SNPs on cell proliferation. Cells were also incubated with or without 100nM CNP or C-ANF$_{4-23}$ (a specific NPR-C agonist) for 24 hours to investigate the effect of this receptor related signalling on cell proliferation.

rs1173771 genotype pattern in these HUASMCs studied is concordant with other three SNPs (rs1173743/rs1173747, rs1173756), thus the genotypes will be referred to as BP-elevating allele homozygotes, heterozygotes and BP-lowering allele homozygotes.

The study revealed that there is a significant difference between genotypes of *NPR3* BP-associated SNPs in HUASMC proliferation, with a markedly increased proliferating rate in BP-elevating allele carriers in contrast to BP-lowering allele homozygous samples (Figure 3.10). Furthermore, treatment of CNP or C-ANF$_{4-23}$ significantly diminished proliferation in HUASMCs, with a trend of genetic difference of drugs inhibitory effect with less inhibition in HUASMCs carrying the BP-elevating allele compared with those of BP-lowering allele homozygotes (Figure 3.11), which is in line with the findings of their effects on *NPR3* gene expression.

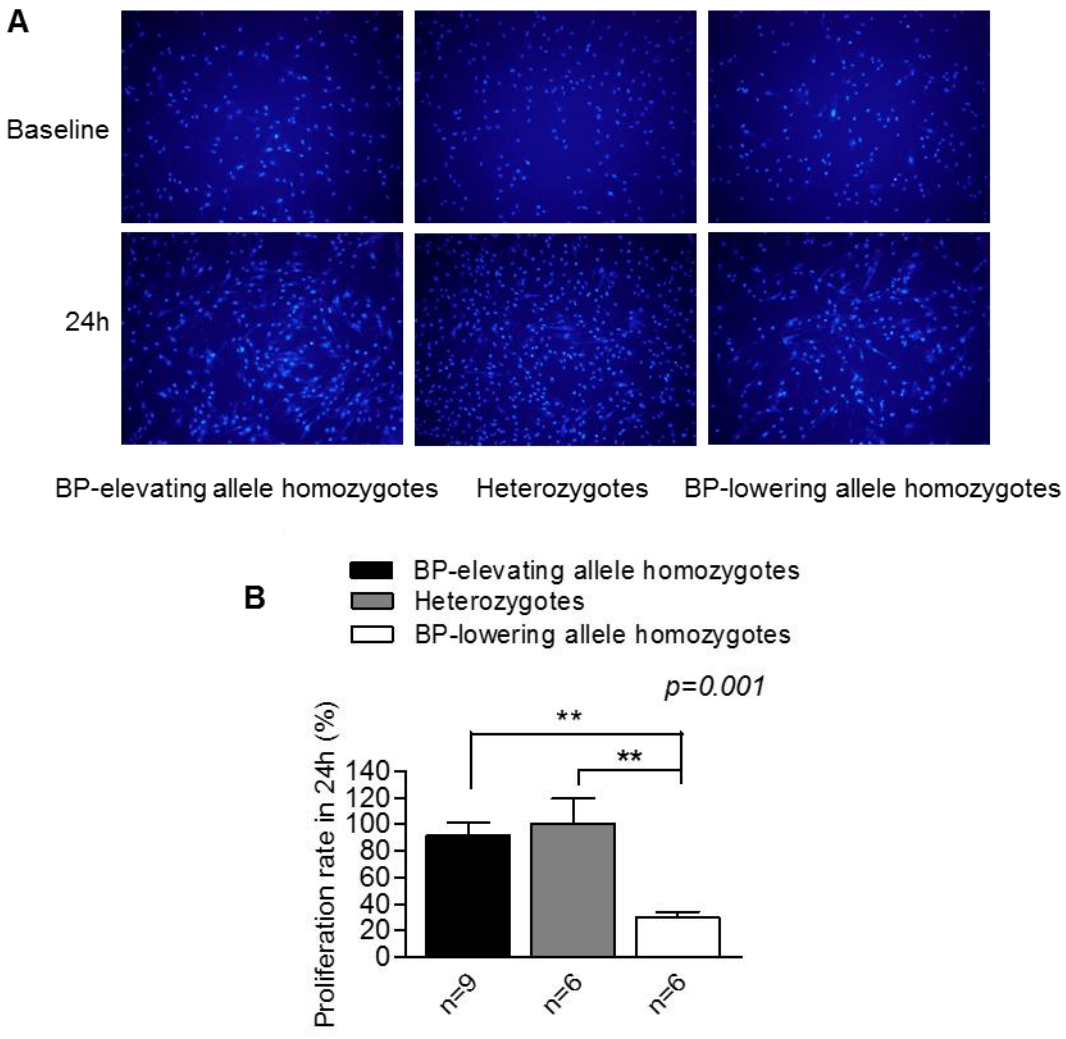

Figure 3.9 Effect of BP-associated variants in the rs1173771 LD block in *NPR3* on HUASMCs proliferation.

A, Representative images showing differences between genotypes in cell density at baseline and in 24h. **B**, Cell proliferation was measured at 24h by cell counting assay (CCK-8). A significantly increased cell growth rate was observed in HUASMCs carrying the BP-elevating allele compared with cells of BP-lowering allele homozygotes (CC). N≥6 for each genotype in at least duplicate. Values are presented as mean ± SEM, *P<0.05, **P<0.01 by one-way ANOVA with Bonferroni correction for a number of tests for different genotypes.

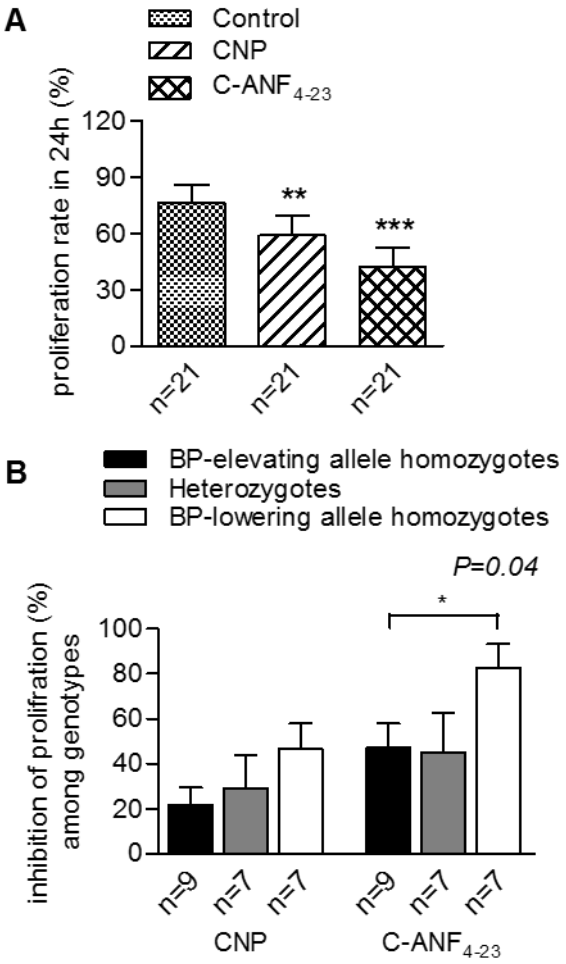

Figure 3.10 Inhibitory effect of CNP/ C-ANF$_{4-23}$ on HUASMC proliferation.

A, C-type natriuretic peptide (CNP) and the NPR-C specific agonist C-atrial natriuretic peptide (C-ANF$_{4-23}$) attenuated HUASMC proliferation. N≥19 for each group in at least duplicate. Values are presented as mean ± SEM, **P<0.01, ***P<0.001 when comparing CNP or C-ANF$_{4-23}$ vs control by Wilcoxon signed-rank test. **B,** when treated with CNP or CANF$_{4-23,}$ the inhibitory effect of drugs in BP-elevating allele homozygotes is less than BP-lowering allele homozygous samples. N≥6 for each genotype running at least duplicate. Values are presented as mean ± SEM, *P<0.05, when comparing BP-elevating allele homozygotes vs BP-lowering allele homozygotes by unpaired t test.

3.2.6 BP-associated variants at the *NPR3* locus have no effect on HUASMC migration

In addition to cell proliferation, I also sought to investigate whether BP-associated variants at the *NPR3* gene locus have an impact on cell migration. Scratch assay, as described in section 2.11, was used here to explore the possible genetic effect of NPR3 variants in primary HUASMCs from different individuals.

The study showed no significant association between SNPs in rs1173771 LD block studied and HUASMCs migration, although treatment of 100nM CNP or C-ANF$_{4-23}$ could inhibit the migration ability of HUASMCs (N≥5 for each genotype). (Figure 3.12), indicating association between these SNPs and BP control is not through regulating cell migration.

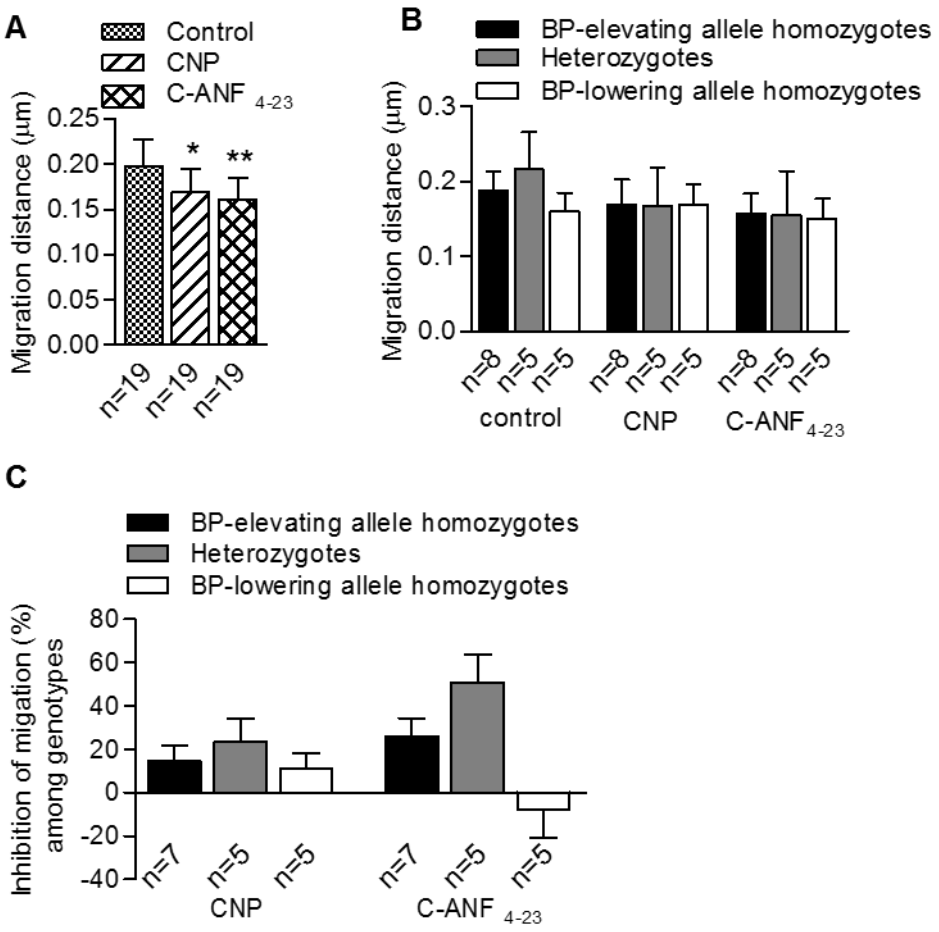

Figure 3.11 No significant effect of blood pressure (BP)-associated variants in rs1173771 LD block at the *NPR3* locus on cell migration in HUASMCs.

A, CNP or C-ANF$_{4-23}$ inhibited the migration rate of HUASMCs in in vitro scratch assay. N=19 for each group. **B**, No association was observed between BP-associated variants and cell migration in HUASMCs with or without CNP/C-ANF$_{4-23}$. **C**, No genetic difference of inhibitory effect of CNP/C-ANF$_{4-23}$ was observed in HUASMCs cell migration. N≥5 for each genotype running at least duplicate. Values are presented as mean ± SEM, Genetic difference among genotypes was analysed by one-way ANOVA with Bonferroni correction for the number of tests for genotypes. *P<0.05, **P<0.01 when CNP/CANF$_{4-23}$ vs control by Wilcoxon signed rank test.

3.2.7 BP-elevating allele of variants in the rs1173771 LD block increases intracellular calcium flux in response to Ang II in HUASMCs.

Calcium flux was carried out by FLIPR with previously optimized fluorescent loading dye, Calcium 6 (see section 2.12.1) in HUAMCs. The aim was to study the impact of BP-associated variants on intracellular calcium changes under stimulation of Ang II and Carbachol (positive control). A preliminary experiment indicated the concentration of EC_{50} of Ang II required to activate calcium flux is approximately 10nM in HUASMCs (see section 2.12.1). Cells were stimulated with 10nM Ang II (EC_{50}), 100nM Ang II ($EC_{80/90}$), or 10mM carbachol. To explore the possible related signalling pathway, cells were also pre-treated with CNP/C-ANF_{4-23} before stimulation.

Cells were plated at a similar density among genotypes and incubated with loading dye calcium 6 (Figure 3.13). No genetic association of intracellular calcium changes was observed in response to carbachol. However, HUASMCs that are either homozygotes for the BP-elevating allele or heterozygotes exhibited an augmented intracellular calcium level in response to Ang II in contrast to BP-lowering allele homozygotes (Figure 3.14). These results imply *NPR3* gene with the risk variant is involved in the intracellular calcium response to Ang II.

We next examined the effect of CNP and the NPR-C specific agonist, C-ANF_{4-23}, on the calcium flux with losartan (1μmol/L) as antagonist control. In the presence of CNP or $CANF_{4-23}$ (1μmol/L), HUASMCs continued to exhibit the same genetic difference in both doses of Ang II-stimulation (Figure 3.15A). CNP or $CANF_{4-23}$ significantly counteracted the augment of intracellular calcium in response to the lower dose of Ang II (10nM), and even under a higher dose of Ang II (100nM), $CANF_{4-23}$ was still effective. However, no significant difference of inhibitory effect of CNP or $CANF_{4-23}$ on

genotype was detected, with a slightly lower effect on BP-elevating allele samples, which is in accordance with its *NPR3* expression level (Figure 3.15).

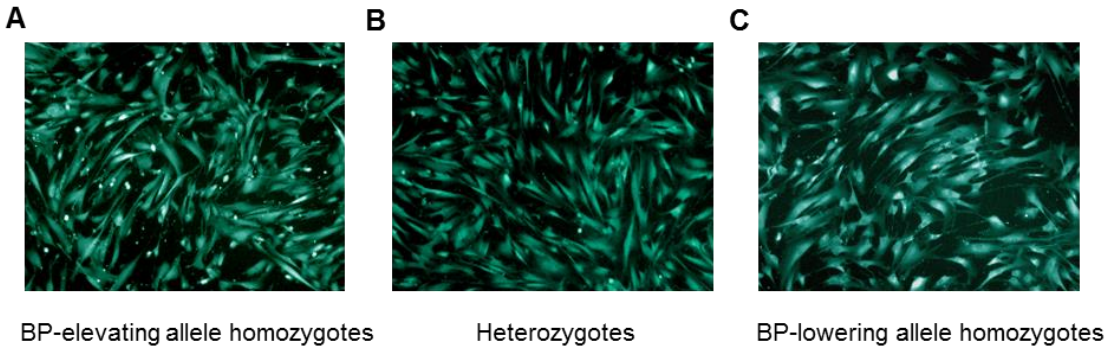

Figure 3.12 Representative figures to show cell density of human umbilical arterial smooth muscle cells in each genotype after incubated with fluorescent loading dye calcium 6.

A, B, C, HUASMCs were plated into cell plate at a similar cell density and images were taken after 2 hours incubation with loading dye calcium 6.

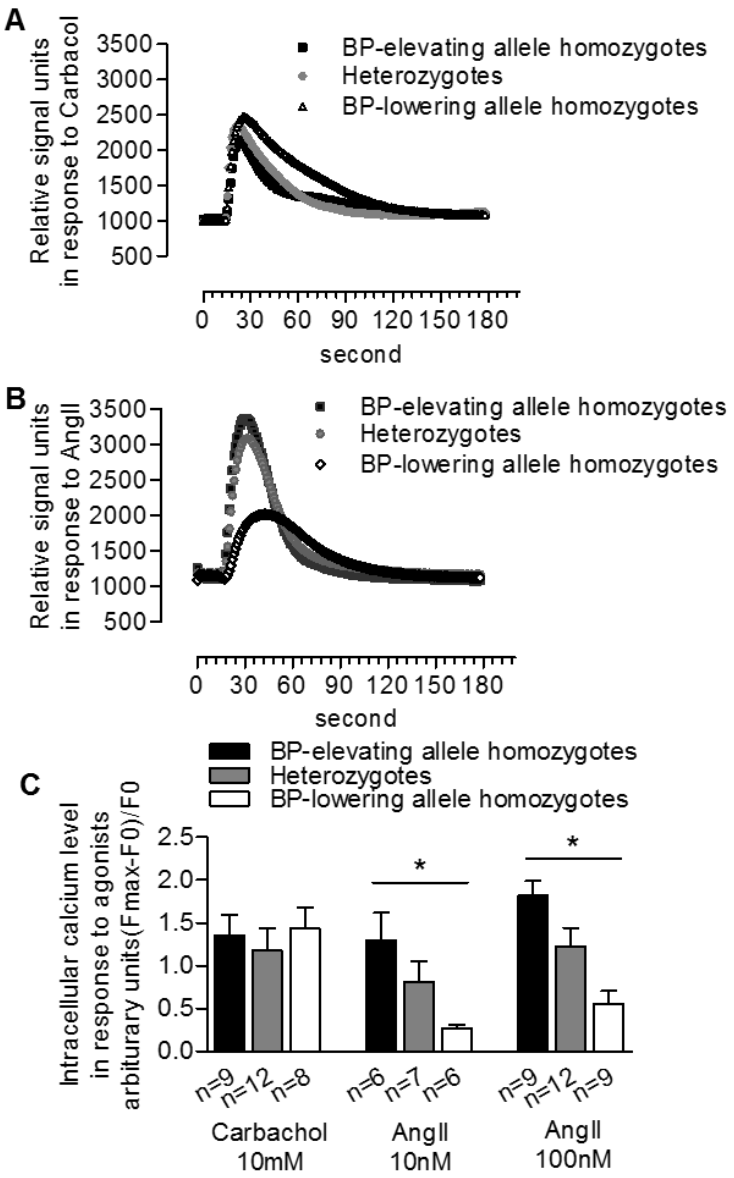

Figure 3.13 Effect of *NPR3* BP-associated variants in the rs1173771 LD block on the intracellular calcium changes induced by angiotensin II (Ang II) in HUASMCs.

Representative traces showing the calcium flux in response to carbachol (1mM) (positive control) (**A**) and angiotensin II (Ang II) (100nM) (**B**) among genotypes using fluorescent imaging plate reader (FLIPR) assay. **C**, A higher Ang II-stimulated intracellular calcium level was observed in BP-elevating allele samples in both lower dose (10nM) and higher dose (100nM) groups, however, no genetic difference was observed in carbachol induced HUASMCs calcium flux. N≥5 for each genotype running at least duplicate. Values are presented as mean ± SEM, *P<0.05, analysed by one-way ANOVA with Bonferroni correction for the number of tests for different genotypes.

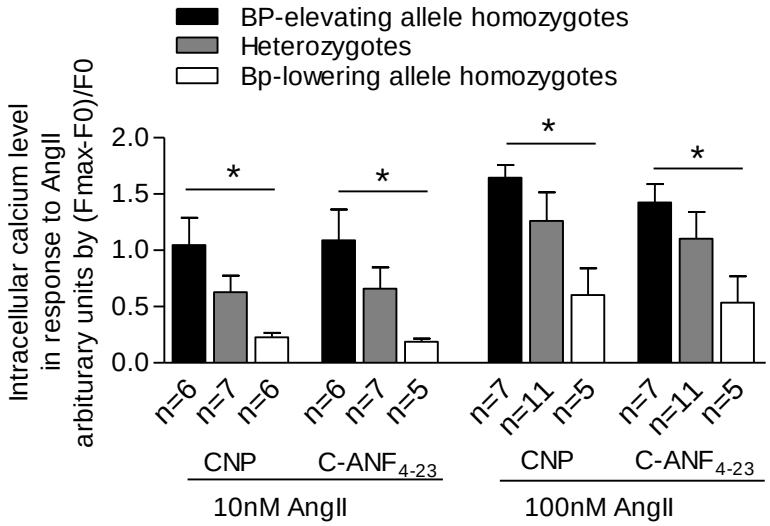

Figure 3.14 Effect of C-type natriuretic peptide and natriuretic peptide receptor C-specific agonist CANF4-23 on angiotensin II induced intracellular calcium changes in HUASMCs.

Cells were treated with C-type natriuretic peptide (CNP, 1μM) or the natriuretic peptide receptor C-specific agonist C-ANF4-23 (1μM). The analysis showed a difference among genotypes with a higher intracellular calcium level in BP-elevating allele (major allele) carrier samples. N≥5 for each genotype running at least duplicate. *P<0.05 by one-way ANOVA with Bonferroni correction for the number of tests for different genotypes.

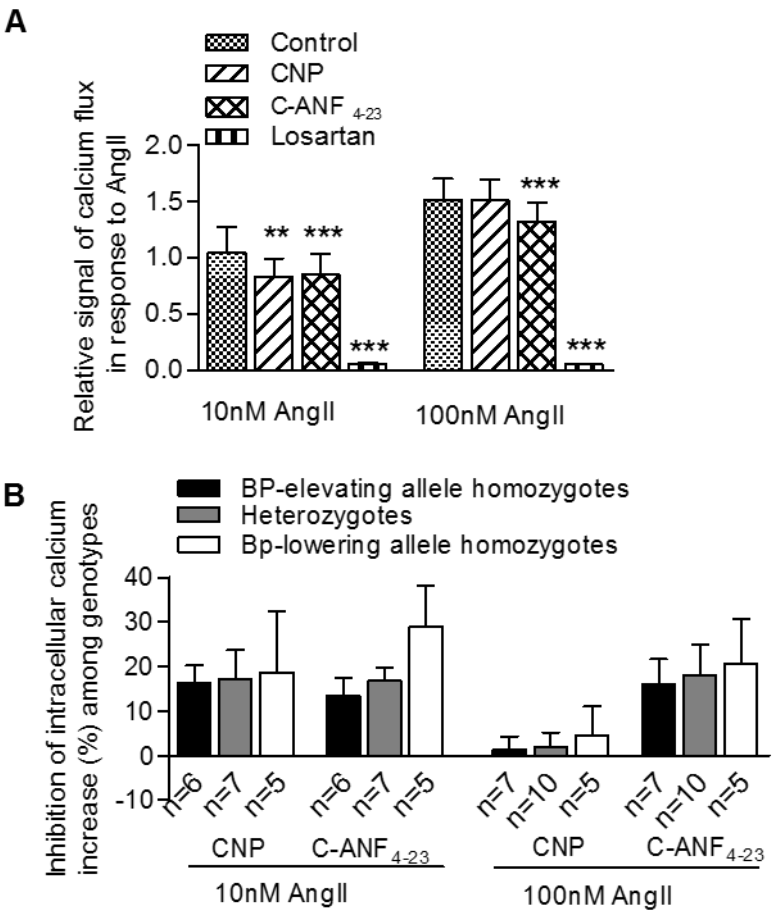

Figure 3.15 Effect of C-type natriuretic peptide and natriuretic peptide receptor C-specific agonist C-ANF$_{4-23}$ on angiotensin II induced intracellular calcium changes in HUASMCs.

Cells were treated with C-type natriuretic peptide (CNP, 1μM), the natriuretic peptide receptor C-specific agonist C-ANF$_{4-23}$ (1μM) and angiotensin II (Ang II) receptor blocker losartan (1μM) as antagonist control. **A**, CNP or CANF$_{4-23}$ could counteract the augment of intracellular calcium in response to the lower dose of Ang II (10nM), even under a higher dose of Ang II (100nM), CANF$_{4-23}$ still could significantly diminish Ang II-stimulated calcium response. N≥20 for each group running at least duplicate. Values are presented as mean ± SEM, **P<0.01, ***P<0.001 when CNP/C-ANF4-23 vs control by Wilcoxon signed rank test. **B**, No significant difference of compound (CNP/CANF$_{4-23}$) inhibitory effect among genotypes in both Ang II groups. N≥5 for each genotype running at least duplicate. Values are presented as mean ± SEM, *P<0.05, analysed by one-way ANOVA with Bonferroni correction for the number of tests for different genotypes.

3.3 Functional study of variants in the rs1421811 LD block in HUASMCs

3.3.1 Effect of BP-associated SNPs on *NPR3* mRNA level in HUASMCs

To see whether there is an impact of BP-associated variants in the rs1421811 LD block in *NPR3* mRNA level of HUASMCs, qRT-PCR data was also analysed based on rs1421811 genotypes. *NPR3* mRNA level was slightly decreased in BP-elevating allele carriers of intronic SNPs rs3762988 and SNP rs7729447 (Figure 3.17 B and C) respectively, but the difference was not statistically significant. However, there was a trend towards lower *NPR3* mRNA level in BP-elevating allele (major allele) carrier samples compared with BP-lowering allele of intronic SNPs rs1421811/rs3828591 (r^2=1.0) (Figure 3.17 D), suggesting a possible impact of these two intronic SNPs on *NPR3* gene expression.

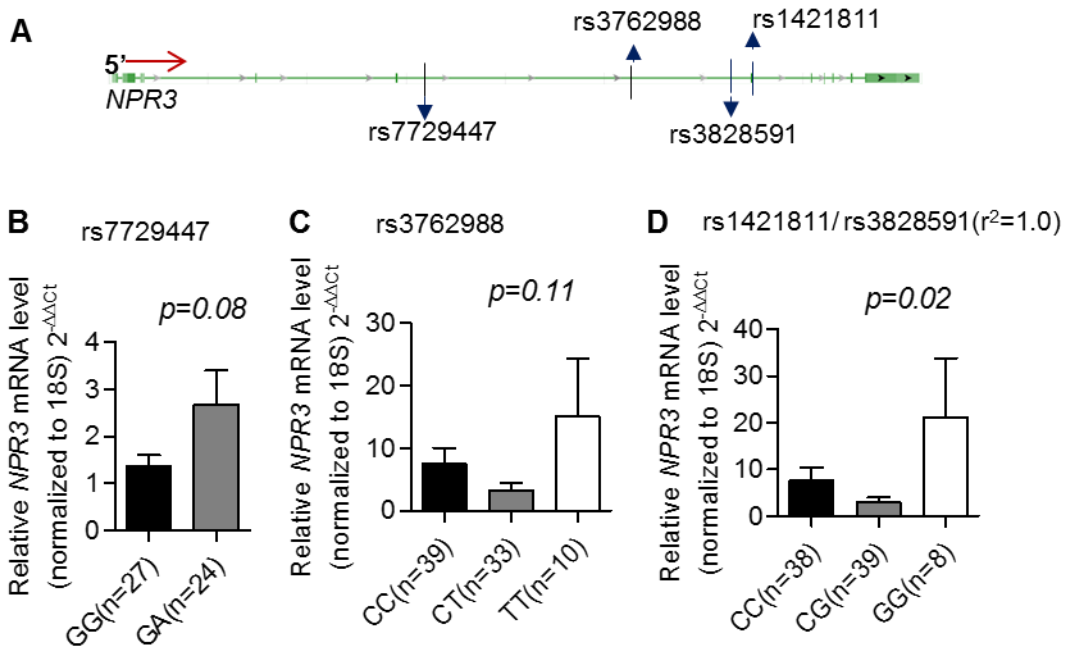

Figure 3.16 Quantitative analysis of mRNA levels of *NPR3* among BP-associated SNPs in rs1421811 LD block in HUASMCs.

A, Genetic positions of BP-associated variants of rs1421811 LD block in *NPR3* gene locus. **B,C,D**, BP-associated variants drove a genotype- dependent effect on *NPR3* gene regulation in HUASMCs with reduced mRNA level of NPR3 in BP-elevating allele homozygous samples, such determined by quantitative reverse-transcription polymerase chain reaction (qRT-PCR) for intronic variants rs7729447(**B**), rs3762988(**C**), rs1421811 and rs3828591 (r^2=1.0) (**D**). Values are presented as mean ± SEM, *P<0.05, analysed by one-way ANOVA with post-test of Bonferroni's multiple comparison test.

3.3.2 No significant effect of variants in the rs1421811 LD block on NPR-C expression level

In the rs1421811 LD block, the BP-lowering allele homozygous samples are very rare, therefore the data was analysed by combining heterozygous and BP-lowering allele homozygous samples together versus BP-elevating allele homozygotes. There were

slightly lower expression levels of NPR-C in BP-elevating allele homozygous HUASMCs compared with the other two genotypes, however, there was no statistically significant association between NPR-C protein level and genotype for any of these SNPs (Figure 3.18).

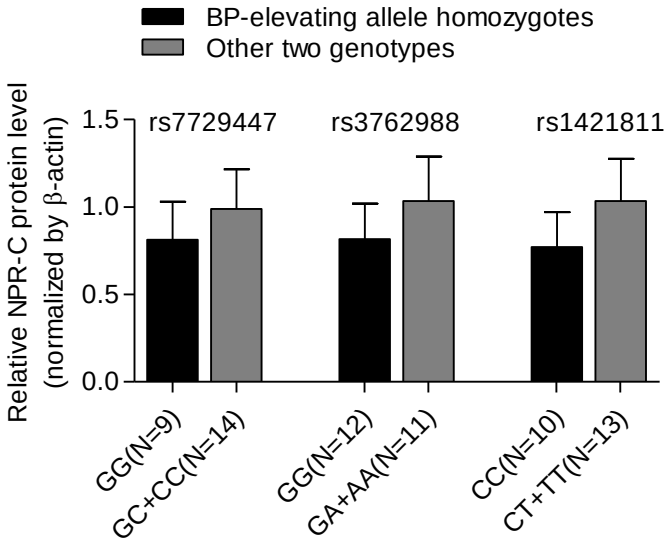

Figure 3.17 Effect of Blood pressure-associated variant in rs1421811 LD block on natriuretic peptide receptor C (NPR-C) protein level in human umbilical arterial smooth muscle cells (HUASMCs).

Western blotting shows NPR-C protein level is slightly lower in HUASMCs with genotype of BP-elevating allele homozygotes compared with other two genotypes, but no significance (N≥9 in each genotype).

3.3.3 No significant association between variants in the rs1421811 LD block at NPR3 gene locus and HUASMC proliferation

The possible genetic difference of variants in rs1421811 LD block in HUASMCs proliferation was also investigated here. The minor allele frequency (MAF) of these variants are low and there is only a few samples (N≤ 3) for BP-lowering allele (minor)

homozygotes harvested in our current collection, hence, the data was analysed by combination with heterozygous and minor allele homozygous. As shown in Figure 3.19, No significant genetic difference among genotypes of all investigated variants in rs1421811 LD block was detected in HUASMCs proliferation, and no genetic difference of compounds inhibitory effect as well.

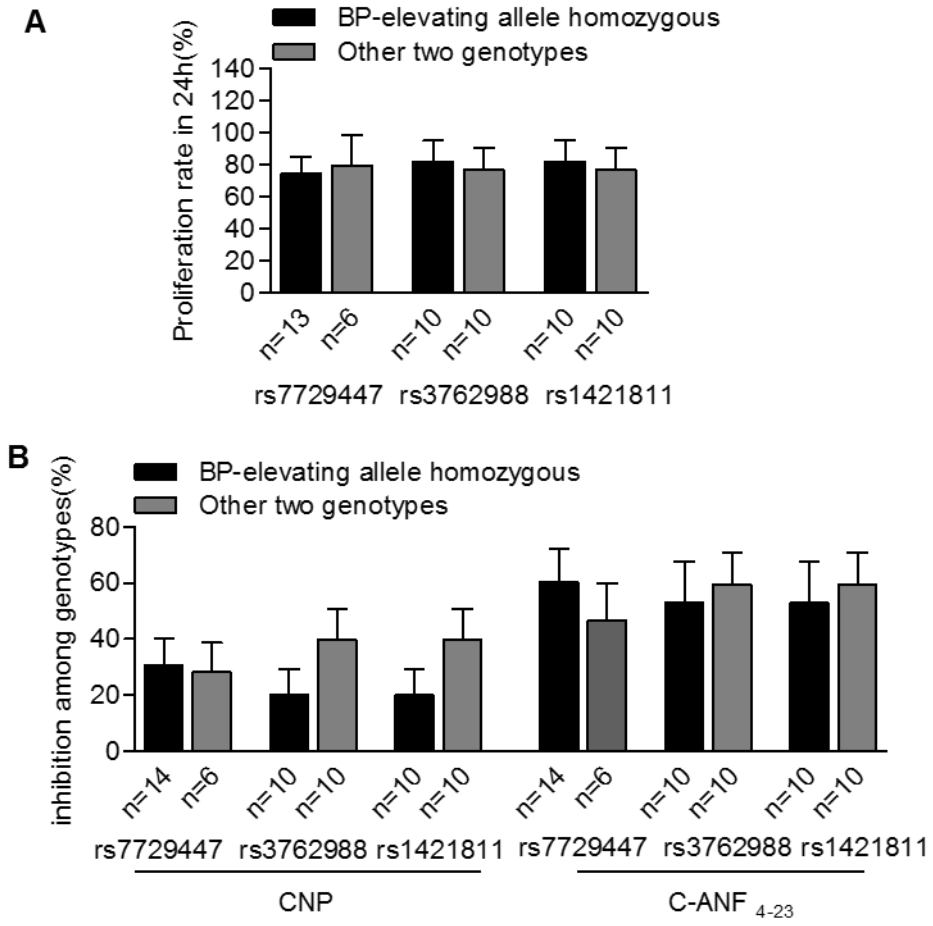

Figure 3.18 No significant effect of BP-associated variant in rs1421811 LD block in *NPR3* on HUASMC proliferation.

A, Cell proliferation was measured at 24h by cell counting assay (CCK-8). No genetic difference was detected among genotypes in HUASMCs proliferation and compounds inhibitory effect. N≥6 in each genotype running at least duplicate. Values are presented as mean ± SEM, data was analysed by unpaired t test between BP-elevating allele homozygous and other two genotypes.

3.3.4 No significant association between variants in the rs1421811 LD block at the *NPR3* gene locus and HUASMC migration

When analysing data for rs1421811 LD block, the BP-lowering allele homozygous samples here is less than 3, thus this genotype was combined with heterozygous. However, no difference was observed between BP-elevating allele homozygous and other two genotypes in migration rate in HUASMCs and in compounds inhibitory effect either (Figure 3.20).

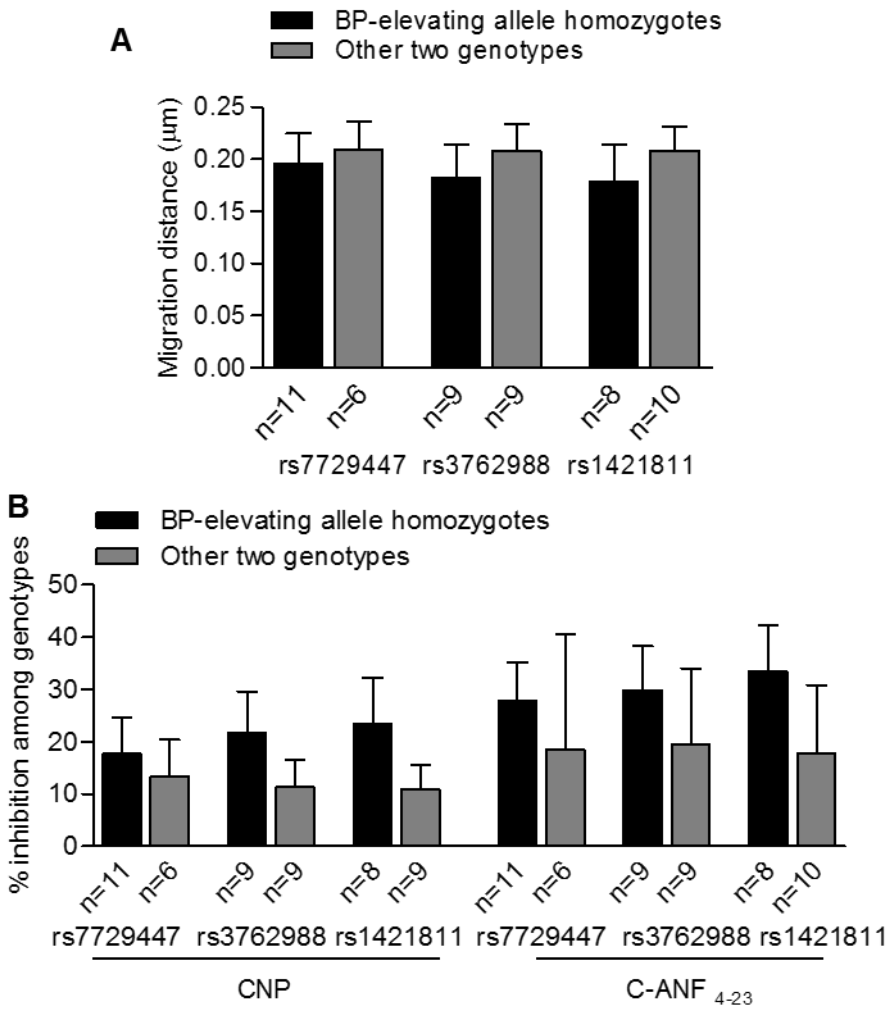

Figure 3.19 No effect of blood pressure (BP)-associated variants in the rs1421811 LD block at the *NPR3* locus on HUASMC migration.

A, No association was observed between BP-associated variants and HUASMCs cell migration. N≥5 in each genotype running at least duplicate. **B,** No genetic difference of compounds (CNP/C-ANF$_{4\text{-}23}$) inhibitory effect was detected in HUASMCs migration. Values are presented as mean ± SEM, Genetic difference among genotypes was analysed by unpaired t test.

3.3.5 Impact of variants in the rs1421811 LD block in HUASMC calcium flux.

No significant genetic association of intracellular calcium changes in response to lower dose of Ang II (10nM) was observed in HUASMCs, although with a slightly higher level in elevating allele homozygotes (N≥5 in each group). However, when induced with 100nM Ang II, it was exhibited a significantly augmented intracellular calcium level in BP-elevating homozygous samples in contrast to other two genotypes (N≥10 in each group) (Figure 3.21).

As indicated in section 3.9.1, CNP or C-ANF$_{4-23}$ significantly counteracted the augment of intracellular calcium in response to the lower dose of Ang II (10nM), and even under a higher dose of Ang II (100nM), C-ANF$_{4-23}$ is still active. However, no significant genetic difference of inhibitory effect of CNP or C-ANF$_{4-23}$ was detected either in HUASMCs for rs1421811 LD block (Figure 3.22).

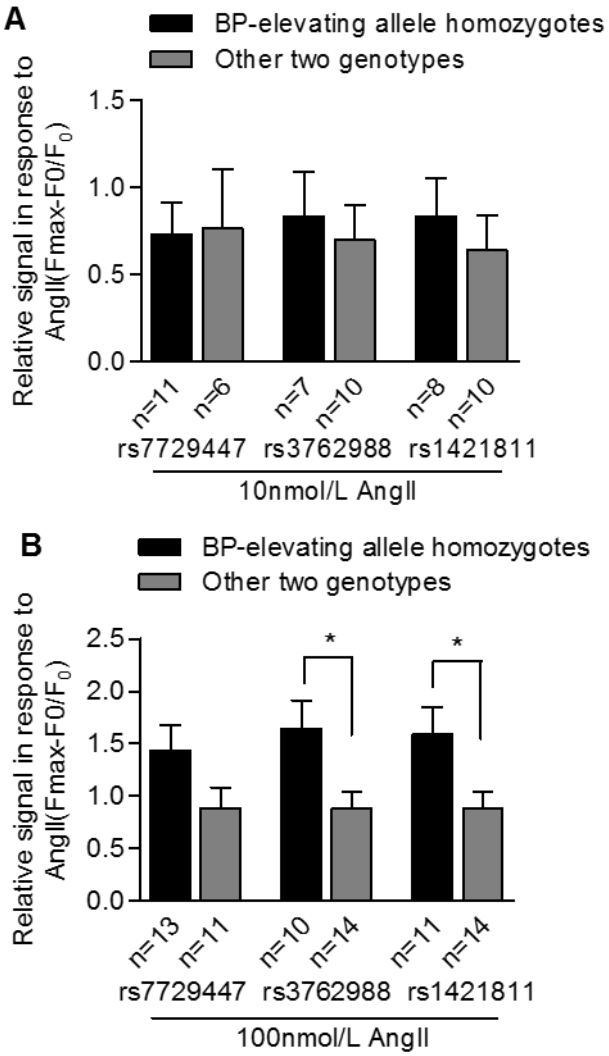

Figure 3.20 Effect of variants in the rs142181 LD block on angiotensin II induced intracellular calcium changes in human umbilical arterial smooth muscle cells. **A**, no significant genetic difference of impact of variants in rs1421811 LD block in intracellular calcium changes in response to Ang II (10nM) was obtained. N≥5 in each genotype running at least duplicate, and difference between genotypes was analysed by unpaired t test. **B**, Significantly genetic influence of variants in rs1421811 LD block in intracellular calcium changes in response to Ang II (100nM) was observed. N≥10 in each genotype running at least duplicate, and *P<0.05 by unpaired t test when compared between genotypes.

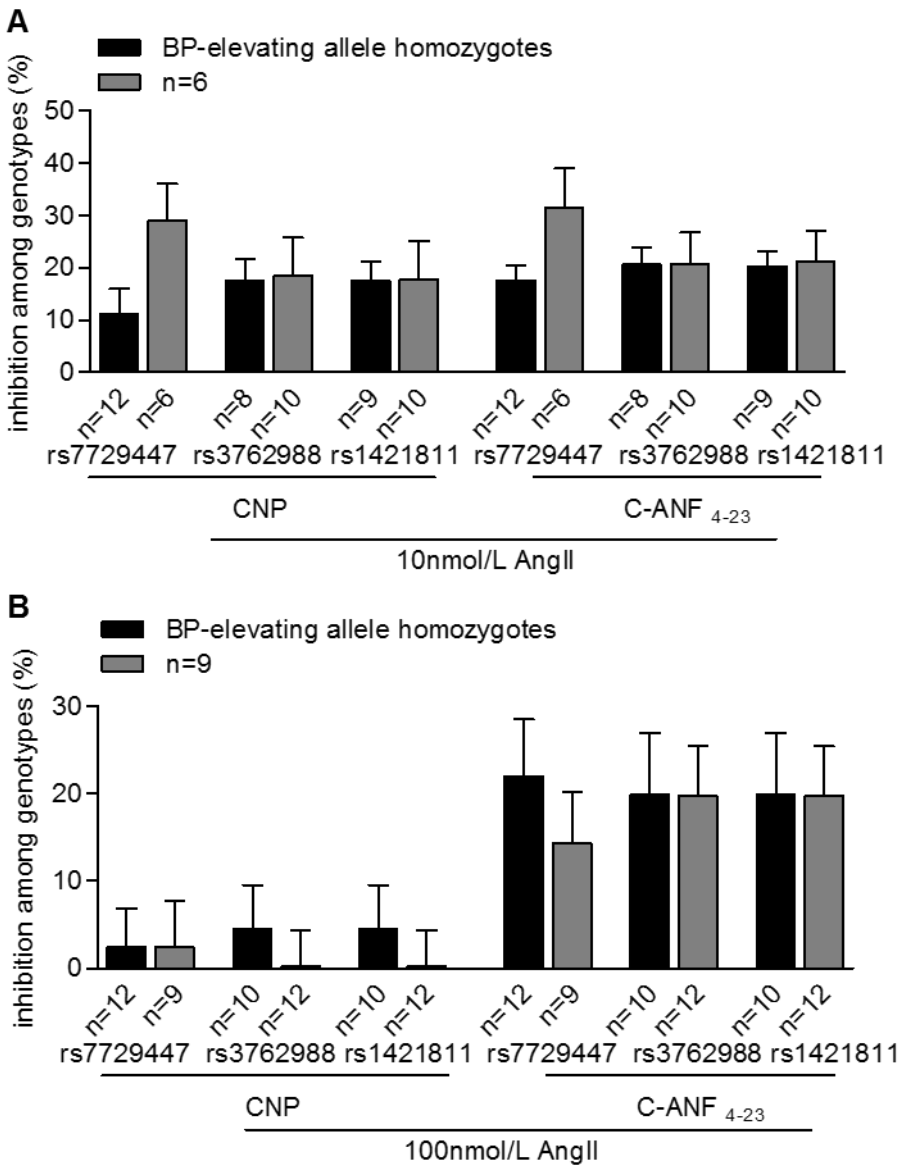

Figure 3.21 No effect of C-type natriuretic peptide and natriuretic peptide receptor C-specific agonist $CANF_{4-23}$ on angiotensin II induced intracellular calcium changes in human umbilical arterial smooth muscle cells.

A, **B**, No significant genetic difference of compounds (CNP/$CANF_{4-23}$) inhibitory effect among genotypes of SNPs in rs1421811 LD block in Ang II groups. N≥5 in each genotype running at least duplicate. Values are presented as mean ± SEM, difference was analysed unpaired t test.

4. Result of Functional study of BP-associated variants at the *NPR3* gene locus in HUVECs

4.1 Genotyping result of BP-associated SNPs at the *NPR3* locus in HUVECs

Genomic DNA of isolated HUVECs from different individuals was genotyped using the KASPar technique described in section 2.3. All of the BP-associated SNP genotyping results in HUVECs were in accordant with Hardy-Weinberg equilibrium as shown in Table 4.1.

Table 4.1 BP-associated SNPs genotyping results in HUVECs and HWE calculation.

	variants in block 1		
Samples in genotype (No)	rs1173743/ rs1173747(r^2=1)	rs1173756	rs1173771
Major allele homozygotes	63	64	76
Heterozygotes	93	94	89
Minor allele homozygotes	34	35	26
HWE calculation			
P-value by Chi-Square Test	0.9623	0.9747	0.9816

	variants in block 2		
Samples in genotype (No)	rs7729447	rs3762988	rs1421811/ rs3828591(r^2=1)
Major allele homozygotes	121	89	99
Heterozygotes	59	71	73
Minor allele homozygotes	5	12	11
HWE calculation			
P-value by Chi-Square Test	0.9338	0.9757	0.9433

HWE= Hardy-Weinberg equilibrium; Major allele is BP-elevating allele; Minor allele is BP-lowering allele.

4.2 Functional study of variants in the rs1173771 LD block in HUVECs

4.2.1 Effect of BP-associated SNPs in the rs173771 LD block on *NPR3* mRNA level in HUVECs

4.2.1.1 No significant difference between genotypes in *NPR3* mRNA in HUVECs.

To investigate whether the BP-associated SNPs is associated with *NPR3* gene regulation, qRT-PCR was also conducted on HUVEC mRNA by SYBR-Green qPCR technique (see section 2.5.1).

In the HUVEC samples, there was a hint of lower relative *NPR3* mRNA level in BP-elevating allele (major allele) carrier samples compared with BP-lowering allele of all the detected SNPs (Figure 4.1). However, the difference was not statistically significant.

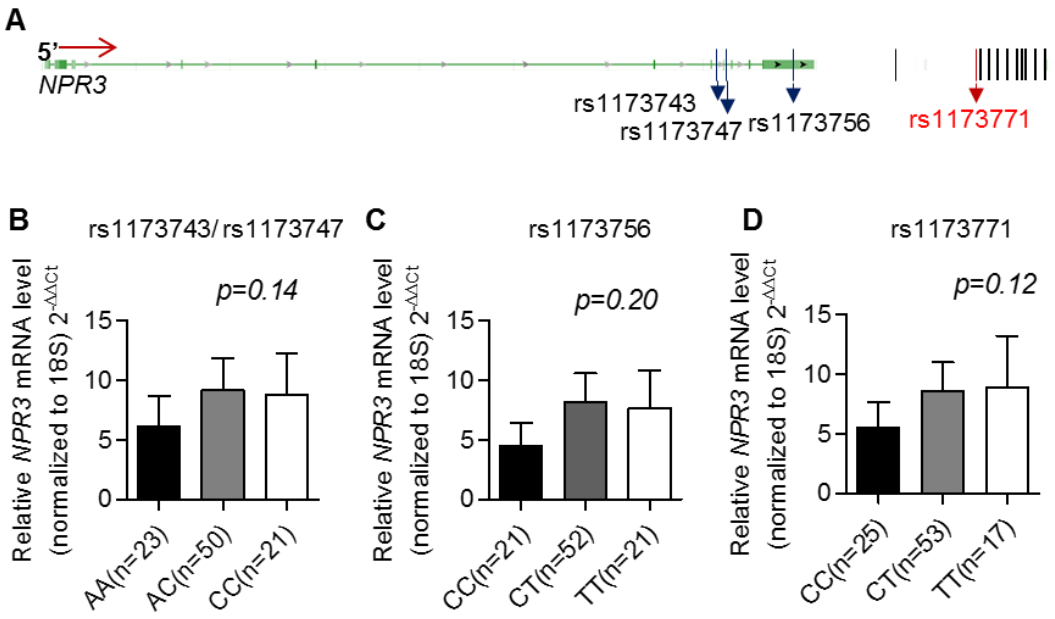

Figure 4.1 Quantitative analysis of mRNA levels of NPR3 among BP-associated SNPs in the rs1173771 LD block in HUVECs.

A, Genetic positions of BP-associated variants of rs1173771 LD block at *NPR3* gene locus. **B,C,D**, BP-associated variants drove a genotype- dependent effect on *NPR3* gene regulation in HUASMCs with a slightly lower NPR3 mRNA level in BP-elevating allele carriers, such determined by quantitative reverse-transcription polymerase chain reaction (qRT-PCR) for intronic variants rs1173743 and rs1173747 (r^2=1.0) (**B**),3'UTR variant rs1173756 (**C**), and 3' flanking region variant rs1173771 (**D**) respectively. Values are presented as mean ± SEM, data were analysed by one-way ANOVA with post-test of Bonferroni's multiple comparison test.

4.2.1.2 Allelic expression imbalance of 3'-UTR SNP rs1173756

In addition of real-time PCR, allelic expression imbalance was performed to investigate the possible genetic influence on *NPR3* mRNA level. This assay was conducted in HUVEC heterozygotes for the 3-UTR SNP rs1173756 (C/T), and the ratio of the two alleles in genomic DNA and cDNA was detected by sequencing and

compared. As shown in Figure 4.2, the expression level of BP-elevating allele (major allele C) was significantly lower in HUVECs.

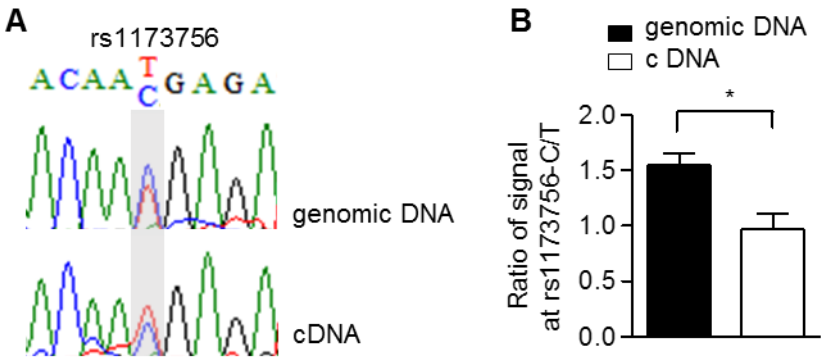

Figure 4.2 Allelic expression imbalance of 3-UTR SNP- rs1173756 in *NPR3* gene in HUVECs.

Sequencing assay for the detection of rs1173756 (C/T) was applied in genomic DNA and corresponding cDNA samples from HUASMC. The peak value of each allele was determined by Peak Picker. Allelic expression imbalance (AEI) between genomic DNA and complementary DNA (cDNA) at the 3' UTR SNP rs1173756 in HUVECs (N=7 pairs), with a lower BP-elevating allele (C) signal in cDNA compared to genomic DNA. *P=0.015 by Wilcoxon signed-rank test.

4.2.2 No effect of BP-associated SNPs on the NPR-C protein level in HUVECs

Western blottoing analysis was conducted to investigate whether BP-associated SNPs influence NPR-C expression in HUVECs samples from different individuals, and the rs1173747 genotype pattern in those samples is concordant with other three BP-associated SNPs (rs1173743, rs1173756 and rs1173771). The analsysis showed slightly lower NPR-C levels in BP-elevating allele homozygotes in contrast to BP-lowering allele homozygotes, but no statistical siginifance (Figure 4.3).

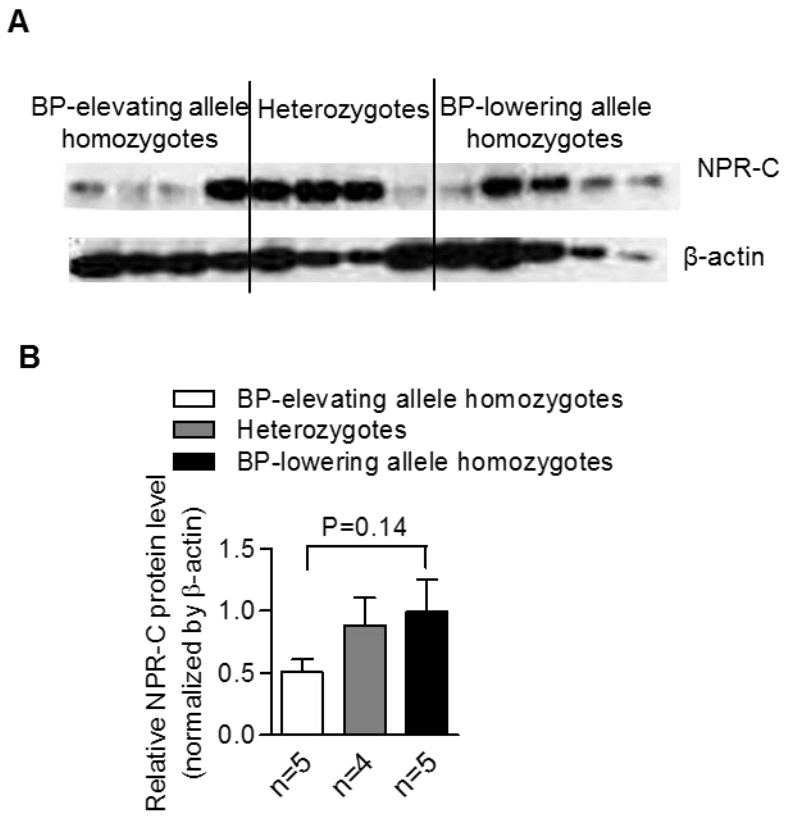

Figure 4.3 No effect of BP-associated variant on NPR3 protein level in HUVECs.

A,B, Western blotting shows NPR-C protein level is lower in HUVECs with genotype of BP-elevating allele homozygotes compared with BP-lowering allele homozygotes, difference was analysed by unpaired t test (N≥4 in each genotype).

4.2.3 Interaction of BP-associated SNP rs1173756 with nuclear proteins from HUVECs

Electrophoretic mobility shift assays (EMSA) were conducted to investigate whether BP-associated SNPs interact with potential nuclear proteins in HUVECs *in vitro*. Biotin-labelled oligos representing DNA fragments flanking the BP-associated SNPs were incubated with HUVEC nuclear extracts.

As shown in Figure 4.4, there was a DNA-protein complex visible for the 3'-UTR SNP rs1173756 probes when incubated with HUVEC nuclear extracts. The intensity of the complex of the rs173756-BP-elevating allele (C) was much lower than the BP-lowering allele (T), indicating a potential allelic difference in nuclear protein binding with this DNA region. This possibility is in accordant with genetic difference of the allelic expression imbalance data with a lower level of BP-elevating allele in mRNA, and may suggest some active transcription factors interacting with the BP-lowering allele. However, this still needs to be verified by following detection with specific or unspecific competitors and molecular mechanism study. Otherwise, complex was not shown in the lanes for intronic SNPs rs173743, rs173747 and intergenic SNP rs173771.

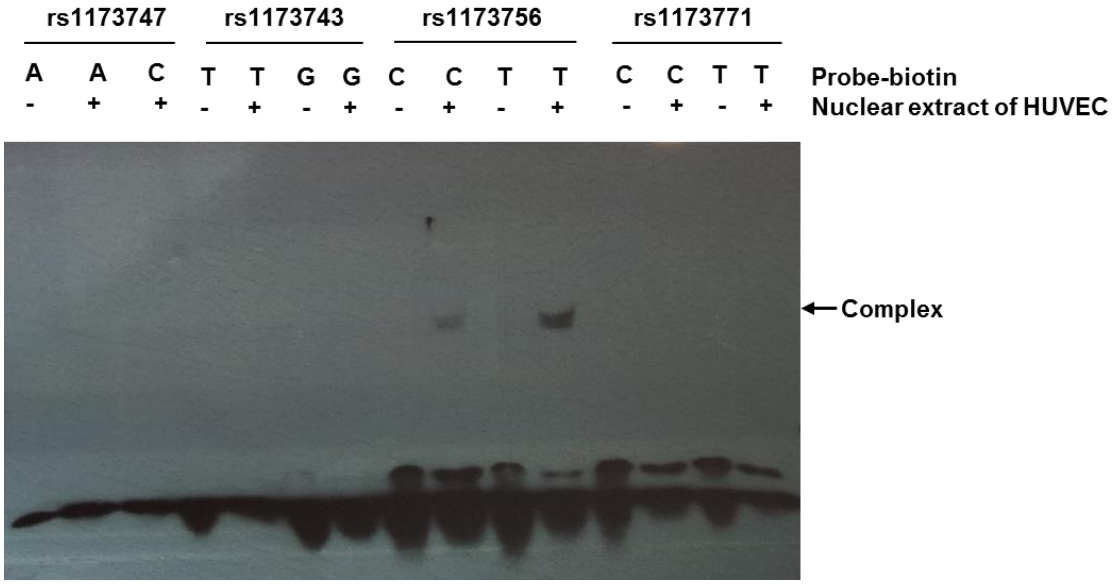

Figure 4.4 Detection of relative binding affinities of DNA sequences flanking BP-associated SNPs to HUVEC nuclear extract *in vitro*.

The biotin-labelled oligos were incubated with HUVEC nuclear extract. Complexes were visible in the lanes of rs1173756-centered flanking oligos with nuclear protein and indicated a potential allelic difference of affinity.

4.2.4 Effect of BP-associated SNPs in HUVECs cell proliferation

It has been shown that binding of NPR-C (as a Gi protein coupled receptor) with CNP could up-regulate HUVEC cell proliferation [133]. Therefore, the primary HUVECs incubated with or without 1nM CNP or C-ANF$_{4-23}$ were analysed by cell counting assay (as described in section 2.10) to explore the possible genetic impact of BP-associated SNPs on HUVECs proliferation.

Again, rs1173771 genotype pattern in these HUVECs studied is concordant with other three SNPs (rs1173743/rs1173747, rs1173756), thus the data were analysed by comparing BP-elevating allele homozygous, heterozygous and BP-lowering allele homozygous groups.

There was no significant difference among genotypes of the *NPR3* BP-associated SNPs in HUVEC proliferation, although there was a slightly higher proliferating rate in BP-lowering allele homozygous samples (Figure 4.5). When incubated with CNP or C-ANF$_{4\text{-}23}$, a slightly higher proliferation rate was observed in CNP and/or C-ANF groups, but with no statistical significance. The genetic difference was not detectable in HUVECs under CNP or C-ANF$_{4\text{-}23}$ as well (Figure 4.6).

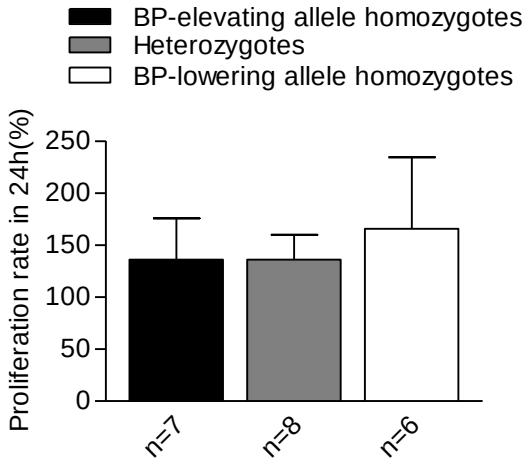

Figure 4.5 No effect of BP-associated variants in the rs1173771 LD block at *NPR3* locus on human umbilical vein endothelial cells proliferation.

Cell proliferation was measured at 24h by cell counting assay (CCK-8). No significant genetic impact was detected in HUVECs, N≥5 for each genotype. Values are presented as mean ± SEM, and difference was analysed by one-way ANOVA with Bonferroni correction of the number of tests for different genotypes.

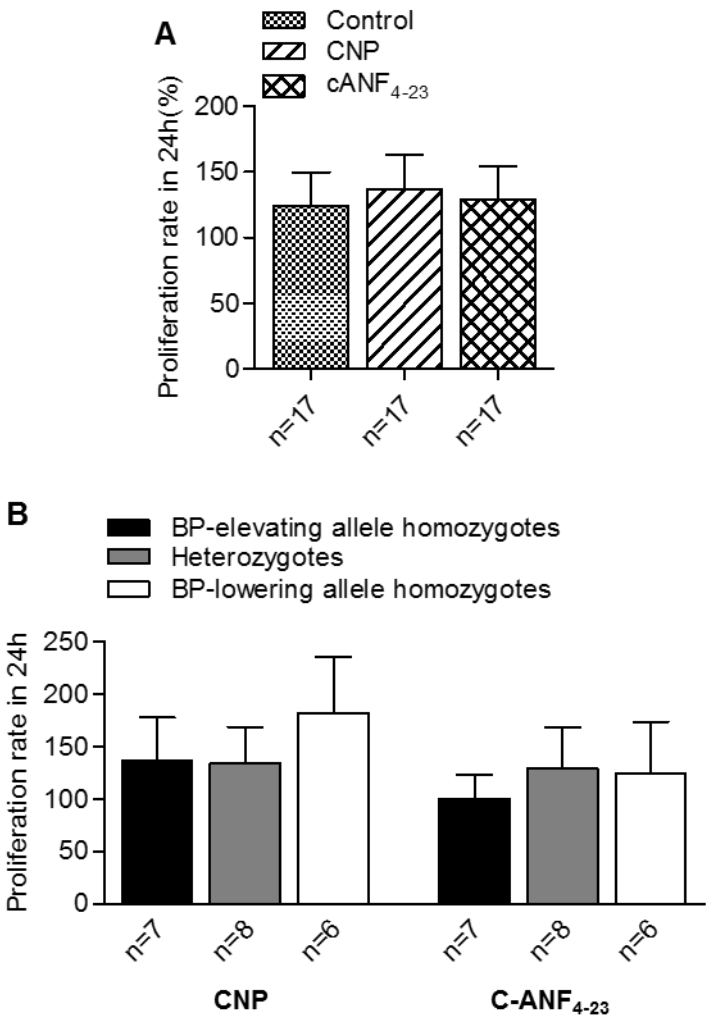

Figure 4.6 No effect of CNP/ CANF$_{4-23}$ on human umbilical vein endothelial cells proliferation.

A, C-type natriuretic peptide (CNP) and NPR-C specific agonist C-atrial natriuretic peptide (C-ANF$_{4-23}$) slightly increased the HUVECs proliferation, but without significance. N≥8 in each genotype. Values are presented as mean ± SEM, difference between CNP or C-ANF$_{4-23}$ and control was compared by Wilcoxon signed-rank test. **B, C,** no significant genetic difference was observed in HUVECs with treatment of CNP or C-ANF$_{4-23}$. N≥5 for each genotype. Values are presented as mean ± SEM, difference was analysed by one-way ANOVA with Bonferroni correction for the number of tests for different genotypes.

4.3 Functional study of variants in the rs1421811 LD block in HUVECs

4.3.1 No effect of BP-associated SNPs on the *NPR3* mRNA level in HUVECs

In the rs421811 LD block, *NPR3* mRNA data also indicated a hint of lower relative expression level in BP-elevating allele (major allele) homozygous samples compared with BP-lowering allele homozygotes, but no significant difference among genotypes (Figure 4.7). For rs7729447, the number of BP-lowering allele homozygotes is only three in current mRNA collection, therefore data was analysed here by combining BP-lowering allele homozygotes and heterozygotes (Figure 4.7 B).

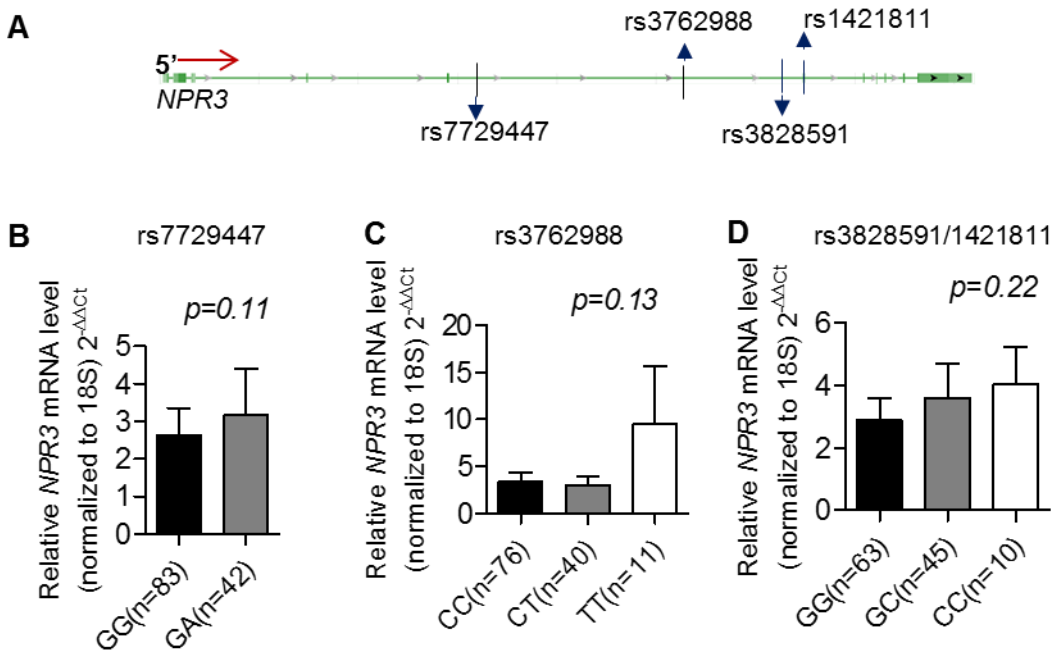

Figure 4.7 Quantitative analysis of mRNA levels of *NPR3* among BP-associated SNPs in the rs1421811 LD block in HUVECs.

A, Genetic positions of BP-associated variants in rs1421811 LD block at *NPR3* gene locus. **B,C,D**, BP-associated variants drove a genotype- dependent effect on NPR3 gene regulation in HUASMCs with a slightly lower NPR3 mRNA level in BP-elevating allele carriers, such determined by quantitative reverse-transcription polymerase chain reaction (qRT-PCR) for rs7729447 (**B**), rs3762988 (**C**), and rs1421811/rs3828591(r^2=1.0) (**D**) respectively. Values are presented as mean ± SEM, data were analysed by one-way ANOVA with post-test of Bonferroni correction.

4.3.2 Effect of BP-associated SNPs on HUVEC proliferation

HUVECs were incubated with or without 1nM CNP, or C-ANF_{4-23} for 24 hours and proliferation was investigated by cell counting assay. The effect of CNP, or C-ANF_{4-23} on cell proliferation see the section 4.2.4. When without treatment, a relatively increased level of proliferation was observed in heterozygotes of SNPs in contrast to their BP-elevating allele homozygotes, but without significance (Figure 4.8).

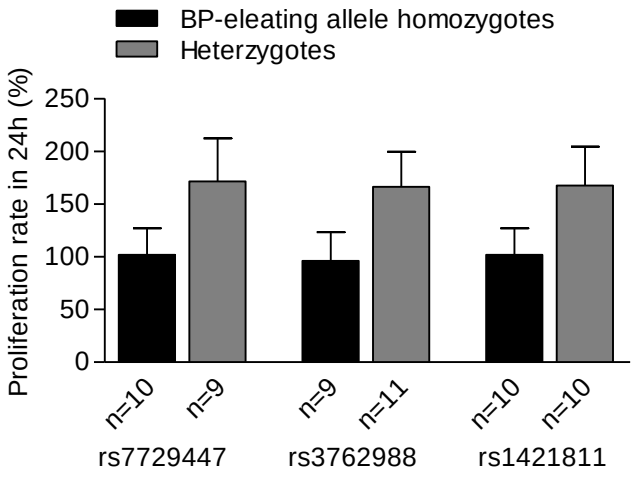

Figure 4.8 No effect of BP-associated variants in the rs1421811 LD block in *NPR3* on human umbilical vein endothelial cells proliferation.

Cell proliferation was measured at 24h by cell counting assay (CCK-8). No significant of genetic impact was implicated in HUVECs, but with a slightly higher proliferating level in heterozygous samples of all detected SNPs. N≥8 in each genotype. Values are presented as mean ± SEM, and difference was analysed by unpaired t test.

5. Discussion and Future work

An increasing number of DNA sequence variations in or near the *NPR3* gene have been reported to be associated with cardiovascular diseases susceptibility, especially phenotypes related to blood pressure regulation.

As described in section 1.5, lead SNPs rs1173771, rs173766 and rs1421811 have been identified as association with blood pressure by GWAS. Moreover, another combined admixture mapping and association analysis of 6303 un-associated African-American participants by the Candidate Gene Association Resource (CARe) consortium has shown variation (rs7726475, A/G) in the 5′-flanking region of the *NPR3* gene has also been significantly associated with inter-individual variation in both systolic (β=2.00; P=8.85×10^{-7}) and diastolic (β=1.04; P=3.64×10^{-6}) blood pressure.[109]

In addition to in the association with blood pressure, other association linking *NPR3* variants to blood pressure have also been demonstrated in related complications. For instance, three SNPs (rs6889608, rs1173773, and rs2270915) in *NPR3* were significantly associated with systolic BP (SBP) in diabetes.[142] rs2270915 (G/A) is a nonsynonymous SNP located in exon 8 of *NPR3* and its association was replicated in the second step population of 2,452 French: AA homozygotes had a lower SBP than G carriers (137.4 ± 19.1 vs. 140.0 ± 20.2 mmHg, P = 0.004). It was also replicated with resequencing study in three ethnic groups (European American, African American, and Han Chinese American) and identified association with difference in SBP.

These studies have demonstrated the association of SNPs at *NPR3* locus with blood pressure regulation and highlighted the potential of *NPR3* in blood pressure control and in the development of hypertension. However, the precise role of those blood-

pressure associated SNPs and *NPR3* in the development of hypertension remains to be elucidated.

NPR3 encodes for the natriuretic peptide receptor C (NPR-C), previously regarded to predominantly function as a systemic clearance receptor that removes natriuretic peptides (NP) from the circulation.[73,75,102] Recently, there is accumulating evidence suggesting a physiological role of NPR-C coupled to adenylyl cyclase / cyclic adenosine monophosphate (cAMP) signal transduction system through inhibitory guanine nucleotide regulatory protein (G_i).[80–82] Upon binding with NPR-C, Gi is able to inhibit adenylyl cyclase, with the subsequently lower intracellular formation of cAMP via Gi-α subunit, and activates phosphoinositide phospholipase C (PLC) and phosphatidyl inositol (PI) by Gi-β/γ subunit.[72,143] Studies have implicated NPR-C in mediating some of the cardio-protective actions of natriuretic peptides and its direct involvement in the pathogenesis of hypertension.

NPR-C homozygous knockout mice have showed an average decrease of 8 mmHg (SBP) than the control which is also associated with an increased half-life of ANP, increased diuresis and reduced ability to concentrate urine. However, a whole body of NPR-C knock out mouse displayed profound skeletal abnormalities, and about 50% of the homozygous knockouts died before weaning.[121] Thus, it is not very practical or proper to use NPR-C knockout mice as model to study blood pressure until possible tissue-specific knockout model is generated.

Herein, we used the “human laboratory” by studying VSMCs and ECs isolated from human umbilical cords of different individuals partitioned by genotype as both represent tissues with high expression levels of NPR-C identified by a previous study

(Khambata, et al. 2011) which was confirmed by our data. These cell types are particularly relevant in the study of blood pressure. Vascular smooth muscle cells (VSMCs) are critically involved in maintaining vascular integrity. Numerous pathophysiological processes with VSMCs hyperplasia, hypertrophy, apoptosis, cell elongation, migration, inflammation and its altered extracellular matrix proteins could contribute to arterial remodelling, finally to the development of hypertension.[144] Endothelial cells (ECs) can release both relaxing and contracting factors that modulate vascular smooth muscle tone and also participate in the pathophysiology of essential hypertension.[145]

With an aim to understand the functional effects of the blood pressure-associated SNPs at the *NPR3* locus, I sought to investigate whether these SNPs have an effect on *NPR3* expression, together with human vascular SMC and endothelial BP-related cell phenotypes *in vitro*.

5.1 BP-associated SNPs in rs1173771 LD block influence *NPR3* gene expression in HUASMCs.

Gene expression studies were conducted on mRNA and protein levels of NPR-C and analysed by genotype. My data showed that a decreased expression level of NPR-C in BP-elevating allele carrier genotypes in human vascular SMCs (see section 3.2.1-3.2.2). Reduced NPR-C mRNA levels were observed in HUASMCs homozygous and heterozygous for BP-elevating (major) allele, as compared with BP-lowering (minor) allele homozygous HUASMCs, by qRT-PCR. This finding was confirmed with the complementary method of allelic expression imbalance analysis using genomic DNA and mRNA from HUASMCs that were heterozygous for 3'-UTR SNP rs1173756.

Consistent with the qRT-PCR results, the BP-elevating allele (C) had lower expression as compared to the BP-lowering allele (T). Protein detection by western blotting subsequently validated a compatibly diminished NPR-C level in BP-elevating allele homozygous group in HUASMCs. In concert, these observations provide strong support for a genetic influence of *NPR3* SNPs on NPR-C expression at a transcriptional level. In the blood pressure GWAS, the major allele C of rs1173771 is indicated association with elevated blood pressure (0.504mmHg for SBP and 0.261 mmHg for DBP).[146] The results presented above also implies the higher blood pressure-associated risk allele C may exert its effect through lower *NPR3* expression and subsequent NPR-C related signalling.

A recent study revealed eight nonsynonymous SNPs in *NPR3* gene have a functional significance by demonstrating their effect on protein expression, which is characterized autophagy-dependent degradation by the incompatible Arg146 variant allozyme with protein conformation. This finding implicated a mechanism of SNPs in altering *NPR3* expression through the protein activity of miss-folding or instability.[147] However, all the BP-associated SNPs in rs1173771 LD block are not located in protein coding region of *NPR3*, they reside in intron, 3 untranslated region and downstream of gene. Therefore, it is hypothesised these BP-associated SNPs may affect the transcription/co-transcription process, and some detection for possible interaction of SNPs with regulatory factors were also conducted in this study.

Chromatin compactness is regarded to reflect its accessibility for the transcription machinery. Euchromatin (loose or open chromatin) is widely regarded as permissible structure for transcription through binding some regulatory elements, whereas heterochromatin (tight or closed chromatin) is more compact and refractory to factors that need to gain access to the DNA .[148] FAIRE was conducted to explore whether

blood-pressure associated variants reside in the open chromatin fragments, to further investigate their potential molecular mechanism on genetic regulation of *NPR3*. FAIRE results indicated the sequencing signals at BP-elevating allele of rs1173756 (C) or rs1173747 (A) were less enriched in FAIRE DNA compared with reference DNA in HUASMCs, which suggests both SNPs may reside in the regulatory elements in open chromatin and has differential function in an allelic-specific manner (see section 3.2.4). Considering the regulation pattern, the BP-lowering alleles may preferentially bind active transcription factors such as enhancers to upregulate the gene expression.

EMSA was also carried out to detect the possible interaction of HUASMC nuclear protein extracts with SNPs flanking DNA fragment *in vitro*. It shows an allelic binding specificity of *NPR3*-rs1173747 with HUASMC nuclear extract, indicating transcriptional or co-transcriptional factor may bind the DNA segment surrounding the BP-lowering allele of rs1173747 DNA fragment *in vitro*. Combined with qRT-PCR results showing a lower *NPR3* gene expression in BP-elevating allele of rs1173747, a possible explanation for this EMSA finding is rs173747 BP-lowering allele may overlap with some active transcriptional factors recognition sites hence upregulating the *NPR3* gene expression. This is also in line with FAIRE data with a preferable enrichment of rs1173747-lowering allele in open chromatin. This is supported by bioinformatics analyses showing rs1173747 being predicted to interact with some histone-modifications or transcription factors such as H3K27AC that upregulate gene expression.

Moreover, AEI, which was only technically possible to be conducted for 3-UTR SNP rs1173756 in this study also indicated a lower mRNA level of BP-elevating allele (C) comparing to BP-lowering allele (T) (see section 3.2.1.2). This finding is accordant with qRT-PCR result of lower *NPR3* mRNA expression in BP-elevating allele

homozygotes and FAIRE data with less enriched sequencing signals at BP-elevating allele of rs1173756 (C) in open chromatin. This also suggests rs1173756 may be a regulatory polymorphisms (rSNPs) or a structural RNA SNPs (srSNPs) interacting with some transcriptional factors, micRNA or other elements which could affect mRNA processing and turnover.

Altogether, the results provide a mechanistic explanation for the association of risk allele in rs1173771 LD block with elevation of blood pressure that may be through a lower *NPR3* expression. Findings from FAIRE, EMSA and AEI also imply the intronic SNP rs1173747 and/or 3-UTR SNP rs1173756 might be the functional SNPs. However, there are limitations of FARIE and EMSA conducted in this subject with absence of transcription factor foot printing, and some other technical limitations such as a relatively lower signal-to-noise ratio in FAIRE compared with ChIP-seq or DNase-seq experiments, leading to a reduced confidence in the sites identified [140]. Thus, it is not very clear of the molecular mechanism behind the genetic regulation at this stage.

5.2 BP-associated SNPs in rs1173771 LD block influence HUASMC proliferation *via* NPR-C signalling pathway.

The increase in vessel wall thickness/lumen (w/l) ratio resulting from vascular remodelling leads to greater vascular reactivity and elevated blood pressure,[149] while human vascular smooth muscle cell proliferation and migration contribute to vascular remodelling in hypertension and atherosclerosis.[150,151] Thus, SMC cell proliferation and migration ability are very relevant phenotypes to blood pressure control.

As a G_i-coupled receptor, NPR-C has been identified as a regulator of vascular SMC proliferation through mitogen-activated protein kinase (MAPK) and PI3-kinase.[152,153] Hobbs et al further investigated the vasoprotective profile of NPR-C, and revealed its binding of CNP could inhibit aortic smooth muscle cells (AoSMC) proliferation mediated by extracellular signal-regulated kinase (ERK) 1/2 phosphorylation.[133]

Here, the cell counting assay was conducted to investigate the cell viability with or without treatment of 100nM CNP or 100nM C-ANF$_{4-23}$. It is shown that treatment of CNP or C-ANF$_{4-23}$ after 24 hours could diminish human VSMCs proliferation in contrast to control group, and this inhibitory effect also revealed a trend of genetic difference with a relatively higher inhibitory influence on BP-lowering allele homozygotes. This is in agreement with their NPR-C expression level among genotypes and all support that stimulation of NPR-C could have an impact on cell proliferation *in vitro* (Figure 3.10).

Independent of CNP or C-ANF$_{4-23}$ exposure, HUASMCs proliferation over 24 hours also showed a remarkable difference between genotypes (Figure 3.9) offering a mechanistic link from the BP-elevating allele, to lower NPR3 expression and subsequently higher VSMCs proliferation. The mechanism behind this kind of intrinsic genetic difference in cell proliferation is currently unclear. The possible explanation may be the presence some autocrine secretion of natriuretic peptides, such as ANP, BNP and CNP, that could activate NPR-C and influence cell proliferation. Some literature have implicated ANP and BNP modulation of vascular cells proliferation. BNP has been shown to exert an anti-proliferative action on human fibroblasts.[154] ANP inhibited the growth of VSMCs *in vitro* and recombinant adenovirus (Ad-RSV)-ANP showed the respect to inhibiting rat VSMC proliferation and migration following

endothelial injury.[155] However, the precise role of NPR-C on vascular cell proliferation is so far unknown.

Furthermore, the possible genetic difference on HUASMCs migration was also detected here. It is shown CNP or C-ANF$_{4-23}$ could slightly inhibit the cell migration, and this is in line with previous finding that CNP or C-ANF$_{4–23}$ directly inhibited rat aortic smooth muscle migration *in vitro*.[111] Whereas, no significant genetic difference was observed among genotypes, although with a slightly higher migration in BP-elevating allele carriers (Figure 3.12), suggesting association between *NPR3* risk variants and BP control might not through regulating cell migration. Moreover, Hobbs et al. found CNP inhibitory effect on migration may be related with NPR-B in their current study (unpublished), providing a support for the concept. However, the limited size (N≥5 in each genotype) of HUASMC samples were utilised in scratch assay, thus future work with more samples might be explored.

Together, it is revealed HUASMCs carrying BP-elevating allele had a higher proliferation than BP-lowering allele homozygotes, with persists even after exposure to CNP or C-ANF$_{4-23}$. The finding of genetic differences in HUASMCs proliferation implies that the risk allele was associated with blood pressure elevation in individuals might partially result from the increased VSMCs proliferation via NPR-C signalling pathway.

5.3 BP-associated SNPs in rs1173771 LD block affect HUASMC calcium flux in response to Ang II

It is widely recognised that augmented intracellular calcium levels have an important role in compacting the vascular tone and precipitating blood pressure elevation.[156] By contraction and relaxation of smooth muscle cells, the luminal diameter of the vasculature was altered, which enables blood vessels to maintain an appropriate blood pressure.[157] Herein, carbachol and Ang II were both utilised to stimulate HUASMCs calcium flux. Optimization work of Ang II concertation in HUASMCs indicated an EC_{50} of approximately 10nM, an EC_{90} of 100nM. Both concertation of Ang II were used here to investigate the possible genetic difference among genotypes and inhibitory effect of CNP or C-ANF_{4-23} on Ang II- stimulated intracellular calcium increase with carbachol as agonist control.

Carbachol, a muscarinic and nicotinic receptor agonist, can increase human SMC intracellular free calcium concentrations.[158] Carbachol-induced contraction is predominantly initiated by M3 muscarinic receptor-mediated activation of the $G_{q/11}$-phospholipase C β-protein kinase C (PKC) and the G12/13-RhoGEF-Rho kinase (ROCK) pathways. However, these pathways and their downstream effectors are not well understood.[159,160] Herein, carbachol was utilised as a control agonist to explore the calcium flux. It is observed there is no genetic difference in carbachol-induced intracellular calcium increase in HUASMCs (Figure 3.13). This confirmed that the samples were able to mount an appropriate Ca^{2+}-response that was independent of genotype. With this, the observed genotype-associated differences in response to Ang II is more likely to be due to the genetic differences itself, rather than confounding factors such as differences in cell viability.

Ang II is an octapeptide hormone exerting vasoconstriction mediated by G_q protein-dependent signalling pathway, which activates PLC and increases cytosolic calcium concentrations.[161] Similarly, NPR-C has been recognized as a G_i protein coupled receptor which may influence PLC via the $G_{i\text{-}\beta/\gamma}$ subunit,[85] suggesting a potential crosstalk between Ang II and NPR-C on intracellular calcium regulation. Thus Ang II was used here to investigate the possible genetic impact of *NPR3* BP-associated variants on calcium flux which may link to NPR-C signalling pathway.

It is observed there was a genetic impact of BP-associated variants on intracellular calcium flux in human VSMCs with an augmented level in BP-elevating allele carriers when stimulated by 10nM or 100nM Ang II (Figure 3.13). This genetic pattern is compatible with their *NPR3* gene expression, indicating risk allele effect on blood pressure occurs by a mechanism of regulating VSMCs calcium flux in response to Ang II.

Here, we showed for the first time that human VSMCs presenting high NPR-C level could blunt the intracellular calcium reaction to Ang II, supporting the potential role of NPR-C in regulating VSMCs calcium current and blood pressure homeostasis. Several studies demonstrated NPR-C could reduce L-type calcium current ($I_{Ca,L}$) via binding with CNP in mouse vascular and sinoatrial node myocytes,[88] and (100nM) Ang II-stimulated mesenteric artery smooth muscle cells calcium flux.[134] Therefore, the effect of *NPR3* variations on the intracellular calcium changes may be through a CNP-related signalling pathway. Indeed, CNP inhibited the observed intracellular calcium response to 10nM Ang II in human umbilical arterial SMCs when pre-treated with CNP *in vitro*, which indicates NPR-C effect on human arterial VSMCs calcium flux might be involve CNP signalling pathway.

However, in my study, CNP did not inhibit the higher Ang II (100nM) stimulated intracellular calcium increase. This is might be explained by pharmacological antagonism. Moyes et al. showed CNP efficiently counteracted to 100nM Ang II-stimulated mesenteric artery smooth muscle cells calcium flux,[134] and implied CNP may have a tissue specificity. However, stimulation of NPR-C by C-ANF$_{4-23}$, mimicking the effect of natriuretic peptides, still displayed inhibitory effect of calcium flux in response to higher Ang II, indicating a possibility of NPR-C effect on HUAMSCs calcium signalling might be via more than CNP.

This thesis is consistent with other studies on NPR-C with other NPs (ANP or BNP) in hypertensive phenotype research. It has been demonstrated that ANP-induced vasodilation was significantly reduced by inhibition of the large-conductance calcium channel,[162] suggesting a link between ANP and calcium flux. BNP attenuated the L-type calcium current in ventricular myocytes.[163] Some future work targeting the interaction between NPR-C with ANP or BNP on human vasculature might be further explored.

5.4 No significant correlation of genetic impact on cell proliferation and calcium flux in response to Ang II

The same pattern was observed in both HUASMCs proliferation and calcium flux in response to Ang II, which was both higher in BP-elevating allele carriers, implicating a possibility of a correlation between these two phenotypes based on genotype.

The current literature indicates an influence of calcium signalling on cell proliferation. It has been revealed that increases in the basal cytosolic calcium concentration could

activate the immediate early genes responsible for inducing resting cells (G_0) to re-enter the cell cycle and promote the initiation of DNA synthesis at the $G_{1/S}$ transition.[164,165] However, when exceeding its normal spatial and temporal boundaries, calcium can result in cell death through both necrosis and apoptosis.[166]

In my study, carbachol was also utilised to induce the HUASMC calcium flux, but no genetic difference was observed, suggesting the intracellular calcium flux was not related to cell proliferation status. Moreover, the correlation analysis between cell proliferation/viability in 24 hours and calcium flux in response to Ang II did not show a significant association as displayed in Figure 5.1. Thus, the genetic impact on Ang II-induced calcium flux was correlated with NPR-C expression level and might be independent from the proliferation via different signalling pathways.

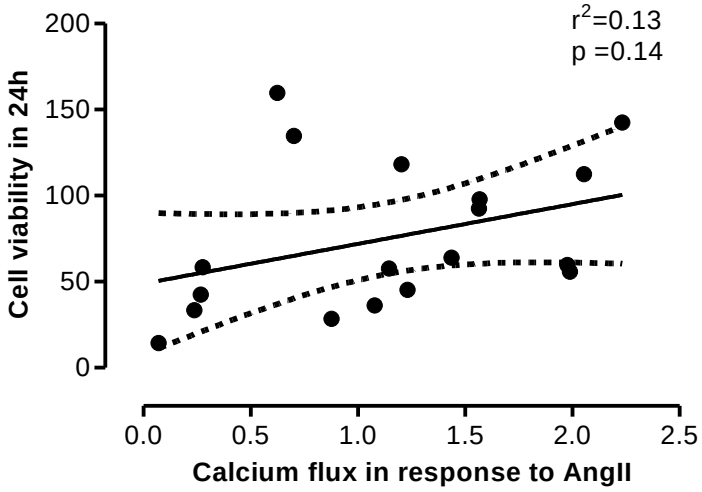

Figure 5.1 No correlation between cell viability in 24 hours and calcium flux in response to Ang II.

HUASMCs (N=20) conducted in both cell viability assay and calcium flux assay were subjected to linear regression analysis, and no significant linear relationship (p=0.14) was found between cell viability in 24 hours and calcium flux in response to Ang II.

5.5 Effect of BP-associated variants in rs173771 LD block on HUVECs

In addition to human VSMC studies, investigation of potential genetic impact of BP-associated variants on HUVECs were also conducted. Gene expression studies were firstly carried out on mRNA and protein levels of NPR-C to explore the possible genetic regulation on NPR3 gene expression in HUVECs. A significant genetic difference was not detected in HUVEC *NPR3* mRNA expression, although with a slightly lower *NPR3* mRNA level in BP-elevating allele carrier genotypes (see section 4.2.1-4.2.2). Complementary method of allelic expression imbalance analysis using genomic DNA and mRNA from HUVECs that were heterozygous for 3'-UTR SNP rs1173756 was conducted and indicated an obvious imbalance of allele's level with a lower expression of the BP-elevating allele (C) in mRNA comparing to the BP-lowering allele (T). Subsequent protein detection by western blotting did not validate a difference of NPR-among genotypes in HUVECs. These gene expression data presented above suggests a weak correlation of BP-associated SNPs with *NPR3* gene expression. However, the positive genetic difference observed in allelic expression imbalance study still could reflect the potential impact on the population individual difference indicated by GWAS study.

Moreover, no significant genetic impact was detected on HUVECs proliferation (section 4.2.4). Together with VSMCs data, it is implied a cell-type dependent specificity of such association mainly on VSMCs rather than ECs. As indicated in Figure 5.2, the expression level of *NPR3* mRNA in HUASMCs was remarkably higher compared with HUVECs, this might explain the cell-type dependent specificity which may link to the different *NPR3* expression levels in these cells. In addition, considering

the dual–capacity of NPR-C in both clearance and signalling pathway, there is a possible concept that NPR-C in VSMC mainly exert the signalling, otherwise, NPR-C in ECs may play a role of the clearance receptor based on their physiological locations in vasculature. However, more study still needs to be conducted to further study the mechanism.

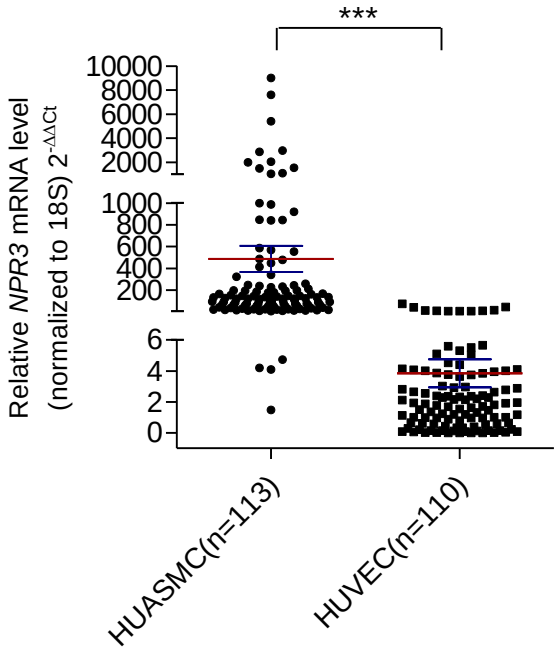

Figure 5.2 A much higher relative expression level of *NPR3* mRNA was detected in HUASMCs compared with HUVECs.

NPR3 mRNA level in HUASMCs and HUVECs were determined by quantitative reverse-transcription polymerase chain reaction (qRT-PCR), N ≥ 110 in each group, values are presented as mean ± SEM, ***P<0.001 analysed by unpaired t-test when HUASMC vs HUVEC.

5.6 Effect of other LD block at *NPR3* gene locus in HUASMCs and HUVECs

A recent hypertension susceptibility study by bespoke gene–centric assay found another BP-associated LD block with lead SNP rs1421811,[70] Although SNP rs421811 is in low LD (r^2=0.13) with rs1173771 LD block indicated by SNAP, its minor allele (G) is indicated as a BP-lowering allele, which is in line with genetic pattern on BP control for variants located in rs173771 LD block with BP-lowering allele being minor allele.

There are 20 SNPs in high LD ($r^2 \geq 0.8$) with rs421811 in this LD block in CEU population, which are either intronic or intergenic variants. Predicted by bioinformatics programs such as ENCODE, a few SNPs (rs421811, rs3828591, rs3762988, rs7729447) with relatively higher score in location of regulatory factors binding sites were chosen as candidates to conduct the functional study in HUASMCs and HUVECs *in vitro*.

Firstly, gene expression data in HUASMCs (see section 3.3.1-3.3.2) revealed a trend of genetic regulation of rs1421811 or rs3828591 (r^2=1.0) on *NPR3* mRNA level with a lower level in BP-elevating allele homozygotes. But this pattern was not validated at the protein level, although with a slightly lower NPR-C protein level in BP-elevating allele homozygote. Cell phenotypes detection for proliferation and migration did not show any genetic difference among genotypes. However, a much higher intracellular calcium flux in response to 100nmol/L Ang II was observed in BP-elevating allele homozygotes compared with other two genotypes (Figure 3.19-B).

Secondly, functional study based on HUVECs presented no significant genetic association with *NPR3* gene expression and cell proliferation, but with a relatively lower levels in BP-elevating allele homozygote (see section 4.3).

In total, current data in HUASMCs show a hint of genetic influence on *NPR3* mRNA expression level and intracellular calcium flux in response to Ang II with a very limited size of BP-lowering allele (minor allele) homozygotes (see section 3.1), in which the direction of genetic impact was not clear or consistent. Therefore, it is not safe to get a solid conclusion based on current data.

5.7 Conclusion

This study demonstrated that the hypertension-associated variants in the rs1173771 LD block exhibited lower NPR-C expression in individuals carrying BP-elevating allele. Human VSMC samples carrying the BP-elevating allele had augmented cell proliferation and Ang II-stimulated intracellular calcium response. However, we did not observe such a genetic association in HUVECs, suggesting a tissue specific impact on vascular smooth muscle. Altogether, the results has provided a mechanistic insight for the association of *NPR3* risk variants with elevation of blood pressure that may be through a lower NPR-C expression and subsequent modification of VSMCs phenotype via NPR-C related pathways.

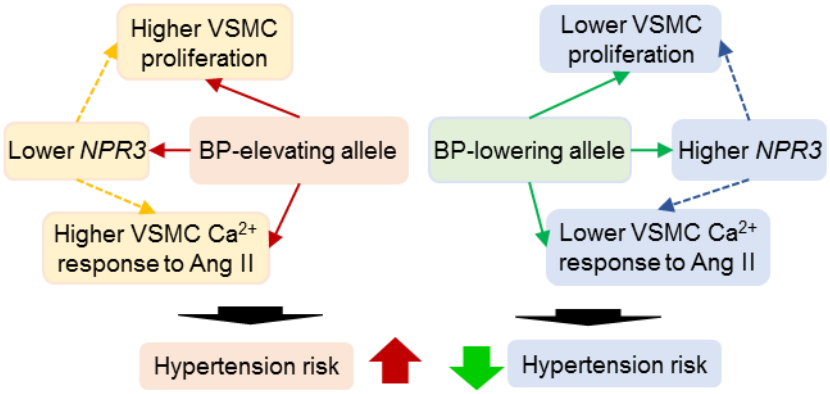

Figure 5.3 A proposed model to show the systemic mechanism between risk variants in natriuretic peptide receptor C (*NPR3*) gene and hypertension risk. The risk variants major allele (BP-elevating allele) presented a lower NPR3 expression and upregulated the human vascular smooth muscle cells proliferation and intracellular calcium changes in response to angiotensin II (AngII) NPR-C signalling pathway, which could lead to high risk for the development of hypertension.

Observations in human VSMCs proliferation and calcium flux studies provide a support for the concept that NPR-C has a physiological impact on blood pressure control. Indeed, C-atrial natriuretic peptide (C-ANF$_{4-23}$), a ring-deleted analog of ANP, is able to specifically interact with NPR-C. It has been demonstrated to attenuate the elevated BP of SHRs *via* decreasing the enhanced oxidative stress.[167] Additionally, C-ANP compound 118, an NPR-C agonist, caused relaxation of isolated mesenteric resistance arteries, an effect blocked by NPR-C antagonism. It also promoted a reduction of blood pressure in wild-type mice, which could be blunted in NPR-C KO mice.[134]

So far, researchers have identified more than 60 genes that harbour variations underlying the risks of hypertension.[45] These newly discovered candidate genes, proteins and their related pathways can represent powerful new drug targets. Here, we conducted a functional study base on the NPR3 locus and provided an evidence

that NPR3 is strongly involved in the development of hypertension, indicating NPR3 can be regarded as a therapeutic target for hypertension.

Moreover, It has been evident that single nucleotide polymorphisms (SNPs) in protein-coding region comprise merely 7% of complex disease-associated variants, while a striking majority of associated SNPs are either intronic or intergenic.[168,169] However, only a small fraction of molecular mechanisms in the development of disease may have been unravelled. Our functional experiments assessing the effect of these intronic and intergenic BP-associated variants on associated-gene regulation and cellular phenotypes have provided one example for this kind of study.

5.8 Future work

5.8.1 Original hypothesis

A number of studies have shown the SNPs within the *NPR3* locus are association with blood pressure in different populations. Additionally, previous work has also revealed the potential role of NPR-C in hypertension. However, the precise role of those blood-pressure associated SNPs and *NPR3* in the development of hypertension has not elucidated. So the major points are to be explored as follows:

1. The possible molecular mechanism associated to BP-associated SNPs at NPR3 locus: whether these SNPs affect *NPR3* gene expression or structural modelling /activity,
2. The role of NPR-C with its associated signalling pathway on cell phenotypes and in the development of hypertension.

5.8.2 Future work

This study have provided a mechanistic explanation for the recently reported association between *NPR3* variants and hypertension susceptibility. However, much more work needs to be done to further investigate the molecular mechanism behind and the role of NPR-C in the development of hypertension.

Some of the future work as discussed as below.

1. The study described in chapter 3.2.1-3.2.4 has shown the genetic regulation of BP-associated SNPs on *NPR3* expression. EMSA and FAIRE data provided a clue that rs1173747 and/or rs1173756 can be functional SNPs as residing in the regulatory elements region, but the precise molecular mechanism still needs to be explored with further experiments. The strategy would be that utilise antibodies targeting candidate transcription factors chosen by bioinformatics prediction to conduct ChIP assay or EMSA to determine whether there is interaction of SNPs flanking region with these transcription factors.

2. The findings indicated in chapter 3.2.5 and 3.2.7 presented a genetic impact of *NPR3* risk variants on HUASMCs proliferation and calcium flux in response to Ang II, even without treatment of CNP or C-ANF$_{4\text{-}23}$. A hypothesis would be there is CNP (maybe even ANP or BNP) present in the growth medium to activate the signalling pathway leading to the genetic difference in proliferation and calcium flux. To validate the hypothesis to elucidate the NPR-C signalling pathway behind, protein detection for CNP/ANP/BNP in growth medium would be done by western blotting, and more work with ANP/BNP on cell proliferation and calcium flux would be possibly conducted as well.

3. Data as described in chapter 3.3 revealed a hint of a genetic influence of BP-associated variants in rs1421811 LD block on *NPR3* mRNA expression level and intracellular calcium flux in response to Ang II. More samples, especially with the minor allele homozygotes would be needed to fully explore effect of the BP-associated SNPs on cell phenotypes, such as, cell proliferation, migration and calcium flux.

6. References

1. Swales JD. Manual of Hypertension. 1995:13-22.

2. Reil JC, Bohm M. The role of heart rate in the development of cardiovascular disease. *Clin Res Cardiol*. 2007;96(9):585-592. doi:10.1007/s00392-007-0537-5.

3. Guyton AC. Blood pressure control--special role of the kidneys and body fluids. *Science (80-)*. 1991;252(5014):1813-1816. http://www.ncbi.nlm.nih.gov/pubmed/2063193.

4. Takeuchi K, Ito S. [Molecular biology in regulation of renal functions: Renin-angiotensin system]. *Nihon Rinsho*. 2006;64 Suppl 2:187-191. http://www.ncbi.nlm.nih.gov/pubmed/16523885.

5. Folkow B, Sivertsson R. Aspects of the Difference in Vascular “Reactivity” between Cutaneous Resistance Vessels and a-V Anastomoses. *Angiologica*. 1964;1:338-345. http://www.ncbi.nlm.nih.gov/pubmed/14264824.

6. Short D. The nature of the increased vascular resistance in chronic hypertension. *Am Hear J*. 1967;73(6):840-841. http://www.ncbi.nlm.nih.gov/pubmed/6026046.

7. Weale FE, Taylor GW, Rothwell-Jackson RL. The Measurement of Regional Vascular Resistance at Operation. *Br J Surg*. 1964;51:627-629. http://www.ncbi.nlm.nih.gov/pubmed/14211723.

8. Cowley Jr. AW. Long-term control of arterial blood pressure. *Physiol Rev*. 1992;72(1):231-300. http://www.ncbi.nlm.nih.gov/pubmed/1731371.

9. Lifton RP, Gharavi AG, Geller DS. Molecular Mechanisms of Human Hypertension. *Cell*. 2001;104(4):545-556. doi:10.1016/S0092-8674(01)00241-0.

10. Maguire JJ, Davenport AP. Regulation of vascular reactivity by established and emerging GPCRs. *Trends Pharmacol Sci*. 2005;26(9):448-454. doi:10.1016/j.tips.2005.07.007.

11. Wirth A, Benyo Z, Lukasova M, et al. G12-G13-LARG-mediated signaling in vascular smooth muscle is required for salt-induced hypertension. *Nat Med*. 2008;14(1):64-68. doi:10.1038/nm1666.

12. El-Atat FA, Stas SN, McFarlane SI, Sowers JR. The relationship between hyperinsulinemia, hypertension and progressive renal disease. *J Am Soc Nephrol*. 2004;15(11):2816-2827. doi:Doi 10.1097/01.Asn.0000133698.80390.37.

13. Schrier RW, Humphreys MH, Ufferman RC. Role of cardiac output and the autonomic nervous system in the antinatriuretic response to acute constriction of the thoracic superior vena cava. *Circ Res*. 1971;29(5):490-498. http://www.ncbi.nlm.nih.gov/pubmed/5120614. Accessed November 23, 2015.

14. Guild SJ, Barrett CJ, Malpas SC. Long-term recording of sympathetic nerve activity: the new frontier in understanding the development of hypertension? *Clin Exp Pharmacol Physiol*. 2005;32(5-6):433-439. doi:CEP4207 [pii] 10.1111/j.1440-1681.2005.04207.x.

15. Wyss JM, Carlson SH. The role of the nervous system in hypertension. *Curr Hypertens Rep*. 2001;3(3):255-262.

http://www.ncbi.nlm.nih.gov/entrez/query.fcgi?cmd=Retrieve&db=PubMed&dopt=Citation&list_uids=11353577.

16. Oparil S, Zaman MA, Calhoun DA. Pathogenesis of hypertension. *Ann Intern Med*. 2003;139(9):761-776. http://www.ncbi.nlm.nih.gov/pubmed/14597461.

17. Roger VL, Go AS, Lloyd-Jones DM, et al. Heart disease and stroke statistics--2012 update: a report from the American Heart Association. *Circulation*. 2012;125(1):e2-e220. doi:10.1161/CIR.0b013e31823ac046.

18. Kearney PM, Whelton M, Reynolds K, Muntner P, Whelton PK, He J. Global burden of hypertension: analysis of worldwide data. *Lancet*. 2005;365(9455):217-223. doi:10.1016/S0140-6736(05)17741-1.

19. Pierdomenico SD, Di Nicola M, Esposito AL, et al. Prognostic value of different indices of blood pressure variability in hypertensive patients. *Am J Hypertens*. 2009;22(8):842-847. doi:10.1038/ajh.2009.103.

20. Sacks FM, Obarzanek E, Windhauser MM, et al. Rationale and design of the Dietary Approaches to Stop Hypertension trial (DASH). A multicenter controlled-feeding study of dietary patterns to lower blood pressure. *Ann Epidemiol*. 1995;5(2):108-118. http://www.ncbi.nlm.nih.gov/pubmed/7795829.

21. Primatesta P, Poulter NR. Improvement in hypertension management in England: results from the Health Survey for England 2003. *J Hypertens*. 2006;24(6):1187-1192. doi:10.1097/01.hjh.0000226210.95936.bc.

22. Tocci G, Rosei EA, Ambrosioni E, et al. Blood pressure control in Italy: analysis of clinical data from 2005-2011 surveys on hypertension. *J Hypertens*. 2012;30(6):1065-1074. doi:10.1097/HJH.0b013e3283535993.

23. Egan BM, Zhao Y, Axon RN. US trends in prevalence, awareness, treatment, and control of hypertension, 1988-2008. *JAMA*. 2010;303(20):2043-2050. doi:10.1001/jama.2010.650.

24. Binder A. A review of the genetics of essential hypertension. *Curr Opin Cardiol*. 2007;22(3):176-184. doi:10.1097/HCO.0b013e3280d357f9.

25. Lloyd-Jones D, Adams R, Carnethon M, et al. Heart disease and stroke statistics--2009 update: a report from the American Heart Association Statistics Committee and Stroke Statistics Subcommittee. *Circulation*. 2009;119(3):e21-e181. doi:10.1161/CIRCULATIONAHA.108.191261.

26. Harrap SB. Where are all the blood-pressure genes? *Lancet*. 2003;361(9375):2149-2151. doi:10.1016/S0140-6736(03)13694-X.

27. Marteau JB, Zaiou M, Siest G, Visvikis-Siest S. Genetic determinants of blood pressure regulation. *J Hypertens*. 2005;23(12):2127-2143. http://www.ncbi.nlm.nih.gov/pubmed/16269952.

28. Williams RR, Hunt SC, Hopkins PN, et al. Genetic basis of familial dyslipidemia and hypertension: 15-year results from Utah. *Am J Hypertens*. 1993;6(11 Pt 2):319S - 327S. http://www.ncbi.nlm.nih.gov/pubmed/8297539.

29. Krzesinski JM, Saint-Remy A. [Essential hypertension, a complex trait]. *Rev Med Liege*. 2012;67(5-6):279-285. http://www.ncbi.nlm.nih.gov/pubmed/22891479.

30. Sebat J, Lakshmi B, Troge J, et al. Large-scale copy number polymorphism in the human genome. *Science (80-)*. 2004;305(5683):525-528. doi:DOI 10.1126/science.1098918.

31. Altshuler D, Durbin RM, Abecasis GR, et al. A map of human genome variation from population-scale sequencing. *Nature*. 2010;467(7319):1061-1073. doi:Doi 10.1038/Nature09534.

32. Brookes AJ. The essence of SNPs. *Gene*. 1999;234(2):177-186. http://www.ncbi.nlm.nih.gov/pubmed/10395891.

33. Collins FS, Brooks LD, Chakravarti A. A DNA polymorphism discovery resource for research on human genetic variation. *Genome Res*. 1998;8(12):1229-1231. http://www.ncbi.nlm.nih.gov/pubmed/9872978.

34. *Genetics of Bone Biology and Skeletal Disease*. Academic Press; 2013. https://books.google.com/books?id=Y0OEkCLIw1QC&pgis=1. Accessed March 9, 2016.

35. Munroe PB, Barnes MR, Caulfield MJ. Advances in Blood Pressure Genomics. *Circ Res*. 2013;112(10):1365-1379. doi:Doi 10.1161/Circresaha.112.300387.

36. Cirulli ET, Goldstein DB. Uncovering the roles of rare variants in common disease through whole-genome sequencing. *Nat Rev Genet*. 2010;11(6):415-425. doi:10.1038/nrg2779.

37. McCarthy MI, Abecasis GR, Cardon LR, et al. Genome-wide association studies for complex traits: consensus, uncertainty and challenges. *Nat Rev Genet*. 2008;9(5):356-369. doi:10.1038/nrg2344.

38. Taylor JG, Choi E-H, Foster CB, Chanock SJ. Using genetic variation to study human disease. *Trends Mol Med*. 2001;7(11):507-512. doi:10.1016/S1471-4914(01)02183-9.

39. Shastry BS. SNPs: impact on gene function and phenotype. *Methods Mol Biol*. 2009;578:3-22. doi:10.1007/978-1-60327-411-1_1.

40. Ong C-T, Corces VG. Enhancer function: new insights into the regulation of tissue-specific gene expression. *Nat Rev Genet*. 2011;12(4):283-293. doi:10.1038/nrg2957.

41. Leff SE, Rosenfeld MG, Evans RM. Complex transcriptional units: diversity in gene expression by alternative RNA processing. *Annu Rev Biochem*. 1986;55:1091-1117. doi:10.1146/annurev.bi.55.070186.005303.

42. El Shamieh S, Visvikis-Siest S. Genetic biomarkers of hypertension and future challenges integrating epigenomics. *Clin Chim Acta*. 2012;414:259-265. doi:DOI 10.1016/j.cca.2012.09.018.

43. Cowley Jr. AW. The genetic dissection of essential hypertension. *Nat Rev Genet*. 2006;7(11):829-840. doi:10.1038/nrg1967.

44. Zhu M, Zhao S. Candidate gene identification approach: progress and challenges. *Int J Biol Sci*. 2007;3(7):420-427. http://www.pubmedcentral.nih.gov/articlerender.fcgi?artid=2043166&tool=pmcentrez&rendertype=abstract. Accessed March 5, 2016.

45. Munroe PB, Barnes MR, Caulfield MJ. Advances in blood pressure genomics. *Circ Res*. 2013;112(10):1365-1379. doi:10.1161/CIRCRESAHA.112.300387.

46. Peleman JD, Wye C, Zethof J, et al. Quantitative trait locus (QTL) isogenic recombinant analysis: a method for high-resolution mapping of QTL within a single population. *Genetics*. 2005;171(3):1341-1352. doi:10.1534/genetics.105.045963.

47. Lalouel JM. Large-scale search for genes predisposing to essential hypertension. *Am J Hypertens*. 2003;16(2):163-166. doi:Pii S0895-7061(02)03201-6 Doi 10.1016/S0895-7061(02)03201-6.

48. Bush WS, Moore JH. Chapter 11: Genome-wide association studies. *PLoS Comput Biol*. 2012;8(12):e1002822. doi:10.1371/journal.pcbi.1002822.

49. Williams SM, Addy JH, Phillips JA, et al. Combinations of variations in multiple genes are associated with hypertension. *Hypertension*. 2000;36(1):2-6. <Go to ISI>://WOS:000088419600002.

50. Zuk O, Schaffner SF, Samocha K, et al. Searching for missing heritability: designing rare variant association studies. *Proc Natl Acad Sci U S A*. 2014;111(4):E455-E464. doi:10.1073/pnas.1322563111.

51. Grada A, Weinbrecht K. Next-generation sequencing: methodology and application. *J Invest Dermatol*. 2013;133(8):e11. doi:10.1038/jid.2013.248.

52. Metzker ML. Sequencing technologies - the next generation. *Nat Rev Genet*. 2010;11(1):31-46. doi:10.1038/nrg2626.

53. Xuan J, Yu Y, Qing T, Guo L, Shi L. Next-generation sequencing in the clinic: promises and challenges. *Cancer Lett*. 2013;340(2):284-295. doi:10.1016/j.canlet.2012.11.025.

54. Dominiczak AF, Brain N, Charchar F, McBride M, Hanlon N, Lee WK. Genetics of hypertension: lessons learnt from mendelian and polygenic syndromes. *Clin Exp Hypertens*. 2004;26(7-8):611-620. http://www.ncbi.nlm.nih.gov/pubmed/15702615.

55. Ehret GB, Caulfield MJ. Genes for blood pressure: an opportunity to understand hypertension. *Eur Heart J*. 2013;34(13):951-961. doi:10.1093/eurheartj/ehs455.

56. Kato N, Julier C. Linkage mapping for hypertension susceptibility genes. *Curr Hypertens Rep*. 1999;1(1):15-24. http://www.ncbi.nlm.nih.gov/pubmed/10981038.

57. Carlson CS, Eberle MA, Kruglyak L, Nickerson DA. Mapping complex disease loci in whole-genome association studies. *Nature*. 2004;429(6990):446-452. doi:10.1038/nature02623.

58. Guo Y, Tomlinson B, Chu T, et al. A genome-wide linkage and association scan reveals novel loci for hypertension and blood pressure traits. *PLoS One*. 2012;7(2):e31489. doi:10.1371/journal.pone.0031489.

59. Levy D, Ehret GB, Rice K, et al. Genome-wide association study of blood pressure and hypertension. *Nat Genet*. 2009;41(6):677-687. doi:10.1038/ng.384.

60. Newton-Cheh C, Johnson T, Gateva V, et al. Genome-wide association study identifies eight loci associated with blood pressure. *Nat Genet*. 2009;41(6):666-676. doi:10.1038/ng.361.

61. Healy DG. Case-control studies in the genomic era: a clinician's guide. *Lancet Neurol*. 2006;5(8):701-707. doi:10.1016/S1474-4422(06)70524-5.

62. Ehret GB. Genome-wide association studies: contribution of genomics to understanding blood pressure and essential hypertension. *Curr Hypertens Rep*. 2010;12(1):17-25. doi:10.1007/s11906-009-0086-6.

63. Newton-Cheh C, Johnson T, Gateva V, et al. Genome-wide association study identifies eight loci associated with blood pressure. *Nat Genet*. 2009;41(6):666-676. doi:10.1038/ng.361.

64. Padmanabhan S, Melander O, Johnson T, et al. Genome-wide association study of blood pressure extremes identifies variant near UMOD associated with hypertension. *PLoS Genet*. 2010;6(10):e1001177. doi:10.1371/journal.pgen.1001177.

65. International Consortium for Blood Pressure Genome-Wide Association S, Ehret GB, Munroe PB, et al. Genetic variants in novel pathways influence blood pressure and cardiovascular disease risk. *Nature*. 2011;478(7367):103-109. doi:10.1038/nature10405.

66. Levy D, Ehret GB, Rice K, et al. Genome-wide association study of blood pressure and hypertension. *Nat Genet*. 2009;41(6):677-687. doi:10.1038/ng.384.

67. Wain L V, Verwoert GC, O'Reilly PF, et al. Genome-wide association study identifies six new loci influencing pulse pressure and mean arterial pressure. *Nat Genet*. 2011;43(10):1005-1011. doi:10.1038/ng.922.

68. He J, Kelly TN, Zhao Q, et al. Genome-Wide Association Study Identifies Eight Novel Loci Associated with Blood Pressure Responses to Interventions in Han Chinese. *Circ Cardiovasc Genet*. 2013. doi:10.1161/CIRCGENETICS.113.000307.

69. Kato N, Takeuchi F, Tabara Y, et al. Meta-analysis of genome-wide association studies identifies common variants associated with blood

pressure variation in east Asians. *Nat Genet*. 2011;43(6):531-538. doi:10.1038/ng.834.

70. Johnson T, Gaunt TR, Newhouse SJ, et al. Blood pressure loci identified with a gene-centric array. *Am J Hum Genet*. 2011;89(6):688-700. doi:10.1016/j.ajhg.2011.10.013.

71. Savoie P, de Champlain J, Anand-Srivastava MB. C-type natriuretic peptide and brain natriuretic peptide inhibit adenylyl cyclase activity: interaction with ANF-R2/ANP-C receptors. *FEBS Lett*. 1995;370(1-2):6-10. http://www.ncbi.nlm.nih.gov/pubmed/7649305.

72. Anand-Srivastava MB. Natriuretic peptide receptor-C signaling and regulation. *Peptides*. 2005;26(6):1044-1059. doi:10.1016/j.peptides.2004.09.023.

73. Suga S, Nakao K, Hosoda K, et al. Receptor selectivity of natriuretic peptide family, atrial natriuretic peptide, brain natriuretic peptide, and C-type natriuretic peptide. *Endocrinology*. 1992;130(1):229-239. http://www.ncbi.nlm.nih.gov/pubmed/1309330.

74. Wong GG. The isolation and identification of cDNA genes by their heterologous expression and function. *Genet Eng (N Y)*. 1990;12:297-316. http://www.ncbi.nlm.nih.gov/pubmed/1366706.

75. Maack T, Suzuki M, Almeida FA, et al. Physiological role of silent receptors of atrial natriuretic factor. *Science (80-)*. 1987;238(4827):675-678. http://www.ncbi.nlm.nih.gov/pubmed/2823385.

76. Ardaillou N, Placier S, Striker L, Striker G, Ardaillou R. Mesangial cells from diabetic NOD mice constitutively express increased density of atrial natriuretic

peptide C receptors. *Kidney Int*. 1999;55(4):1293-1302. doi:10.1046/j.1523-1755.1999.00393.x.

77. Zhou H, Murthy KS. Identification of the G protein-activating sequence of the single-transmembrane natriuretic peptide receptor C (NPR-C). *Am J Physiol Cell Physiol*. 2003;284(5):C1255-C1261. doi:10.1152/ajpcell.00520.2002.

78. Leitman DC, Andresen JW, Kuno T, Kamisaki Y, Chang JK, Murad F. Identification of multiple binding sites for atrial natriuretic factor by affinity cross-linking in cultured endothelial cells. *J Biol Chem*. 1986;261(25):11650-11655. http://www.ncbi.nlm.nih.gov/pubmed/3017939.

79. Maack T. Role of atrial natriuretic factor in volume control. *Kidney Int*. 1996;49(6):1732-1737. http://www.ncbi.nlm.nih.gov/pubmed/8743487.

80. Anand-Srivastava MB. Platelets from spontaneously hypertensive rats exhibit decreased expression of inhibitory guanine nucleotide regulatory protein. Relation with adenylyl cyclase activity. *Circ Res*. 1993;73(6):1032-1039. http://www.ncbi.nlm.nih.gov/pubmed/8222075.

81. Anand-Srivastava MB, Sairam MR, Cantin M. Ring-deleted analogs of atrial natriuretic factor inhibit adenylate cyclase/cAMP system. Possible coupling of clearance atrial natriuretic factor receptors to adenylate cyclase/cAMP signal transduction system. *J Biol Chem*. 1990;265(15):8566-8572. http://www.ncbi.nlm.nih.gov/pubmed/2160462.

82. Anand-Srivastava MB, Srivastava AK, Cantin M. Pertussis toxin attenuates atrial natriuretic factor-mediated inhibition of adenylate cyclase. Involvement of inhibitory guanine nucleotide regulatory protein. *J Biol Chem*. 1987;262(11):4931-4934. http://www.ncbi.nlm.nih.gov/pubmed/3031034.

83. Pagano M, Anand-Srivastava MB. Cytoplasmic domain of natriuretic peptide receptor C constitutes Gi activator sequences that inhibit adenylyl cyclase activity. *J Biol Chem*. 2001;276(25):22064-22070. doi:10.1074/jbc.M101587200.

84. Gilman AG. G-Proteins - Transducers of Receptor-Generated Signals. *Annu Rev Biochem*. 1987;56:615-649. doi:DOI 10.1146/annurev.biochem.56.1.615.

85. Mouawad R, Li Y, Anand-Srivastava MB. Atrial natriuretic peptide-C receptor-induced attenuation of adenylyl cyclase signaling activates phosphatidylinositol turnover in A10 vascular smooth muscle cells. *Mol Pharmacol*. 2004;65(4):917-924. doi:10.1124/mol.65.4.917.

86. Hashim S, Li Y, Anand-Srivastava MB. Small cytoplasmic domain peptides of natriuretic peptide receptor-C attenuate cell proliferation through Gialpha protein/MAP kinase/PI3-kinase/AKT pathways. *Am J Physiol Hear Circ Physiol*. 2006;291(6):H3144-H3153. doi:10.1152/ajpheart.00327.2006.

87. Murthy KS, Teng B, Jin J, Makhlouf GM. G protein-dependent activation of smooth muscle eNOS via natriuretic peptide clearance receptor. *Am J Physiol*. 1998;275(6 Pt 1):C1409-C1416. http://www.ncbi.nlm.nih.gov/pubmed/9843699.

88. Rose RA, Lomax AE, Giles WR. Inhibition of L-type Ca2+ current by C-type natriuretic peptide in bullfrog atrial myocytes: an NPR-C-mediated effect. *Am J Physiol Hear Circ Physiol*. 2003;285(6):H2454-H2462. doi:10.1152/ajpheart.00388.2003.

89. Chabrier PE, Roubert P, Lonchampt MO, Plas P, Braquet P. Regulation of atrial natriuretic factor receptors by angiotensin II in rat vascular smooth

muscle cells. *J Biol Chem*. 1988;263(26):13199-13202. http://www.ncbi.nlm.nih.gov/pubmed/2843514.

90. Yoshimoto T, Naruse M, Naruse K, et al. Angiotensin II-dependent down-regulation of vascular natriuretic peptide type C receptor gene expression in hypertensive rats. *Endocrinology*. 1996;137(3):1102-1107. doi:10.1210/endo.137.3.8603580.

91. Boumati M, Li Y, Anand-Srivastava MB. Modulation of ANP-C receptor signaling by endothelin-1 in A-10 smooth muscle cells. *Arch Biochem Biophys*. 2002;401(2):178-186. doi:10.1016/S0003-9861(02)00044-9.

92. Kishimoto I, Yoshimasa T, Suga S, et al. Natriuretic Peptide Clearance Receptor Is Transcriptionally down-Regulated by Beta(2)-Adrenergic Stimulation in Vascular Smooth-Muscle Cells. *J Biol Chem*. 1994;269(45):28300-28308. <Go to ISI>://WOS:A1994PV77200079.

93. Katafuchi T, Mizuno T, Hagiwara H, Itakura M, Ito T, Hirose S. Modulation by NaCl of atrial natriuretic peptide receptor levels and cyclic GMP responsiveness to atrial natriuretic peptide of cultured vascular endothelial cells. *J Biol Chem*. 1992;267(11):7624-7629. http://www.ncbi.nlm.nih.gov/pubmed/1348507.

94. Sun JZ, Oparil S, Lucchesi P, Thompson JA, Chen YF. Tyrosine kinase receptor activation inhibits NPR-C in lung arterial smooth muscle cells. *Am J Physiol Cell Mol Physiol*. 2001;281(1):L155-L163. <Go to ISI>://WOS:000169546800021.

95. Arejian M, Li Y, Anand-Srivastava MB. Nitric oxide attenuates the expression of natriuretic peptide receptor C and associated adenylyl cyclase signaling in

aortic vascular smooth muscle cells: role of MAPK. *Am J Physiol Circ Physiol*. 2009;296(6):H1859-H1867. doi:DOI 10.1152/ajpheart.01108.2008.

96. Agui T, Xin X, Cai Y, et al. Opposite actions of transforming growth factor-beta 1 on the gene expression of atrial natriuretic peptide biological and clearance receptors in a murine thymic stromal cell line. *J Biochem*. 1995;118(3):500-507. http://www.ncbi.nlm.nih.gov/pubmed/8690708.

97. Ardaillou N, Blaise V, Placier S, Amestoy F, Ardaillou R. Dexamethasone upregulates ANP C-receptor protein in human mesangial cells without affecting mRNA. *Am J Physiol Fluid Electrolyte Physiol*. 1996;270(3):F440-F446. <Go to ISI>://WOS:A1996UA04800009.

98. Sarzani R, Paci VM, Zingaretti CM, et al. Fasting inhibits natriuretic peptides clearance receptor expression in rat adipose tissue. *J Hypertens*. 1995;13(11):1241-1246. http://www.ncbi.nlm.nih.gov/pubmed/8984120.

99. Carini R, De Cesaris MG, Splendore R, et al. Mechanisms of hepatocyte protection against hypoxic injury by atrial natriuretic peptide. *Hepatology*. 2003;37(2):277-285. doi:10.1053/jhep.2003.50033.

100. Chen YF. Atrial natriuretic peptide in hypoxia. *Peptides*. 2005;26(6):1068-1077. doi:10.1016/j.peptides.2004.08.030.

101. Li H, Oparil S, Meng QC, Elton TS, Chen YF. Selective downregulation of ANP-clearance-receptor gene expression in lung of rats adapted to hypoxia. *Am J Physiol*. 1995;268(2 Pt 1):L328-L335. http://www.ncbi.nlm.nih.gov/pubmed/7864153.

102. Nagase M, Ando K, Katafuchi T, Kato A, Hirose S, Fujita T. Role of natriuretic peptide receptor type C in dahl salt-sensitive hypertensive rats. *Hypertension*. 1997;30(2):177-183. <Go to ISI>://WOS:A1997XQ40900006.

103. Li YX, Cheng KC, Asakawa A, et al. Role of musclin in the pathogenesis of hypertension in rat. *PLoS One*. 2013;8(8):e72004. doi:10.1371/journal.pone.0072004.

104. Dessi-Fulgheri P, Sarzani R, Tamburrini P, et al. Plasma atrial natriuretic peptide and natriuretic peptide receptor gene expression in adipose tissue of normotensive and hypertensive obese patients. *J Hypertens*. 1997;15(12 Pt 2):1695-1699. http://www.ncbi.nlm.nih.gov/pubmed/9488224.

105. Anand-Srivastava MB. Atrial natriuretic peptide-C receptor and membrane signalling in hypertension. *J Hypertens*. 1997;15(8):815-826. http://www.ncbi.nlm.nih.gov/pubmed/9280203.

106. Costa MA, Elesgaray R, Balaszczuk AM, Arranz C. Role of NPR-C natriuretic receptor in nitric oxide system activation induced by atrial natriuretic peptide. *Regul Pept*. 2006;135(1-2):63-68. doi:10.1016/j.regpep.2006.04.002.

107. Villar IC, Panayiotou CM, Sheraz A, et al. Definitive role for natriuretic peptide receptor-C in mediating the vasorelaxant activity of C-type natriuretic peptide and endothelium-derived hyperpolarising factor. *Cardiovasc Res*. 2007;74(3):515-525. doi:10.1016/j.cardiores.2007.02.032.

108. Ehret GB, Munroe PB, Rice KM, et al. Genetic variants in novel pathways influence blood pressure and cardiovascular disease risk. *Nature*. 2011;478(7367):103-109. doi:10.1038/nature10405.

109. Zhu X, Young JH, Fox E, et al. Combined admixture mapping and association analysis identifies a novel blood pressure genetic locus on 5p13: contributions from the CARe consortium. *Hum Mol Genet*. 2011;20(11):2285-2295. doi:10.1093/hmg/ddr113.

110. Johnson T, Gaunt TR, Newhouse SJ, et al. Blood pressure loci identified with a gene-centric array. *Am J Hum Genet*. 2011;89(6):688-700. doi:10.1016/j.ajhg.2011.10.013.

111. Cahill PA, Hassid A. ANF-C-receptor-mediated inhibition of aortic smooth muscle cell proliferation and thymidine kinase activity. *Am J Physiol*. 1994;266(1 Pt 2):R194-R203. http://www.ncbi.nlm.nih.gov/pubmed/8304541.

112. Levin ER, Frank HJ. Natriuretic peptides inhibit rat astroglial proliferation: mediation by C receptor. *Am J Physiol*. 1991;261(2 Pt 2):R453-R457. http://www.ncbi.nlm.nih.gov/pubmed/1652217.

113. Naruko T, Itoh A, Haze K, et al. C-Type natriuretic peptide and natriuretic peptide receptors are expressed by smooth muscle cells in the neointima after percutaneous coronary intervention. *Atherosclerosis*. 2005;181(2):241-250. doi:10.1016/j.atherosclerosis.2005.01.023.

114. Liu Y, Abendschein D, Woodard GE, et al. Molecular imaging of atherosclerotic plaque with (64)Cu-labeled natriuretic peptide and PET. *J Nucl Med*. 2010;51(1):85-91. doi:10.2967/jnumed.109.066977.

115. Hobbs A, Foster P, Prescott C, Scotland R, Ahluwalia A. Natriuretic peptide receptor-C regulates coronary blood flow and prevents myocardial ischemia/reperfusion injury: novel cardioprotective role for endothelium-

derived C-type natriuretic peptide. *Circulation*. 2004;110(10):1231-1235. doi:10.1161/01.CIR.0000141802.29945.34.

116. Hystad ME, Oie E, Grogaard HK, et al. Gene expression of natriuretic peptides and their receptors type-A and -C after myocardial infarction in rats. *Scand J Clin Lab Invest*. 2001;61(2):139-150. http://www.ncbi.nlm.nih.gov/pubmed/11347981.

117. Becker JR, Chatterjee S, Robinson TY, et al. Differential activation of natriuretic peptide receptors modulates cardiomyocyte proliferation during development. *Development*. 2013. doi:10.1242/dev.100370.

118. Nakatsuji H, Maeda N, Hibuse T, et al. Reciprocal regulation of natriuretic peptide receptors by insulin in adipose cells. *Biochem Biophys Res Commun*. 2010;392(1):100-105. doi:10.1016/j.bbrc.2010.01.008.

119. Sarzani R, Dessi-Fulgheri P, Paci VM, Espinosa E, Rappelli A. Expression of natriuretic peptide receptors in human adipose and other tissues. *J Endocrinol Invest*. 1996;19(9):581-585. http://www.ncbi.nlm.nih.gov/pubmed/8957740.

120. Belo NO, Sairam MR, Dos Reis AM. Impairment of the natriuretic peptide system in follitropin receptor knockout mice and reversal by estradiol: implications for obesity-associated hypertension in menopause. *Endocrinology*. 2008;149(3):1399-1406. doi:10.1210/en.2007-0572.

121. Matsukawa N, Grzesik WJ, Takahashi N, et al. The natriuretic peptide clearance receptor locally modulates the physiological effects of the natriuretic peptide system. *Proc Natl Acad Sci*. 1999;96(13):7403-7408. doi:10.1073/pnas.96.13.7403.

122. Yanaka N, Akatsuka H, Kawai E, Omori K. 1,25-Dihydroxyvitamin D3 upregulates natriuretic peptide receptor-C expression in mouse osteoblasts. *Am J Physiol*. 1998;275(6 Pt 1):E965-E973. http://www.ncbi.nlm.nih.gov/pubmed/9843738.

123. Dauphinee SM, Eva MM, Yuki KE, Herman M, Vidal SM, Malo D. Characterization of two ENU-induced mutations affecting mouse skeletal morphology. *G3*. 2013;3(10):1753-1758. doi:10.1534/g3.113.007310.

124. Estrada K, Krawczak M, Schreiber S, et al. A genome-wide association study of northwestern Europeans involves the C-type natriuretic peptide signaling pathway in the etiology of human height variation. *Hum Mol Genet*. 2009;18(18):3516-3524. doi:10.1093/hmg/ddp296.

125. Bocciardi R, Giorda R, Buttgereit J, et al. Overexpression of the C-type natriuretic peptide (CNP) is associated with overgrowth and bone anomalies in an individual with balanced t(2;7) translocation. *Hum Mutat*. 2007;28(7):724-731. doi:10.1002/humu.20511.

126. Rubattu S, Sciarretta S, Morriello A, Calvieri C, Battistoni A, Volpe M. NPR-C: a component of the natriuretic peptide family with implications in human diseases. *J Mol Med*. 2010;88(9):889-897. doi:10.1007/s00109-010-0641-2.

127. Nishikimi T, Maeda N, Matsuoka H. The role of natriuretic peptides in cardioprotection. *Cardiovasc Res*. 2006;69(2):318-328. doi:10.1016/j.cardiores.2005.10.001.

128. Woodard GE, Rosado JA. Natriuretic peptides in vascular physiology and pathology. *Int Rev Cell Mol Biol*. 2008;268:59-93. doi:10.1016/S1937-6448(08)00803-4.

129. Chen HH, Burnett Jr. JC. C-type natriuretic peptide: the endothelial component of the natriuretic peptide system. *J Cardiovasc Pharmacol*. 1998;32 Suppl 3:S22-S28. http://www.ncbi.nlm.nih.gov/pubmed/9883743.

130. Stingo AJ, Clavell AL, Heublein DM, Wei CM, Pittelkow MR, Burnett Jr. JC. Presence of C-type natriuretic peptide in cultured human endothelial cells and plasma. *Am J Physiol*. 1992;263(4 Pt 2):H1318-H1321. http://www.ncbi.nlm.nih.gov/pubmed/1384363.

131. Honing ML, Smits P, Morrison PJ, Burnett Jr. JC, Rabelink TJ. C-type natriuretic peptide-induced vasodilation is dependent on hyperpolarization in human forearm resistance vessels. *Hypertension*. 2001;37(4):1179-1183. http://www.ncbi.nlm.nih.gov/pubmed/11304521.

132. Chauhan SD, Nilsson H, Ahluwalia A, Hobbs AJ. Release of C-type natriuretic peptide accounts for the biological activity of endothelium-derived hyperpolarizing factor. *Proc Natl Acad Sci U S A*. 2003;100(3):1426-1431. doi:10.1073/pnas.0336365100.

133. Khambata RS, Panayiotou CM, Hobbs AJ. Natriuretic peptide receptor-3 underpins the disparate regulation of endothelial and vascular smooth muscle cell proliferation by C-type natriuretic peptide. *Br J Pharmacol*. 2011;164(2b):584-597. doi:10.1111/j.1476-5381.2011.01400.x.

134. Moyes AJ, Khambata RS, Villar I, et al. Endothelial C-type natriuretic peptide maintains vascular homeostasis. *J Clin Invest*. 2014;124(9):4039-4051. doi:10.1172/JCI74281.

135. Caniffi C, Elesgaray R, Gironacci M, Arranz C, Costa MA. C-type natriuretic peptide effects on cardiovascular nitric oxide system in spontaneously

hypertensive rats. *Peptides*. 2010;31(7):1309-1318. doi:10.1016/j.peptides.2010.03.030.

136. Skau M, Goetze JP, Rehfeld JF, Jensen R. Natriuretic pro-peptides in idiopathic intracranial hypertension. *Regul Pept*. 2010;164(2-3):71-77. doi:10.1016/j.regpep.2010.05.009.

137. Itoh T, Nagaya N, Murakami S, et al. C-type natriuretic peptide ameliorates monocrotaline-induced pulmonary hypertension in rats. *Am J Respir Crit Care Med*. 2004;170(11):1204-1211. doi:10.1164/rccm.200404-455OC.

138. Sangaralingham SJ, Huntley BK, Martin FL, et al. The aging heart, myocardial fibrosis, and its relationship to circulating C-type natriuretic Peptide. *Hypertension*. 2011;57(2):201-207. doi:10.1161/HYPERTENSIONAHA.110.160796.

139. Grobmyer SR, Kuo A, Orishimo M, Okada SS, Cines DB, Barnathan ES. Determinants of binding and internalization of tissue-type plasminogen activator by human vascular smooth muscle and endothelial cells. *J Biol Chem*. 1993;268(18):13291-13300. http://www.ncbi.nlm.nih.gov/pubmed/7685759.

140. Simon JM, Giresi PG, Davis IJ, Lieb JD. Using formaldehyde-assisted isolation of regulatory elements (FAIRE) to isolate active regulatory DNA. *Nat Protoc*. 2012;7(2):256-267. doi:10.1038/nprot.2011.444.

141. Liang C-C, Park AY, Guan J-L. In vitro scratch assay: a convenient and inexpensive method for analysis of cell migration in vitro. *Nat Protoc*. 2007;2(2):329-333. doi:10.1038/nprot.2007.30.

142. Saulnier PJ, Roussel R, Halimi JM, et al. Impact of natriuretic peptide clearance receptor (NPR3) gene variants on blood pressure in type 2 diabetes. *Diabetes Care*. 2011;34(5):1199-1204. doi:10.2337/dc10-2057.

143. Gilman AG. G proteins: transducers of receptor-generated signals. *Annu Rev Biochem*. 1987;56:615-649. doi:10.1146/annurev.bi.56.070187.003151.

144. Berk BC. Vascular smooth muscle growth: autocrine growth mechanisms. *Physiol Rev*. 2001;81(3):999-1030. http://www.ncbi.nlm.nih.gov/pubmed/11427690.

145. Puddu P, Puddu GM, Zaca F, Muscari A. Endothelial dysfunction in hypertension. *Acta Cardiol*. 2000;55(4):221-232. http://www.ncbi.nlm.nih.gov/pubmed/11041120.

146. Ehret GB, Munroe PB, Rice KM, et al. Genetic variants in novel pathways influence blood pressure and cardiovascular disease risk. *Nature*. 2011;478(7367):103-109. doi:10.1038/nature10405.

147. Pereira NL, Lin D, Pelleymounter L, et al. Natriuretic peptide receptor-3 gene (NPR3): nonsynonymous polymorphism results in significant reduction in protein expression because of accelerated degradation. *Circ Cardiovasc Genet*. 2013;6(2):201-210. doi:10.1161/CIRCGENETICS.112.964742.

148. Clapier CR, Cairns BR. The biology of chromatin remodeling complexes. *Annu Rev Biochem*. 2009;78:273-304. doi:10.1146/annurev.biochem.77.062706.153223.

149. Korner PI, Angus JA, Bobik A, Jennings GL. Amplifier function of resistance vessels and the left ventricle in hypertension. *J Hypertens Suppl*. 1991;9(2):S31-S40; discussion S40-S41.

http://www.ncbi.nlm.nih.gov/pubmed/1838766. Accessed November 22, 2015.

150. Heagerty AM, Aalkjaer C, Bund SJ, Korsgaard N, Mulvany MJ. Small artery structure in hypertension. Dual processes of remodeling and growth. *Hypertension*. 1993;21(4):391-397. http://www.ncbi.nlm.nih.gov/pubmed/8458640. Accessed October 14, 2015.

151. Owens GK. Regulation of differentiation of vascular smooth muscle cells. *Physiol Rev*. 1995;75(3):487-517. http://www.ncbi.nlm.nih.gov/pubmed/7624392. Accessed November 22, 2015.

152. El Andalousi J, Li Y, Anand-Srivastava MB. Natriuretic peptide receptor-C agonist attenuates the expression of cell cycle proteins and proliferation of vascular smooth muscle cells from spontaneously hypertensive rats: role of Gi proteins and MAPkinase/PI3kinase signaling. *PLoS One*. 2013;8(10):e76183. doi:10.1371/journal.pone.0076183.

153. Li Y, Hashim S, Anand-Srivastava MB. Intracellular peptides of natriuretic peptide receptor-C inhibit vascular hypertrophy via Gqalpha/MAP kinase signaling pathways. *Cardiovasc Res*. 2006;72(3):464-472. doi:10.1016/j.cardiores.2006.08.012.

154. Huntley BK, Sandberg SM, Noser JA, et al. BNP-induced activation of cGMP in human cardiac fibroblasts: interactions with fibronectin and natriuretic peptide receptors. *J Cell Physiol*. 2006;209(3):943-949. doi:10.1002/jcp.20793.

155. Larifla L, Déprez I, Pham I, et al. Inhibition of vascular smooth muscle cell proliferation and migration in vitro and neointimal hyperplasia in vivo by adenoviral-mediated atrial natriuretic peptide delivery. *J Gene Med*. 2012;14(7):459-467. doi:10.1002/jgm.2639.

156. Hill-Eubanks DC, Werner ME, Heppner TJ, Nelson MT. Calcium signaling in smooth muscle. *Cold Spring Harb Perspect Biol*. 2011;3(9):a004549. doi:10.1101/cshperspect.a004549.

157. Rensen SSM, Doevendans PAFM, van Eys GJJM. Regulation and characteristics of vascular smooth muscle cell phenotypic diversity. *Neth Heart J*. 2007;15(3):100-108. http://www.pubmedcentral.nih.gov/articlerender.fcgi?artid=1847757&tool=pmcentrez&rendertype=abstract. Accessed June 4, 2015.

158. Kropp BP, Zhang Y, Tomasek JJ, et al. Characterization of cultured bladder smooth muscle cells: assessment of in vitro contractility. *J Urol*. 1999;162(5):1779-1784. http://www.ncbi.nlm.nih.gov/pubmed/10524934. Accessed November 1, 2015.

159. Fleichman M, Schneider T, Fetscher C, Michel MC. Signal transduction underlying carbachol-induced contraction of rat urinary bladder. II. Protein kinases. *J Pharmacol Exp Ther*. 2004;308(1):54-58. doi:10.1124/jpet.103.058255.

160. Kitazawa T, Eto M, Woodsome TP, Brautigan DL. Agonists trigger G protein-mediated activation of the CPI-17 inhibitor phosphoprotein of myosin light chain phosphatase to enhance vascular smooth muscle contractility. *J Biol Chem*. 2000;275(14):9897-9900.

http://www.ncbi.nlm.nih.gov/pubmed/10744661. Accessed November 23, 2015.

161. Mehta PK, Griendling KK. Angiotensin II cell signaling: physiological and pathological effects in the cardiovascular system. *Am J Physiol Cell Physiol*. 2007;292(1):C82-C97. doi:10.1152/ajpcell.00287.2006.

162. Matsumoto T, Watanabe S, Yamada K, et al. Relaxation Induced by Atrial Natriuretic Peptide Is Impaired in Carotid but Not Renal Arteries from Spontaneously Hypertensive Rats Due to Reduced BKCa Channel Activity. *Biol Pharm Bull*. 2015;38(11):1801-1808. doi:10.1248/bpb.b15-00527.

163. Sodi R, Dubuis E, Shenkin A, Hart G. B-type natriuretic peptide (BNP) attenuates the L-type calcium current and regulates ventricular myocyte function. *Regul Pept*. 2008;151(1-3):95-105. doi:10.1016/j.regpep.2008.06.006.

164. Berridge MJ. Calcium signalling and cell proliferation. *Bioessays*. 1995;17(6):491-500. doi:10.1002/bies.950170605.

165. Capiod T. Cell proliferation, calcium influx and calcium channels. *Biochimie*. 2011;93(12):2075-2079. doi:10.1016/j.biochi.2011.07.015.

166. Berridge MJ, Lipp P, Bootman MD. The versatility and universality of calcium signalling. *Nat Rev Mol Cell Biol*. 2000;1(1):11-21. doi:10.1038/35036035.

167. Li Y, Sarkar O, Brochu M, Anand-Srivastava MB. Natriuretic peptide receptor-C attenuates hypertension in spontaneously hypertensive rats: role of nitroxidative stress and Gi proteins. *Hypertension*. 2014;63(4):846-855. doi:10.1161/HYPERTENSIONAHA.113.01772.

168. Pennisi E. The Biology of Genomes. Disease risk links to gene regulation. *Science*. 2011;332(6033):1031. doi:10.1126/science.332.6033.1031.

169. Hindorff LA, Sethupathy P, Junkins HA, et al. Potential etiologic and functional implications of genome-wide association loci for human diseases and traits. *Proc Natl Acad Sci U S A*. 2009;106(23):9362-9367. doi:10.1073/pnas.0903103106.

7. Appendix

Reagents, buffers and solution

1L 10X phosphate buffered saline (PBS) – 1X is to be autoclaved

- 80g NaCl
- 2.0g KCl
- 14.4g Na2HPO4
- 2.4g KH2PO4
- Up to volume with ddH_2O

500ml 0.2% w/v gelatin – to be autoclaved

- 1.0g Gelatin
- Up to volume with ddH_2O

500ml 0.04% w/v gelatin – to be autoclaved

- 0.2g Gelatin
- Up to volume with ddH_2O

50ml 1x lysis buffer for DNA extraction

- 500µl 1M Tris pH 8.0
- 1ml 0.5 M EDTA, pH 8.0
- 100µl 5M NaCl,
- 2.5ml 10 % SDS
- Up to volume with ddH_2O

100ml RIPA lysis buffer

- 3ml 5 M NaCl
- 1ml 0.5 M EDTA, pH 8.0
- 5ml 1 M Tris, pH 8.0
- 1ml Triton-X-100
- 5ml 10% sodium deoxycholate
- 1ml 10% SDS
- 84ml ddH_2O

2L 10x running buffer

- 60.4 g Tris base
- 288 g Glycine
- 20 g SDS
- Up to volume with ddH_2O

1L 1.5 M Tris, pH 8.8

- 181.65 g Tris base
- Adjust the pH to 8.8 with concentrated HCl
- Up the volume to 1 L with ddH_2O

1L 1.5 M Tris, pH 6.8 (stock buffer for stacking gels)

- Dissolve 181.65 g Tris base
- Adjust the pH to 6.8 with concentrated HCl
- Up the volume to 1 L with ddH_2O

4L 10x Transfer buffer:

- 121.1 g Tris base
- 576 g Glycine
- Up the volume to 4 L with ddH_2O

1L 1x Transfer buffer:

- 700 mL cold ddH_2O
- 100 mL 10x Transfer buffer
- 200 mL Methanol

4L 10x TBS:

- 96.3 g Tris base
- 320 g NaCl
- Adjust the pH to 7.6 with concentrated HCl
- Bring up the volume to 4 L with ddH_2O

1L 1x TBST:

- 100ml 10xTBS
- Add 1 mL Tween-20
- up the volume to 1 L with ddH_2O

200ml 5% blocking solution

- 10g non-fat milk
- Up the volume to 200ml with 1x TBST

50ml 1x Annealing buffer

- 500µL 1M Tris, pH8.0,
- 2.5ml 5M NaCl,

- 100µl 0.5M EDTA, pH8.0
- up the volume with ddH_2O

50ml 1x buffer A for nuclear protein extraction

- 500µL 1MHEPES, PH 7.9
- 500µL 1M KCl
- 100µl 0.5M EDTA, pH8.0
- 20 µl NP-40
- up the volume to 50ml with ddH_2O

  Add 40 µl 25XPI in 960µl when used

10ml 1x buffer B for nuclear protein extraction

- 100µL 1MHEPES, PH 7.9
- 800µL 5M NaCl
- 20µl 0.5M EDTA,pH8.0
- 1ml Glycerol
- Up the volume to 10ml with ddH_2O

  Add 40 µl 25XPI in 960µl when used